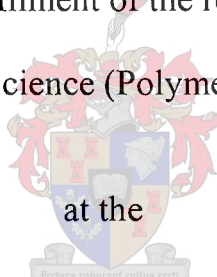


**Preparation of polymer-clay nanocomposites using
emulsion polymerization: Influence of clay modifiers on
the final nanocomposites morphology**

by
Nagi Greesh

Thesis presented in partial fulfilment of the requirements for the degree of

Master of Science (Polymer Science)



at the

University of Stellenbosch

Promoter: Prof. R. D. Sanderson

Stellenbosch

Co -promoter: P.C. Hartmann

December 2006

Declaration

I, the undersigned, hereby declare that the work contained in this thesis is my original work and has not previously in its entirety or in part been submitted at any university for a degree.

Signature:

Date: ...23.1.111.2006

Abstract

Modification of clay surfaces is an essential requirement for the formation of polymer-clay nanocomposites. The clay surface can usually be modified by the replacement of inorganic cations on the clay surface by cationic surfactants. Further, clay has the ability to adsorb some organic compounds that have specific functional groups, such as sulphate and amides, by the formation of hydrogen bonds between these functional groups and hydroxyl groups of the clay. Therefore a clay surface can be treated using non-cationic organic compounds.

The main objective of this study was to modify a clay surface using 2-acrylamido-2-methyl-1-propanesulphonic acid (AMPS), and investigate the interaction occurring between AMPS and clay. The adsorption behaviour of AMPS was compared to organic molecules having similar groups namely: Sodium 1-allyloxy-2-hydroxypropyl (Cops), N-isopropylacrylamide (NIPA) and Methacryloyloxy (MET). An understanding of the type of interaction between clay and organic modifier is useful in terms of understanding the mechanism of clay exfoliation in emulsion polymerization.

The properties and structure of nanocomposites were characterized using SAXS, TEM, DMA, and TGA. The structure of the nanocomposite was affected by the type of clay modifiers. Nanocomposites prepared using AMPS show an exfoliated structure, while other nanocomposites, i.e. those prepared using Cops, NIPA, and MET showed structures between intercalated and partially exfoliated. The mechanical and thermal properties of nanocomposites were found to be strongly dependent on the degree of clay distribution through the polymer matrix. The nanocomposites with exfoliated structures were found to have higher T_g values, improved mechanical properties, and also better thermal stability than nanocomposites with intercalated structures.

Opsomming

Die wysiging van 'n kleioppervlak is 'n belangrike vereiste vir die vorming van polimeer-klei-nanosamestellings. Gewoonlik kan die kleioppervlak gewysig word deur die anorganiese katione op die kleioppervlak te vervang met kationiese sepe. Boonop het die klei die vermoë om sekere organiese verbindings met spesifieke funksionele groepe, b.v. sulfate en amiede, te absorbeer. Dit vind plaas d.m.v. die vorming van waterstofbindings tussen hierdie funksionele groepe en die hidroksielgroepe van die klei. Die kleioppervlakke kan dus met nie-kationiese organiese verbindings behandel word.

Die hoofdoel van hierdie studie was om die kleioppervlak met 2-akriëlamido-2-metiel-1-propaansulfoonsuur (AMPS) te wysig, en die interaksie tussen AMPS en klei te bestudeer. Die adsorpsiegedrag van AMPS is met organiese verbindings met soortgelyke groepe vergelyk (naamlik: natrium-1-alieleksi-2-hidroksiepropiel (Cops), N-isopropielakriëlamied (NIPA) en metakriëloleksi (MET)). 'n Begrip van die tipe interaksie tussen die klei en die organiese wysiger is nuttig om die meganisme van kleiskilfering (Eng. clay exfoliation) in emulsiepolimerisasie beter te verstaan.

Die eienskappe en struktuur van die nanosamestellings is met behulp van SAXS, TEM, DMA en TGA bepaal. Daar is bevind dat die tipe kleimodifiseerder 'n invloed op die struktuur van die nanosamestellings gehad het. Nanosamestellings wat met AMPS berei is, het 'n geskilferde struktuur (Eng. exfoliated structure) gehad, terwyl die ander nanosamestellings (d.w.s. dié wat met Cops, NIPA en MET berei is) het strukture tussen dié van geïnterkaleerde (Eng. intercalated) en gedeeltelike verskilfering (Eng. partially exfoliated) gehad het. Die meganiese en termiese eienskappe van die nanosamestellings het grootliks afgehang van die graad van kleiverspreiding in die polimeermatriks. Die nanosamestellings met 'n geskilferde struktuur het hoër T_g -waardes, beter meganiese eienskappe, asook beter termiese stabiliteit gehad as nanosamestellings met geïnterkaleerde strukture.

Acknowledgements

Firstly I would thank **Allah**, without whom this thesis would certainly not have been possible, and this degree not obtained. Thank you Allah for the prayers that were answered. You inspired- but most of all, thank you for the strength to persevere. I love You with all my heart.

Secondly I give my thanks to the following people for their contributions to this study.

My beloved parents, who have stood by me through all the good and bad times. Thank you for giving me life and walking the distance with me.

Prof. R.D. Sanderson, my study leader, for the chance he gave to me to do something different and individual, and giving me the opportunity to finish it. Thank you Doc for the constant encouragement and your eternal optimism.

Dr. P. Hartmann, for your advice and guidance throughout this study.

Dr. Margie Hurndall, for the time spent helping me write my thesis.

Dr. Matthew Tonge, thank you for your useful advice.

Valeska Cloete, thank you for the use of the coating laboratory and making things available.

Mohamed Jaffer (University of Cape Town) is thanked for doing TEM analysis.

Centre of Macromolecules and Materials Science (Libya) for the financial support of this research.

The coating group, thank you for being my companions for the past few years. I love you guys and look forward to working with you in future.

List of contents

List of Tables.....	vi
List of Figures	vii
List of Abbreviations	xi
Chapter 1: Introduction and objectives	1
1.1 Introduction.....	1
1.2 Objectives	3
1.3 References.....	4
Chapter 2: Polymer-clay nanocomposites: Theoretical background.....	5
2.1 Introduction.....	5
2.2 Types and structures of clay minerals	7
2.3 Surface treatment of clay	10
2.3.1 Ion exchange with organic cations	11
2.3.2 Treatment of clay by interaction of organic molecules in clay galleries	14
2.4 Polymer clay-nanocomposite structure.....	16
2.5 References.....	18
Chapter 3: Synthesis and characterization of nanocomposites: Theoretical background.....	21
3.1 Introduction.....	21
3.2 Methods used to synthesize polymer clay nanocomposites	21
3.2.1 Solution method.....	21
3.2.2 Melt blending synthesis	23

3.2.3 Template method	25
3.2.4 In-situ intercalative polymerization	26
3.2.4.1 Preparation of nanocomposites using emulsion free radical polymerization	27
3.3 Characterization of the structure of the nanocomposites.....	29
3.3.1 X-ray diffraction	29
3.3.2 Transmission electron microscopy	31
3.4 Determination of the properties of nanocomposites.....	31
3.4.1 Thermal stability.....	32
3.4.2 Dynamic mechanical analysis.....	34
3.5 References.....	37
Chapter 4: Experimental.....	41
4.1 Introduction.....	41
4.2 Materials	41
4.3 Modification of Na ⁺ -MMT with various compounds.....	42
4.4 Functionalization of Na ⁺ -MMT by AMPS at different pH values	42
4.5 Characterization of organoclays	43
4.5.1 FT-IR spectroscopy	43
4.5.2 Small angle X-ray scattering	43
4.5.3 Thermogravimetric analysis (TGA)	44
4.6 Synthesis of poly(styrene-co-butylacrylate) nanocomposites	44
4.6.1 Synthesis of poly (styrene-co-butylacrylate) nanocomposites by batch emulsion polymerization	44

4.6.2 Synthesis of poly(styrene-co-butylacrylate) nanocomposites by semi-batch emulsion polymerization	46
4.7 Synthesis of poly(styrene-co-butylacrylate)	46
4.8 Characterization of poly(styrene-co-butylacrylate) nanocomposites	46
4.8.1 Small angle X-ray scattering	47
4.8.2 Transmission electron microscopy	47
4.8.3 Scanning electron microscopy	47
4.8.4 Dynamic mechanical analysis.....	47
4.8.5 Gel permeation chromatography	47
4.8.6 Thermogravimetric analysis	48
4.9 References.....	48
Chapter 5: The interaction mechanism of AMPS with clay	49
5.1 Introduction.....	49
5.2 Clay surface modification by AMPS	51
5.2.1 Determination of the amount of AMPS adsorbed in the clay galleries	52
5.2.2 The organization of AMPS in the clay galleries.....	55
5.3 Determination of types of interaction between AMPS and clay	59
5.3.1 Characterization of AMPS-MMT by FT-IR.....	59
5.3.2 Investigation into the interaction between AMPS and clay via ion exchange .	61
5.3.3 pH dependence of Na ⁺ -MMT surface modified using AMPS.....	61
5.4 Investigation into the interaction between AMPS and clay via adsorption.....	64
5.4.1 Adsorption via sulphate groups	65
5.4.1.1 FT-IR characterization of Cops-MMT and MET-MMT	65

5.4.1.2 Amounts of Cops and MET inside the clay galleries	66
5.4.1.3 Study of d-spacing of AMPS-MMT, MET-MMT and Cops-MMT by SAXS	68
5.4.2 Interaction via the amide groups.....	69
5.4.2.1 Characterization of NIPA-MMT using FT-IR.....	70
5.4.2.2 Amount of NIPA inside the clay galleries	70
5.4.2.3 Study of the <i>d</i> -spacing of NIPA-MMT and AMPS-MMT	72
5.4 References.....	73
Chapter 6: Characterization of poly(styrene-co-butylacrylate)-clay nanocomposites	76
6.1 Introduction.....	76
6.2 Synthesis of poly(styrene-co-butylacrylate).....	76
6.3 Nanocomposites via batch emulsion polymerization	78
6.3.1 Analysis of the composition of poly(styrene-co-butylacrylate) nanocomposites by FT-IR	78
6.3.2 Characterization of nanocomposite structure	79
6.3.2.1 Characterization of nanocomposite structures by SAXS.....	80
6.3.2.2 Characterization of nanocomposite structures by TEM	85
6.3.2.3 Study of the morphology of nanocomposites using SEM	88
6.3.3 Determination of the molecular weights of nanocomposites	89
6.3.4 Study of the thermal properties of nanocomposites	91
6.3.5 Study of the mechanical properties of nanocomposites	94
6.4 Nanocomposites via semi-batch emulsion polymerization	97
6.4.1 Characterization of the structure nanocomposites prepared via semi-batch emulsion polymerization.	98
6.4.3 Study of the thermal stability of nanocomposites synthesized via semi-batch emulsion polymerization, by TGA	101

6.4 References.....	102
Chapter 7: Conclusions and recommendations	104
7.1 Conclusions.....	104
7.2 Recommendations for future work	105
Appendixes	107
Appendix A: The amount of Amps onto clay vs. time of clay modification.....	107
Appendix B: FT-IR spectra of modified clay	108
Appendix C: FT-IR spectra of poly(S-co-BA) nanocomposites	109
Appendix D: T_g measurement by using DMA.....	112

List of Tables

Chapter: 2

Table 2.1: Formula of commonly used 2:1 layered phyllosilicates	9
--	---

Chapter: 4

Table 4. 1: Formulations for the preparation of nanocomposites using AMPS	45
--	----

Chapter: 5

Table 5.1: Clay modifiers used in this study	50
Table 5.2: Initial AMPS concentrations and the quantities of AMPS inside clay galleries	54
Table 5.3: FT-IR results for Na ⁺ -MMT and AMPS-MMT	60
Table 5.4: Quantities of organic modifiers inside the clay galleries	67

Chapter: 6

Table 6.1: FT-IR data of poly (S-co-BA)-clay nanocomposites (at 100% CEC).....	79
Table 6.2: Variation of molecular mass and polydispersity index (PDI) with clay loading of the poly(S-co-BA)-clay nanocomposites	90
Table 6.3 : TGA data for poly(S-co-BA) nanocomposites at similar clay loading (10%)	93
Table 6.4: T_g values and storage modulus of nanocomposites	95

List of Figures

Chapter: 2

- Fig. 2.1:** a) Silica tetrahedron and tetrahedral units arranged in a hexagonal network, and
b) cation octahedron and octahedral units arranged in a sheet7
- Fig. 2.2:** Structure of 2:1 phyllosilicates9
- Fig. 2.3:** The arrangement of charges on the surface of silicate layers.....10
- Fig. 2.4:** Schematic representation of clay surface treatment by ion-exchange reaction. 13
- Fig. 2.5:** Representation of the arrangement of water molecules around Na^+ ions15
- Fig. 2.6:** Types of nanocomposite structures: (a) conventional, (b) intercalated and (c) exfoliated. (Note: (a) layers number 500-1000, (b) layers number up to 1000 but can also tend toward a single figure depending on an extent of intercalation, and (c) individual layers loosened from 1000 sheets per single clay particle.).....16

Chapter: 3

- Fig. 3.1:** Schematic representation of the preparation of nanocomposites via the solution method.22
- Fig. 3.2:** Schematic representation of the preparation of nanocomposites via the melt blending method.24
- Fig. 3.3:** Schematic representation of the preparation of nanocomposites via in-situ polymerization.26
- Fig. 3.4:** X-Ray patterns of three layered silicates structures: (a) conventional, (b) intercalated, (c) exfoliated30

Chapter: 5

- Fig. 5.1:** pH values of centrifuged water vs. the number of washings for 100% CEC AMPS.52

- Fig. 5.2:** Thermal gravimetric curves of: (a) pristine Na^+ -MMT and Na^+ -MMT with different AMPS concentrations: (b) 25% CEC (c) 50%CEC (d) 75% CEC (e) 100% CEC (f) 130% CEC. (The insert shows thermal decomposition of dried AMPS.)53
- Fig. 5.3:** SAXS patterns of (a) pristine Na^+ -MMT, and AMPS-MMT samples with different AMPS concentrations b) 10%, c) 25%, d) 50%, f) 75%, g) 100% and h) 130% CEC of clay.....56
- Fig. 5.4:** Interlayer distances of Na^+ -MMT and AMPS-MMT vs. AMPS concentration. 57
- Fig. 5.5:** Schematic representation of the arrangement of AMPS molecules inside silicate layers: (a) mono-layer, (b) bi-layer, (c) paraffin-type mono-layer and (d) paraffin-type bi-layer58
- Fig. 5.6:** Thermal gravimetric curves of (a) Na^+ -MMT, and AMPS-MMT at different pH values: (b) 0.63 (c) 1.81 (d) 2.8 (e) 3.5 and (f) 6.0.....62
- Fig. 5.7:** SAXS traces for AMPS-MMT prepared at different pH values.....63
- Fig. 5.8:** TGA thermograms of (a) Na^+ -MMT, (b) Cops-MMT, (c) MET-MMT, and (d) AMPS-MMT. (The insert shows thermal decomposition of dried Cops, MET and AMPS).66
- Fig. 5.9:** SAXS patterns for (a) Na^+ -MMT, (b) AMPS-MMT, (c) MET-MMT and (d) Cops-MMT68
- Fig. 5.10:** Two possibilities for the interaction between NIPA and clay via hydrogen bonding between amide group of NIPA and (a) hydroxyl groups of silicate, and (b) with water molecules coordinated to the interlayer cations.....71
- Fig. 5.11:** TGA thermograms of (a) Na^+ -MMT, (b) NIPA-MMT, (c) AMPS-MMT. The insert shows thermal decomposition of dried NIPA and AMPS.71
- Fig. 5.12:** SAXS patterns for (a) Na^+ -MMT, (b) AMPS-MMT, and (c) NIPA-MMT.....72

Chapter: 6

- Fig. 6.1:** ^1H NMR spectrum of poly(styrene-co-butylacrylate). Note that the distribution of monomer units in the copolymer is expected to be random.....77
- Fig. 6.2:** SAXS patterns for poly(styrene-co-butylacrylate) nanocomposites: (A)

- poly(styrene-co-butylacrylate)-AMPS nanocomposites i-v represent nanocomposites containing 1%, 3%, 5%, 7% and 10% clay respectively, (B) poly(styrene-co-butylacrylate)-NIPA nanocomposites i-iv represent nanocomposites containing 1%, 3%, 7% and 10% clay respectively, (C) poly(styrene-co-butylacrylate)-Cops nanocomposites i-v representing nanocomposites containing 1%, 5%, 7% and 10% clay, (D) poly(styrene-co-butylacrylate)-MET-nanocomposites i-iv representing nanocomposites containing 1%, 5%, 7% and 10% clay respectively.81
- Fig. 6.3:** TEM images of intercalated poly(S-co-BA)-AMPS nanocomposites containing: (A) 1% clay, and (B) 5% clay loading.....85
- Fig. 6.4:** TEM images for partially exfoliated poly(S-co-BA)-AMPS nanocomposites at: (A) 7% clay loading, and (B) exfoliated poly(S-co-BA)-AMPS nanocomposites at 10% clay loading.85
- Fig. 6.5:** TEM images for intercalated poly(S-co-BA)-NIPA nanocomposites at: (A) 1% clay loading and (B) 3% clay loading.86
- Fig. 6.6:** TEM images for poly(S-co-BA)-NIPA nanocomposites at different clay loadings: (A) 7% and (B) 10% clay.....87
- Fig. 6.7:** TEM image of intercalated structure of poly(S-co-BA)-Cops nanocomposites at 10% clay loading.87
- Fig. 6.8:** TEM image of poly(S-co-BA)-MET nanocomposite at 10% clay loading.....88
- Fig. 6.9:** SEM images of (A) poly(S-co-BA)-AMPS nanocomposite containing 10% clay, and (B) poly(S-co-BA)-Cops nanocomposite containing 10% clay.89
- Fig. 6.10:** (A-D) Thermal stability of poly(S-co-BA)-clay nanocomposites as a function of clay loading. The inserts show the amount of clay in the thermograms, as a percentage and the organic compounds used to make the organoclays: (A) Poly(S-co-BA)-AMPS nanocomposites (B) Poly(S-co-BA)-MET nanocomposites (C) Poly(S-co-BA)-Cops nanocomposites (D) Poly(S-co-BA)-NIPA nanocomposites.91
- Fig. 6.11:** Comparison of the thermal stability of four different nanocomposites at similar clay loadings. The thermogram of poly(S-co-BA) is included as a reference. .92
- Fig. 6.12:** Variation of (A) storage modulus and (B) $\tan \delta$ vs. temperature for (i) pure

poly(S-co-BA) and for different nanocomposites at 10% clay loading: (ii) poly(S-co-BA)-cops nanocomposite, (iii) poly(S-co-BA)-NIPA nanocomposite, (iv) poly(S-co-BA)-MET nanocomposite, and (v) poly(S-co-BA)-AMPS nanocomposite.96

Fig. 6.13: T_g values vs. clay content of four types of nanocomposites97

Fig. 6.14: TEM image of poly(S-co-BA)-AMPS nanocomposite at 3% clay loading.....98

Fig. 6.15: TEM image of a poly(S-co-BA)-AMPS nanocomposite at 10% clay loading. 99

Fig. 6. 16: TEM image for poly(S-co-BA)-AMPS at 15 % clay loading.99

Fig. 6.17: SAXS patterns for poly(S-co-BA)-AMPS nanocomposites at different clay loading: (i) 3%, (ii) 15% and (iii) 10%.....100

Fig. 6.18: Thermal stability of poly(S-co-BA)-AMPS nanocomposites at different clay loading. Pure poly(S-co-BA) is included in the figure as reference.....101

List of Abbreviations

AMPS	2-acrylamido-2-methyl-1-propanesolphonic acid
AMPS-MMT	Montmorillonite modified by AMPS
°C	Degree Celsius
CTAB	Cetyltrimethylammonium bromide
CEC	Cation exchange capacity
Cops	Sodium 1-allyloxy-2-hydroxypropyl sulphonate
<i>d</i>	Interlayer distance
DMA	Dynamic mechanical analysis
FT-IR	Fourier transform infrared
G'	Storage modulus
G''	Loss modulus
GPC	Gel permeation chromatography
MMT	Montmorillonite clay
MET - MMT	Montmorillonite modified by MET
\bar{M}_n	Number average molecular mass
\bar{M}_w	Weight average molecular weight
\bar{M}_w/\bar{M}_n	Polydispersity index
Na ⁺ -MMT	Montmorillonite clay containing sodium ions
NMR	Nuclear magnetic resonance
NIPA	N-isopropyl acrylamide

NIPA- MMT	Montmorillonite modified by NIPA
PCNS	Polymer - clay nanocomposites
Poly(S-co-BA)	Poly(styrene-co-butylacrylate)
Poly(S-co-BA)-AMPS	Poly (styrene-co-butylacrylate) with AMPS
Poly(S-co-BA)-Cops	Poly (styrene-co-butylacrylate) with Cops
Poly(S-co-BA) NIPA	Poly (styrene-co-butylacrylate) with NIPA
Poly(S-co-BA) MET	Poly (styrene-co-butylacrylate) with MET
PEO	Poly(ethylene oxide)
PVA	Poly(vinyl alcohol)
SAXS	Small angle scattering
SDBS	Sodium dodecyl benzenesulphonate
SEM	Scanning electron microscopy
TGA	Thermogravimetric analysis
TEM	Transmission electron microscopy
T_g	Glass transition temperature
THF	Tetrahydrofuran
UV	Ultraviolet
WAXD	Wide angle X-ray diffraction
Wt	Weight
XRD	X-ray diffraction

Introduction and objectives

1.1 Introduction

Often polymeric materials require certain properties to satisfy certain application needs. One of the ways in which the properties of a polymer can be modified is by addition of a second selected component. New composite materials can then be produced with improved properties. Inorganic fillers are commonly used as a second component in polymers to reduce the cost and to improve a variety of physical properties, such as stiffness, strength, thermal stability, etc.¹ Different types of fillers are presently being used in industry, such as glass fibres, mineral fillers, metallic fillers, etc. In conventional composites materials, these types of fillers range in size from several microns to a few millimetres¹⁻³.

Clay is one of the most abundant natural and inexpensive filler materials. Clay was introduced in the nanotechnology field as a new type of filler to produce polymer-clay nanocomposites⁴. Depending on the ordering and degree of clay dispersion in a polymer matrix there are three types of nanocomposites that can be distinguished (i.e. conventional composites, intercalated and exfoliated)⁵.

A polymer-clay nanocomposite is a polymer that contains nanometer-sized clay particles. Such a nanocomposite can have favourable properties, like high stiffness and barrier resistance. Optimal properties are usually obtained when clay is fully exfoliated into single silicate layers^{6,7}. During exfoliation, the clay particles do not only become much smaller but simultaneously their shape is changed from cubical blocks to flat platelets.

The preparation of polymer-clay nanocomposites requires a good compatibility between the clay surface and the polymers or monomers¹. The swellable clays such as montmorillonite are hydrophilic and therefore incompatible with hydrophobic polymers or monomers⁸. Furthermore, the clay platelets are bound to each other by Van der Waals

Introduction and objectives

forces, which make the interlayer in the clay very narrow. The hydrophilicity of clay can be changed by surface modification of clay^{6,8}.

The surface modification of clay can be typically performed by ion exchange of surface inorganic cations (e.g. Na⁺, K⁺, Ca²⁺) by organic cationic surfactants. However, the clay surface can also be modified using organic molecules with weaker interactions such as hydrogen bonds⁹.

Successful preparation of nanocomposites strongly depends on the organic modifier used and its type of interaction with the clay surface.

Recently many researchers focused on the preparation of polymer-clay nanocomposite latexes using emulsion and miniemulsion polymerization, some studies showed that clay can be successfully exfoliated in these conditions, using various organic clay modifiers, providing some type of interaction with the clay surface prior to polymerization^{7,8,10-13}.

An interesting study showed that the use of 2-acrylamido-2-methyl-1-propanesulphonic acid (AMPS) as clay modifier successfully promoted exfoliation of clay upon copolymerization of styrene and butylacrylate in emulsion. The authors indisputably produced exfoliated nanocomposites. However, their statement about the type of interaction between AMPS and clay is questionable¹³.

Since the type of interaction between the organic modifier and clay plays an important role on successfully achieving a proper exfoliation, the real type of interaction occurring between clay and AMPS ought to be elucidated, so as to better understand the mechanism of exfoliation in emulsion polymerization.

The present work is divided into two main parts. The first part is devoted to the study of the type of interactions existing between AMPS and clay. Adsorption behaviour of AMPS into clay was compared to various organic molecules with similar chemical groups namely: Sodium 1-allyloxy-2-hydroxypropyl sulphonate (Cops), N-isopropylacrylamide (NIPA), Methacryloyloxy-undecan-1-yl sulphate (MET).

The second part of the present work focuses on the preparation of poly(styrene-co-butylacrylate)-clay nanocomposites by emulsion polymerization using

Introduction and objectives

these different clay modifiers.

Correlations between the structure of the final nanocomposites obtained with the degree of interaction and modification of the original clay used, will lead to a better understanding on the mechanism by which in-situ intercalative polymerization in emulsion occurs.

1.2 Objectives

Hence the specific objectives of this study were to:-

- Modify Na⁺-MMT using different concentrations of 2-acrylamido-2-methyl-1-propanesulphonic acid (AMPS), and characterize AMPS-MMT samples using FT-IR, TGA and SAXS.
- Study the interaction mechanism between AMPS and clay (i.e. whether by ion exchange or adsorption), by modifying the clay using other organic modifiers which are similar to AMPS in terms of their chemical functional groups, namely (sodium 1-allyloxy-2-hydroxypropyl sulphonate (Cops), N-isopropylacrylamide (NIPA) and methacryloyloxyundecan-1-yl sulphate (MET)).
- Synthesize four different poly(styrene-co-butylacrylate)-clay nanocomposites via batch emulsion polymerization, using four different organic modifiers (AMPS, Cops, NIPA, and MET) as clay modifiers, and then characterize the structures of the nanocomposites using SAXS and TEM.
- Determine the thermal stability of the synthesized nanocomposites using TGA, and compare their thermal stability to that of the pure poly(styrene-co-butylacrylate).
- Determine the mechanical properties and T_g of the synthesised nanocomposites using DMA and compare them with those of the virgin poly(styrene-co-butylacrylate).
- Study the effect of the monomer feed rate on the morphology and properties of nanocomposites, by synthesizing nanocomposites via a semi-batch process using

Introduction and objectives

a slow feeding rate, characterizing the structures and properties, and comparing the results to those results obtained from batch emulsion polymerization.

1.3 References

- (1) Utracki, L. A.; Kamal, M. R. *The Arabian Journal for Science and Engineering*, **2002**, *27*, 43 - 67.
- (2) Eitan, A.; Fisher, F. T.; Andrews, R.; Brinson, L. C.; Schadler, L. S. *Composites Science and Technology* **2006**, *66*, 1162 - 1173.
- (3) Okada, A.; Usuki, A. *Journal of Materials Research* **1995**, *3*, 109 - 117.
- (4) Rosorff, M. In *Nano Surface Chemistry*; Marcel Dekker Inc: New York and Basel, 2002; pp 653 - 673.
- (5) Lebaron, P. C.; Wang, Z.; Pinnavaia, T. J. *Applied Clay Science* **1999**, *15*, 11 - 29.
- (6) Alexandre, M.; Dubois, P. *Materials Science and Engineering*, **2000**, *28*, 1 - 63.
- (7) Choi, Y. S.; Choi, M. H.; Wang, K. H.; Kim, S. O.; Kim, Y. K.; Chung, I. J. *Macromolecules* **2001**, *34*, 8978 - 8985.
- (8) Noh, M. W.; Lee, D. C. *Polymer Bulletin* **1999**, *42*, 619 - 626.
- (9) Yariv, S.; Cross, H. *Organo-Clay Complexes and Interactions*; Marcel Dekker, Inc: New York and Basel, 2002.
- (10) Choi, Y. S.; Wang, K. H.; Xu, M.; Chung, I. J. *Chemistry of Materials* **2001**, *14*, 2936 - 2939.
- (11) Zeng, C.; Lee, L. J. *Macromolecules* **2001**, *34*, 4098 - 4103.
- (12) Qutubuddin, S.; Tajuddin, Y. *Polymer Bulletin* **2002**, *48*, 143 - 149.
- (13) Xu, M.; Choi, Y. S.; Kim, Y. K.; Wang, K. H.; Chung, I. J. *Polymer* **2003**, *44*, 6387 - 6395.

Polymer-clay nanocomposites: Theoretical background**2.1 Introduction**

Polymer materials are often reinforced with fillers to improve their mechanical properties. Such materials are widely used in many areas including transportation, construction and electronics ¹. One of the most common classes of reinforcing materials is fibrous fillers in a randomly dispersed state. The degree of reinforcement depends on the rigidity and aspect ratio of the filler itself, and the adhesive bond between the filler and polymer matrix. For instance, in order to improve adhesive strength between the matrix and the fillers, the surface (e.g. of glass or carbon fibres) is organically treated ². The size of such fillers is of the order of microns, which is large compared to the size of polymers, which are of nanometer order. This significant difference in size between polymer and filler often results in the deterioration in properties of the composite, such as decreased ductility, poor mouldability and poor surface smoothness in moulded articles. The use of fillers can also offer a route to the production of inexpensive polymeric materials ²⁻⁴.

The focus of the present study is on clay-reinforced polymeric nanocomposites (PCNs). The advantages of using clays as polymer fillers are their availability, low cost, and high aspect ratio (i.e. surface to volume or length to thickness with platelets) ². Polymer-clay nanocomposites themselves have several advantages: (a) they are lighter in weight compared to the same polymer filled with other types of fillers, due to the achievement of property enhancement even at small clay loadings, (b) they have enhanced flame retardance and thermal stability and (c) they exhibit enhanced barrier properties ^{1,5,6}.

Depending on the ordering and degree of clay dispersion in a polymer matrix there are three types of PCNs that can be distinguished ⁷.

Conventional composites are formed when the polymer chains are unable to penetrate

Theoretical background

between the layers of the silicate particles of the clay⁸⁻¹⁰.

Intercalated structures are formed when one or more polymer chains intercalate between the layers of clay. Therefore, the interlayer spacing is increased but the ordered layer structure of the clay particles is retained^{10,11}.

Exfoliated composites arise where the clay particles are completely delaminated and the silicate layers do not show any ordering in their arrangement. This type of PCN has improved mechanical and thermal properties relative to intercalated and conventional materials, due to the homogeneous dispersion of clay in the polymer matrix, as well as large interfacial areas between the clay layers and the polymer matrix¹¹⁻¹³.

Polymer-clay nanocomposites are relatively new materials. They exhibit a large increase in tensile strength, modulus and heat distortion temperature compared to the virgin polymers^{13,14}. They also show reduced permeability to gases¹⁵, and a smaller thermal coefficient of expansion¹⁶. All of these property improvements can be realized without a loss of polymer clarity². Further, it has been found that nanocomposites impart flame retardance not present in the virgin polymers. These improvements in properties at relatively low clay loadings (typically 2-10%) have stimulated intensive research in both industry and academia over the past decade¹⁵⁻¹⁷.

Pristine clay is naturally hydrophilic, and polymers are often hydrophobic^{14,18}. The hydrophilic nature of clay impedes its homogeneous dispersion in a polymer matrix. The first major breakthrough in addressing this problem was in 1987, when Fukushima and Inagaki¹⁹ from TCRD in Japan replaced inorganic cations in clay galleries with alkylammonium surfactants. They successfully compatibilized a clay surface with hydrophobic polymer matrices¹⁹.

Usually clays are modified with alkylammonium surfactants for two purposes. The first is to widen the gallery spacing of the layered silicate and to enable polymers or monomers to penetrate more easily into the clay layer spaces. The second is to tether alkylammonium molecules on silicate surfaces and make silicate layers compatible with hydrophobic polymers²⁰.

Theoretical background

The first successful nanocomposite, reported by the Toyota research group, was in the form of a Nylon 6/clay nanocomposite obtained by in situ polymerization. By adding only 4.2% clay the following was achieved: 50% enhanced strength and an increase in heat distortion by 80°C, compared to the neat Nylon 6. It was this discovery that gave rise to the new engineering materials called polymer-clay nanocomposites¹⁴.

2.2 Types and structures of clay minerals

Clay minerals are called layered silicates because of their stacked structure of 1-nm silicate sheets with a variable basal distance⁵. Generally there are two building blocks that can form the silicate layer clays, as shown in Fig. 2.1: the silica (Si) tetrahedral and the aluminium (Al) octahedral⁵.

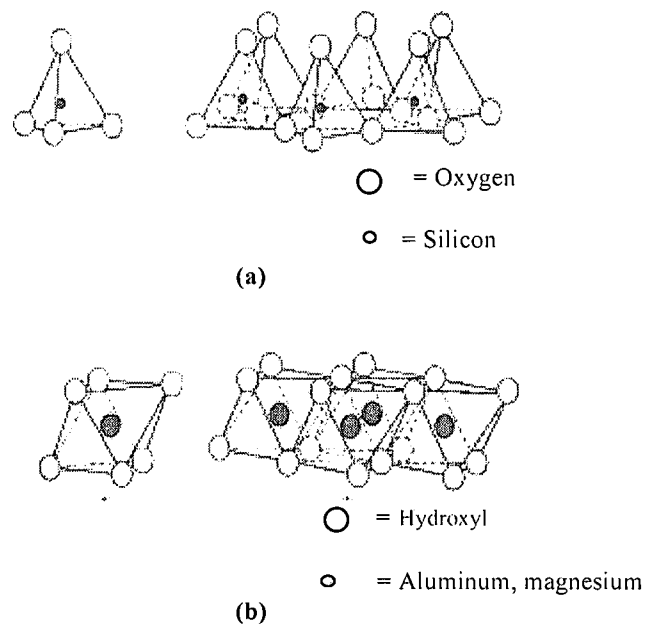


Fig. 2.1: a) Silica tetrahedron and tetrahedral units arranged in a hexagonal network, and b) cation octahedron and octahedral units arranged in a sheet⁵.

The silica tetrahedral groups are arranged to form a sheet of tetrahedron units, and the aluminium octahedral units are joined together to form a sheet of octahedral units. Depending on the number and combination of structural units (tetrahedral and octahedral sheets), the clay minerals can be divided into two types, 1:1 and 2:1 phyllosilicates^{5,13,21}.

(i) 1:1 phyllosilicates: “Non-swelling” clays such as kaolinite consist of units of single

Theoretical background

sheets of silica tetrahedra between alumina octahedral sheets ²¹.

(ii) *2:1 phyllosilicates*: These are known as “swelling” clays, where the layer of minerals is composed of one central octahedral sheet sandwiched between two tetrahedral sheets, condensed in one unit layer designated as 2:1. The most common clays that have a 2:1 structure are smectites (e.g. montmorillonite, saponite, etc.), mica, and chlorites ²¹.

The layered silicates used to form nanocomposites belong to the same structure of 2:1 phyllosilicates. Their crystal lattice consists of two-dimensional, 1-nm thick layers, which are made up of two tetrahedral sheets of silica fused to an edge-shaped octahedral sheet of alumina or magnesia. Depending on the particular silicate the lateral dimensions of the layers can be about 300 Å or more. The layers organize themselves to form stacks with regular Van der Waals gaps in between them, called the interlayer or the gallery ^{1,5,7,13,14,22}.

Naturally the layers undergo isomorphic substitution within them, which includes replacement of one ion for another of similar size (for example, Al^{3+} is replaced by Mg^{2+} or by Fe^{2+} , or Mg^{2+} is replaced by Li^+). This leads to a change in the total charge and the location of the charge on the mineral ^{5,10,13,21,23}. Isomorphic substitution within the layer generates negative charges that are normally counterbalanced by hydrated alkali or alkaline earth cations (such as Na^+ , K^+ and Ca^{2+}) residing in the interlayer ^{7,14}. Because of the relatively weak forces between the layers (due to the layered structure), interaction of various molecules, and even polymers, between the layers is possible.

Ion-exchange reactions with cation surfactants, including primary, tertiary and quaternary ammonium or phosphonium ions, render the normally hydrophilic silicate surface organophilic, which makes possible the intercalation of many polymers. The role of the alkyl ammonium cations in the organosilicates is to reduce the surface energy of the inorganic host and improve the wetting characteristics with the polymer ^{5,13,24-26}.

Theoretical background

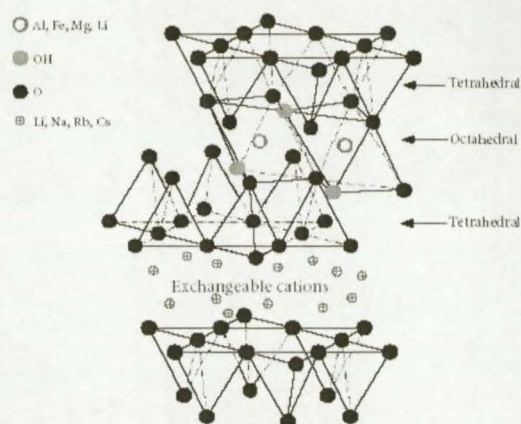


Fig. 2.2: Structure of 2:1 phyllosilicates ²⁴.

The commonly used layered silicates are montmorillonite, hectorite and saponite ^{7,14}. Details on the structure and chemistry of these layered silicates are given in Fig. 2.2 and Table 2.1. All of these silicates are characterized by a large active surface area (700-800 m²/g in the case of montmorillonite), a moderate negative surface charge (cation exchange capacity) and layer morphology, and are regarded as hydrophobic colloids of the constant-charge type ^{1,24}. The layer charge indicated by the chemical formula is only to be regarded as an average over the whole crystal because the charge varies from layer to layer (within certain bounds). Only a small proportion of the charge-balancing cations is located at the external crystal surface, with the majority being present in the interlayer space ²⁷.

Table 2.1: Formula of commonly used 2:1 layered phyllosilicates ¹³

2:1 phyllosilicate	General formula
Montmorillonite	$M_x (Al_{4-x} Mg_x) Si_8 O_{20} (OH)_4$
Hectorite	$M_x (Mg_{6-x} Li_x) Si_8 O_{20} (OH)_4$
Saponite	$M_x (Mg_x) (Si_{8-x} Al_x) O_{20} (OH)_4$

The cations are exchangeable for others in solution. The presence of the cations in the galleries of silicate makes the silicate layers completely hydrophilic, and completely compatible with hydrophilic polymers such as poly(ethylene oxide) (PEO) and poly(vinyl alcohol) (PVOH) ¹⁴. On the other hand, these silicate layers are poorly compatible with hydrophobic polymers. The stacks of clay platelets are held tightly together by

Theoretical background

electrostatic forces ^{14,18}.

Fig. 2.3 shows that the counterions are attracted to the net negative charge within the clay platelets. The counterions can be shared by two neighbouring platelets, resulting in stacks of platelets that are held tightly together. This makes the penetration of polymers or monomer(s) into the galleries of silicate more difficult. For these reasons, the clay must be treated before it can be used to make nanocomposite materials ¹⁸.

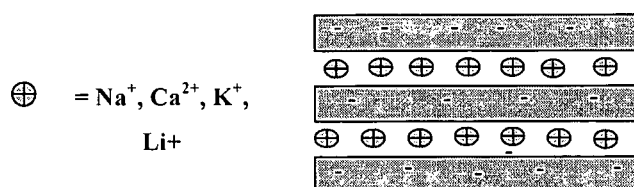


Fig. 2.3: The arrangement of charges on the surface of silicate layers.

2.3 Surface treatment of clay

The mechanical properties of nanocomposites are affected by the dispersion state of silicate particles in the polymer matrix ²⁰. Polymer-clay nanocomposites usually have improved mechanical and thermal properties when the dispersion of silicate layers in the polymer matrix is high (exfoliated structure). The main focus in producing nanocomposites here is to obtain an exfoliated system. ^{13,20,28,29} There are two main problems that can retard the preparation of nanocomposites. The first one is the high hydrophilicity of silicate layers that makes them incompatible with hydrophobic polymers. The second is the narrow basal spacing of silicate layers that makes the penetration of polymer into the silicate interlayer very difficult ^{13,29}. In order to overcome these problems, the clay surface must be modified.

The modification of clay to render it 'organophilic' is an essential requirement for the successful formation of polymer-clay nanocomposites. There are different ways to modify 2:1 clay minerals: (1) ion exchange with organic cations, (2) adsorption, (3) binding of inorganic and organic cations, mainly at the edges of the clay, (4) grafting of organic compounds; (5) reaction with acids and (6) physical treatment such as by ultrasound and plasma ³⁰. Ion exchange with organic cations will be discussed in more

Theoretical background

detail in Section 2.3.1, while all the other methods will be discussed in Section 2.3.2

2.3.1 Ion exchange with organic cations

A popular and relatively easy method of modifying the clay surface, making it more compatible with an organic matrix, is ion exchange³⁰. The cations are not strongly bound to the clay surface, so cationic small molecules can replace the cations present on the clay surface. These cationic small molecules can be simple inorganic cations, such as Cd^{2+} , which can be precipitated using SH^- to give CdS nanoparticles in-between the clay layers, thereby creating potential nanoreactors³⁰.

The most common cationic surfactants used in ion-exchange reactions for the synthesis of PCNs are primary, secondary, and quaternary alkyl ammonium or alkylphosphonium cations¹⁴. The exchange of inorganic cations by organic ions in clay galleries not only makes the organoclay surface compatible with the monomer or polymer matrix but also decreases the interlayer cohesive energy of clay platelets by expanding the d-spacing, i.e. more room is created for polymer chains to enter into these spaces. This facilitates the penetration of polymers or monomers into the clay galleries^{7,13,31}.

The length of the alkyl ammonium cations influence the hydrophobicity of the silicate layers³². Zhang *et al.*³³ investigated the effect of surfactant chain length and found that as the alkyl chain length increases, the miscibility between monomer and clay increases, leading to an exfoliated structure³³. The chain length of the organic modifier within the silicate galleries plays a crucial role in determining the dispersion behaviour in nanocomposites³². The chain length of surfactant also has effects on the mechanical behaviour of nanocomposites. Xie *et al.*³⁴ synthesized PS-nanocomposites using surfactants with different chain lengths. They found that the longer the alkyl chain length that the surfactant possessed, the higher was the glass transition temperature of the PS-nanocomposite³⁴.

The orientation of the surfactant in the galleries depends on its chemical structure and the charge density of the clay itself. Increasing the surfactant chain length or charge density of the clay leads to larger d-spacing and interlayer volume^{16,29}.

Theoretical background

Additionally, the alkylammonium or alkylphosphonium cations can provide functional groups that can react with the polymer matrix or, in some cases, initiate the polymerization of monomers to improve the strength of the interface between the silicate layers and the polymer matrix ¹⁴.

In order to make polymer-clay nanocomposites, all clay particles must be completely separated into individual clay layers (see Fig. 2.4). Exfoliating clay in a polymer matrix is not simple, because electrostatic forces hold the silicate sheets tightly together. To solve these problems, a liquid needs to penetrate between individual sheets. The separation of individual sheets is easily achieved in water, especially with smectite clays like hectorite, montmorillonite and saponite; their ionic charge is just high enough to let water enter the inter-gallery spaces and swell the clay. During this swelling procedure the distance between the clay platelets is increased and the strength of the ionic bond is decreased ³⁵.

Other minerals with neutral layers, like talc, cannot be swollen in water, because talc has no inter-gallery cations. This makes the talc crystal hydrophobic, making it impossible for water to enter the inter-gallery space. On the other hand, mica has a too high concentration of interlayer cations. This makes the binding strength between the clay layers too strong for water to enter the inter-gallery space ³⁵.

Depending on the charge density of the clay and the ionic surfactant, different arrangements of the ions are possible. In general, the longer the surfactant chain length and the higher the charge density of the clay, the further apart the clay layers will be forced. This is expected since both of these parameters contribute to increasing the volume occupied by the intergallery surfactant ⁷.

Theoretical background

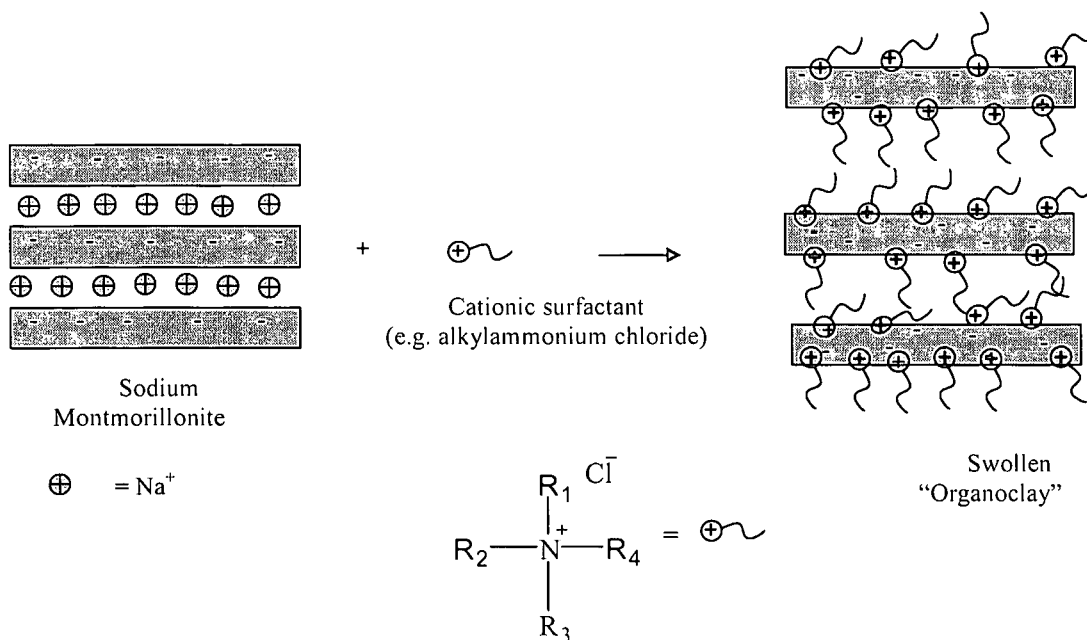


Fig. 2.4: Schematic representation of clay surface treatment by ion-exchange reaction.

The total number of replaceable small inorganic cations is governed by the moderate negative surface charge called the cation exchange capacity (CEC), i.e. the maximum number of exchangeable sites. The CEC values are different for different types of clays; they range from 80-120 meq/100 g of clay (milliequivalent per 100 g of clay)²⁴.

The morphology and properties of nanocomposites are often greatly influenced by the properties of the organic cations used as clay modifiers. Zhang *et al.*³³ investigated the effects of reactive intercalating agents (clay modifiers) with different lengths of alkyl chains on the morphology and properties of PS-nanocomposites. They synthesized different PS-nanocomposites by using ion-exchange reactions, using four different surfactants. Exfoliated structures were obtained when reactive surfactants that had polymerizable groups were used, while intercalated structures were obtained when non-reactive surfactants were used.

Surfactants used for the synthesis of polystyrene-clay nanocomposites range from alkyl to aromatic-containing ammonium surfactants^{33,36}. The head group of a clay modifier plays an important role in terms of the structure of nanocomposites. Intercalated

Theoretical background

structures were obtained with a surfactant having CH₃ in the head group, while exfoliated PS-nanocomposites were achieved with a surfactant having a benzyl in the head group. Both of these nanocomposites structures were achieved under similar conditions using suspension polymerization. The presence of the benzyl group improved the compatibility with styrene so that formation of the exfoliated structure was easier. Polystyrene-clay nanocomposites with organo-MMT-containing benzyl units similar to styrene show a higher thermal stability than other PS-organo-MMT nanocomposites. This indicates that the structure and properties of the surfactant used in the preparation of organo-MMT plays a very important role in determining the properties of the final polymer-clay nanocomposites³⁴.

The ion exchange of cationic surfactants onto a homo-ionic montmorillonite dispersed in water was found to be independent of the size of the hydrophilic head group of the cationic surfactant, and its pH²⁷.

2.3.2 Treatment of clay by interaction of organic molecules in clay galleries

There are several reasons that prompted researchers in the field of nanocomposites to search for alternative methods to modify clay surfaces. The low thermal stability of quaternary ammonium compounds commonly used to modify the clay surface generally leads to decomposition products that impart undesirable colour and odour, and also degrades the properties of the composite³⁷. In addition, the commercial availability of quaternary ammonium compounds is limited. In order to obtain fully exfoliated nanocomposites the modifier should be thermodynamically compatible with the polymer. Here, in order to produce nanocomposites, alternative methods to modify the clay are used. The physicochemical properties of mineral clay allow the interaction between clay and non-cationic organic molecules to take place.

Interactions between organic molecules and clay are very common in nature. Such interactions include cation exchange (explained in the previous section), and adsorption of polar and non-polar molecules.²¹ The organic molecules that have partial negative charge can interact with exchangeable cations via formation of ion-dipole bonds. Therefore, those organic molecules can be used as clay modifiers. This phenomenon was

Theoretical background

first used with different types of glycols³⁷. The organic polar molecules can be adsorbed by mineral clay by the formation of a coordination bond between the exchangeable cation and the organic molecules or by proton transfer from interlayer water to the organic molecules, or vice versa²¹.

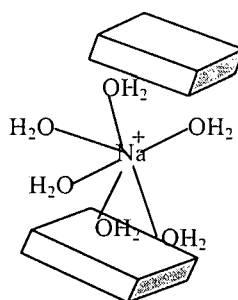


Fig. 2.5: Representation of the arrangement of water molecules around Na⁺ ions²¹.

Neutral molecules penetrate into the interlayer spaces of clay when the energy that results from the adsorption process is enough to overcome the interaction between silicate layers. Clay can form interlayer complexes with many types of uncharged molecules. The presence of water molecules in the interlayer space of the clay (see Fig. 2.5) leads to the creation of some competition between water molecules and uncharged organic molecules for ligand positions around the exchangeable cations. The adsorption of uncharged organic molecules increases as the concentration of organic molecules increases and as the volume of water in the system is lowered.

Some studies have been carried out on the interaction between clay and organic molecules, such as amide compounds. The interaction between amides and Na⁺-MMT was investigated by Tahoun and Mortland³⁸. When amides are adsorbed by Na⁺-MMT, they can be protonated. The degree of protonation depends on the acid strength of exchangeable cations and the polarization of the adsorbed water by the cations. Both functional groups of an amide (carbonyl and amine) form hydrogen bonds with water molecules. In this case water works as bridges between the amide molecules and exchangeable cations in the silicate interlayer. The interaction between urea molecules and clay was studied by Mortland³⁹. Molecular urea is bound to the exchangeable cation via water molecule bridges. The CO group of urea molecules coordinates the metallic cation.

Theoretical background

Stutzmann and Siffert⁴⁰, using IR spectroscopy, studied the adsorption mechanism and fine structure of complexes obtained between Na⁺-MMT and acetamide and polyacrylamide. The adsorption takes place on the external surface of the clay particles. The organic molecules are protonated on the surface and adsorbed by electrostatic force. There are two adsorption possibilities: strong, irreversible adsorption, which corresponds to the formation of chemisorbed molecules, or the more important adsorption of molecules retained by the formation of hydrogen bonds.

2.4 Polymer clay-nanocomposite structure

Depending on the nature of the components used (layer silicate, organic cation and polymer matrix) and the method of preparation, three different types of nanocomposite structure may be obtained when the clay particles are dispersed in a monomer or polymer matrix (see Fig 2.6)¹³.

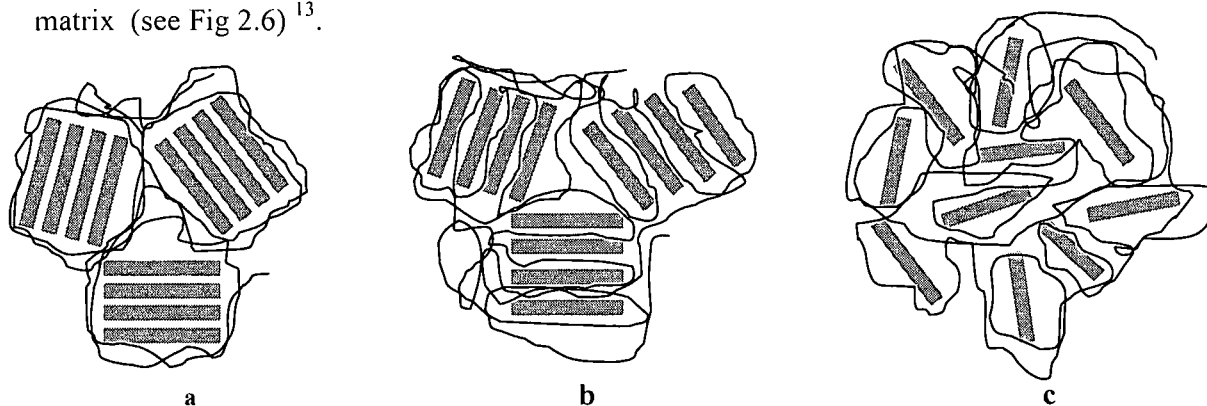


Fig. 2.6: Types of nanocomposite structures: (a) conventional, (b) intercalated and (c) exfoliated¹¹. (Note: (a) layers number 500-1000, (b) layers number up to 1000 but can also tend toward a single figure depending on an extent of intercalation, and (c) individual layers loosened from 1000 sheets per single clay particle.)

Conventional composites: This type of composite contains clay tactoids, with the layers aggregated in an un-intercalated face-to-face form. In this case the clay tactoids are dispersed simply as a segregated phase, as illustrated in Fig. 2.6(a), and the polymer chains are unable to intercalate between the silicate sheets. In this case there is no change in the d-spacing of the clay, which is around 1.15 nm¹⁸. This results in the composites having poor mechanical properties^{7,11,12}.

Intercalated nanocomposites: Here the polymer is located in the clay galleries, expanding the clay structure, but retaining some long-distance register between the platelets. Only a

Theoretical background

few polymer chains penetrate in between clay galleries, as is illustrated in Fig. 2.6(b). This type of nanocomposite shows a slight improvement in mechanical and thermal properties relative to pure polymer^{7,12,24}. and has fire retardant properties⁴¹.

Exfoliated nanocomposites: This type of structure can be formed when all individual clay layers are fully separated from each other, and are no longer close enough to interact with one another. The average distances between the segregated layers are dependent on the clay loading, and they are evenly distributed throughout the polymer matrix. Exfoliated nanocomposites show greater homogeneity than intercalated nanocomposites^{7,11,24}.

Exfoliated polymer-clay nanocomposites improve mechanical performance. The homogeneous dispersion of clay into the polymer matrix provides an enormous surface area, and leads to a high interfacial area between platelets and the polymer matrix²⁴. This huge interfacial area leads to restrictions in free volume, chain mobility and conformation, relaxation behaviour, and thermal transitions⁴². Polymer chains that are close to the clay interface have lower free volume than the bulk polymer. This may begin to explain why nanocomposites have unusual properties, such as increased toughness with longer elongation, and improved barrier properties¹.

2.5 References

- (1) Giannelis, E. P.; Krishnamooti, R.; Manias, E. *Advances in Polymer Science* **1999**, *138*, 107 - 147.
- (2) Utracki, L. A. In *Polymer-Containing Polymeric Nanocomposites*; Rapra Technology Limited: U.K, 2004; Vol. 1, pp 1 - 430.
- (3) Messermith, P. B. *Journal of Materials Research* **1992**, *7*, 2599 - 2607.
- (4) Okada, A.; Usuki, A. *Journal of Materials Research* **1995**, *3*, 109 - 117.
- (5) Utracki, L. A.; Kamal, M. R. *The Arabian Journal for Science and Engineering*, **2002**, *27*, 43 - 67.
- (6) Giannelis, P. E. *Advanced Materials* **1996**, *8*, 29 - 40.
- (7) Lebaron, P. C.; Wang, Z.; Pinnavaia, T. J. *Applied Clay Science* **1999**, *15*, 11 - 29.
- (8) Jeon, H.; Jung, H.; Hudson, S. *Polymer Bulletin* **1998**, *41*, 107 - 113.
- (9) Carrado, K. A.; Xu, L. *Chemistry of Materials* **1998**, *10*, 1440 - 1445.
- (10) Noh, M. W.; Lee, D. C. *Polymer Bulletin* **1999**, *42*, 619 - 626.
- (11) Chen, B. *British Ceramic Transactions* **2004**, *6*, 241 - 249.
- (12) Choi, Y. S.; Xu, M.; Chung, I. J. *Polymer* **2003**, *44*, 6989 - 6994.
- (13) Ray, S.; Okamoto, M. *Progress in Polymer Science* **2003**, *28*, 1539 - 1641.
- (14) Nalwa, H. S. In *Encyclopedia of Nanoscience and Nanotechnology*; American Scientific Publishers: California, 2004; Vol. 8, pp 791 - 843.
- (15) Messermith, P. B.; Giannelis, E. P. *Journal of Polymer Science: Part A: Polymer Chemistry* **1995**, *33*, 1047 - 1057.
- (16) Gilman, J. W. *Applied Clay Science* **1999**, *15*, 31 - 49.
- (17) Yano, K.; Usuki, A.; Okada, A.; Kurachi, T.; Kamigaito, O. *Journal of Polymer Science: Part A: Polymer Chemistry* **1993**, *31*, 2493 - 2498.
- (18) Xu, M.; Choi, Y. S.; Kim, Y. K.; Wang, K. H.; Chung, I. J. *Polymer* **2003**, *44*, 6387 - 6395.
- (19) Fukushima, Y.; Inagaki, S. *Journal of Inclusion Phenomena and Macrocyclic Chemistry* **1987**, *5*, 473 - 482.
- (20) Xu, M.; Choi, Y. S.; Wang, K. H.; Kim, J. H.; Chung, I. *Macromolecules*

Theoretical background

- Research* **2003**, *11*, 410 - 417.
- (21) Shmuel, Y.; Harold, C. *Organo-Clay Complexes and Interactions*; Marcel Dekker, Inc: New York and Basel, 2002.
- (22) Lee, S.; Kim, J. *Journal of Polymer Science: Part B: Polymer Physics*, **2004**, *42*, 246 - 252.
- (23) Luckham, P. F.; Rossi, S. *Advances in Colloid and Interface Science* **1999**, *82*, 43 - 92.
- (24) Alexandre, M.; Dubois, P. *Materials Science and Engineering*, **2000**, *28*, 1 - 63.
- (25) Burnside, S. D.; Giannelis, E. P. *Chemistry of Materials* **1995**, *7*, 1597 - 1600.
- (26) Messersmith, P. B.; Giannelis, E. P. *Chemistry of Materials* **1994**, *6*, 1719 - 1725.
- (27) Rosorff, M. In *Nano Surface Chemistry*; Marcel Dekker Inc: New York and Basel, 2002; pp 653 - 673.
- (28) Meneghetti, P.; Qutubuddin, S. *Langmuir* **2003**, *20*, 3424 - 3430.
- (29) Choi, Y. S.; Chung, I. J. *Macromolecules Research* **2003**, *11*, 425 - 430.
- (30) Bergaya, F.; Lagaly, G. *Applied Clay Science* **2001**, *19*, 1 - 3.
- (31) Fischer, H. *Materials Science and Engineering* **2003**, *23*, 763 - 772.
- (32) Ranade, A.; Souza, N. D.; Thellen, C.; Ratto, J. *Polymer International* **2005**, *54*, 875 - 881.
- (33) Zhang, W. A.; Chen, D. Z.; Xu, H. Y.; Chen, X. F.; Fang, Y. E. *European Polymer Journal* **2003**, *39*, 2323 - 2328.
- (34) Xie, W.; Hwu, J.; George, J.; Thand, M.; Pan, W. P. *Polymer Engineering and Science* **2003**, *43*, 214 - 222.
- (35) Fischer, S. In *TNO Industrial Technology, Eindhoven, The Netherlands*.
- (36) Sadhu, S.; Bhowmick, A. K. *Journal of Applied Polymer Science* **2004**, *92*, 698 - 709.
- (37) Beall, G. W.; Goss, M. *Applied Clay Science* **2004**, *27*, 179 - 186.
- (38) Tahoun, S. A.; Mortland, M. M. *Soil Science* **1966**, *102*, 314 - 321.
- (39) Mortland, M. M. *Clay Minerals* **1966**, *6*, 143 - 156.
- (40) Stutzmann, T.; Siffert, B. *Clays and Clay Minerals* **1977**, *25*, 392 - 406.
- (41) Gilman, J. W.; Jackson, C. L.; Morgan, A. B.; Harris, R. *Chemistry of Materials* **2000**, *12*, 1866 - 1873.

Theoretical background

- (42) Froio, D.; Ziegler, D.; Orroth, C.; Thellen, C.; Lucciarini, J.; Ratto, J. A.
ANTEC 2004, 2422 - 2426.

Synthesis and characterization of nanocomposites: Theoretical background

3.1 Introduction

This chapter is divided in two main parts. The first presents a literature survey on the different methods that have been used to synthesis nanocomposite materials. Depending on the starting materials and synthesis techniques, the preparative methods used to synthesize nanocomposites are divided into four main groups: solution, melt blending, template, and in-situ intercalative polymerization. Section 3.2 introduces these methods and points out their respective advantages and disadvantages.

The second part of this chapter describes the characterization methods that are used to determine the structure and properties of nanocomposite materials. X-ray diffraction (XRD) and transmission electron microscopy (TEM) are the best methods for determining the types of nanocomposite structures (conventional, exfoliated or intercalated). Section 3.3 provides more details about these two techniques. Dynamic mechanical analysis (DMA) is used to determine the mechanical properties and thermogravimetric analysis (TGA) is used to determine the thermal stability of nanocomposites.

A review of the relationship between nanocomposite structures and their properties is presented in Section 3.3.

3.2 Methods used to synthesize polymer clay nanocomposites

The following methods are commonly used to synthesize nanocomposites materials:

3.2.1 Solution method

Here the organoclay and the polymer are dissolved in a polar organic solvent. The polymer chains migrate between the silicate layers. Due to the weak forces between the silicate layers, the solvent separates the layers, thereby allowing the polymer to adsorb

Theoretical background

onto the surfaces of individual silicate platelets. The solvent is then allowed evaporate, leaving nanocomposites behind. The final structure depends on the thermodynamics of the multi-component mixture and the rates of diffusion and adsorption of polymers into the silicate system ¹⁻³. A schematic representation of the solution method is shown in Fig. 3.1.

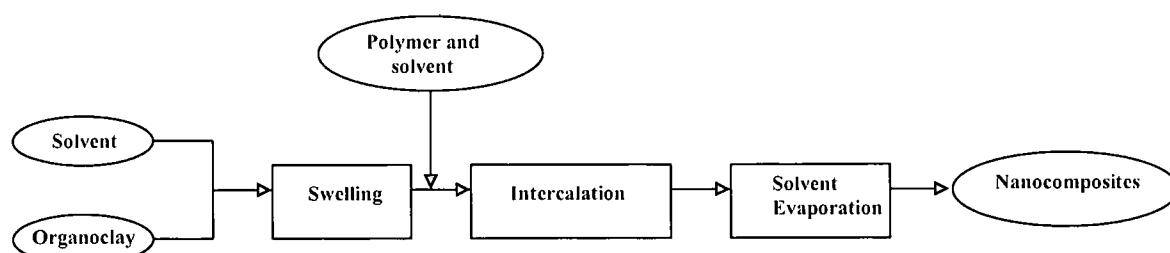


Fig. 3.1: Schematic representation of the preparation of nanocomposites via the solution method.

This route can be used to synthesize nanocomposites from polymers with little or no polarity. From a commercial point of view, however, this route involves the use of large quantities of organic solvents, which is environmentally unfriendly and economically prohibitive ^{3,4}. It is also believed that a small quantity of solvent remains in the final product at the polymer-clay interface, and this will lead to the creation of weaker interfacial interaction between the polymer and the clay surfaces ² and give later emissions problems.

Various polymer-clay nanocomposites, using polymers like poly(vinyl acetate) (PVA) ⁵, polyethylene (PE) ⁶, and poly(ethylene oxide) (PEO) ⁶, have been synthesized using this method.

Depending on the polymer matrix used, the solution method can be used to prepare different nanocomposite structures even if the experiments are carried out under similar conditions. Jeon *et al.* ⁶ synthesized two different types of nanocomposites: a nitrile-based copolymer and a polyethylene-based polymer. In the case of the nitrile-based copolymer partially exfoliated nanocomposites were obtained by dissolving the copolymer in dimethylformamide (DMF) in the presence of the modified clay, and then as the solvent was evaporated the nanocomposites were obtained. The completely exfoliated structure of a high-density polyethylene nanocomposite was obtained by using a similar technique, in which the polyolefin chains were dissolved in a mixture of xylene

Theoretical background

and benzonitrile. These two syntheses indicate that the solution method can provide quite different results, depending on the polymer matrix. In other words, it does mean that for every type of polymer one has to find a suitable layered clay, organic modifier and solvent.

The Toyota CRD group ⁷ investigated the effect of the types of clay on the structure and properties of polyamide nanocomposites synthesized with different types of clay via the solution method. Hectorite, saponite, montmorillonite and synthesized mica were used as pristine layered silicates. The cation exchange capacity (CEC) values of these four types were 55, 100, 110 and 119 meq/100g respectively. All were modified with dodecylammonium salt by a cation exchange reaction, and all nanocomposites were synthesized by the solution method under the same conditions. Exfoliated nanocomposites were obtained when montmorillonite and mica clay were used, while a partially exfoliated structure was obtained when hectorite and saponite were used. The reason for this could be due to the greater interaction between the polyamide matrix and the organoclay-modified montmorillonite or synthetic mica compared to the interaction between the polyamide matrix with the other types of clay ^{2,7}.

Although the solution method is widely used to synthesize nanocomposite materials there are some problems or disadvantages associated with this method. The presence of solvent leads to the generation of some competition between the solvent and polymer chains, reducing the possibility of polymer entering the clay galleries ⁸.

3.2.2 Melt blending synthesis

The melt blending process involves mixing the layered silicate, by annealing statically or under shear, with the polymer while heating the mixture above the softening point of the polymer. During the annealing process, the polymer chains diffuse from the bulk polymer melt into the galleries between the silicate layers ^{3,4,9-12}.

The technique of melt blending is particularly attractive due to its versatility and compatibility with existing processing infrastructure and is beginning to be used for commercial applications ¹³. The structure of nanocomposites formed via polymer melt intercalation depends upon the thermodynamic interaction between the polymer and the

Theoretical background

silicate as well as the transportation of polymer chains from the bulk melt into the silicate interlayer¹⁴.

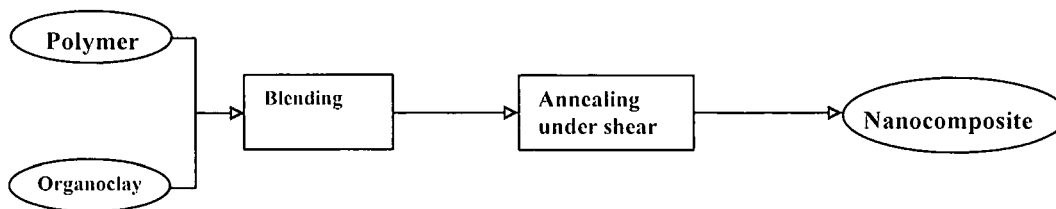


Fig. 3.2: Schematic representation of the preparation of nanocomposites via the melt blending method.

Vaia *et al.*¹⁵ used the direct polymer melt method to form intercalated poly(ethylene oxide) by heating the polymer and silicate together at 80°C for 6 h. Other polymer exfoliated nanocomposites such as polystyrene¹⁵, polyamides, polyesters, polycarbonate, polyphosphazene and polysiloxanes can also be synthesized by this method¹.

Morgan and Gilman¹⁶ synthesized polystyrene-layered silicate nanocomposites using melt intercalation by two different methods: (a) static melt intercalation by mixing and grinding dried powders of polystyrene and modified clay in a pestle and mortar and then heating the mixture at 170°C in vacuum, and (b) extrusion melt intercalation by extrusion of the mixture under nitrogen.

Vaia *et al.*¹⁷ prepared an intercalated polystyrene nanocomposite via polymer melt intercalation. The organoclay was produced by treating the clay using long-chain primary and quaternary alkylammonium-exchanged clays. The organoclay was mixed with commercially available PS at a temperature above the T_g , via melt processing. The diffusion of PS into the clay galleries is slow, and depends on many factors, including polymer molecular weight, processing temperature, surfactant properties, and interactions between the polymer and the organoclay.

Hasegawa *et al.*¹⁸ used polystyrene of different molecular weights to prepare nanocomposites by melt intercalation. An exfoliated structure was obtained only with applied shear during melt compounding of the clay modified with PS of high \bar{M}_w . This result means that the mechanical driving force is important for the exfoliation of clay in a polymer melt.

Theoretical background

The direct melt intercalation of polypropylene and polyethylene in the silicate galleries seemed to be impossible due to the absence of polar groups in their backbones^{3,19-22}. This problem was however overcome when Usuki *et al.*²³ used PP modified with polar groups for intercalation into clay galleries, followed by melt-compounding of organoclay with bulk polypropylene to prepare nanocomposites. Only a limited degree of clay exfoliation was achieved by this method.

The use of the melt intercalation method to synthesize nanocomposite materials is limited due to the following²⁴.

- During high-temperature processing the low thermal stability of the clay modifier leads to a decrease in the distance between clay sheets due to degradation of the clay modifier during processing. This also leads to a loss in hydrophobicity of the clay surface, and it becomes hydrophilic again^{25,26}. This was confirmed by Park *et al.*²⁷ who discovered that the interlayer distance of clay galleries decreased as the temperature increased to 200-280°C due to degradation of surfactant in the clay gallery, which leads to interruption of intercalation between polymer and the clay.
- This method seems unsuitable for producing certain polymers, such as amorphous polystyrene, even though polystyrene can be intercalated into the clay via weak interaction between the phenyl group of polystyrene and the clay surface. Upon heating, this interaction becomes weaker between polystyrene and clay and leads to a decrease in the interlayer spacing²⁸.

3.2.3 Template method

This method is useful for water soluble monomers or polymers. Some success has been achieved with polymers such as poly(vinylpyrrolidone) (PVPyr), poly(acrylonitrile) (PAN), poly(dimethyldiallylammonium) (PDDA) and poly(aniline) (PANI)³. This method is based on directly crystallizing silicate clays hydrothermally from a gel containing organics and organometallics, including polymers⁸.

The typical method for in situ hydrothermal crystallization of the polymer-hectorite clays

Theoretical background

involves creating a 2 wt% gel of silica sol, magnesium hydroxide sol, lithium fluoride, and polymer in water. This method is used with water soluble polymers, and refluxing is typically carried out for 2 days⁸. The selected modifiers are usually positively charged, to encourage incorporation into the gallery space via electrostatic interaction. By using this method the layered silicate can be highly dispersed in a one-step process^{3,8}. This method is far less well developed for layered silicates and thus is of no significance in the present study.

3.2.4 In-situ intercalative polymerization

A schematic representation of the in situ intercalative process is shown in Fig. 3.3. In this method the layered silicate is swollen within the liquid monomer or monomer solution so the polymer formation can occur between the intercalated sheets. Polymerization can be initiated either by heat or radiation, by the diffusion of a suitable initiator, or by an organic initiator^{2,3,10,29-32}.

As in other synthesis methods, the compatibility between monomers and modified clay is important here in order to obtain a high dispersion of silicate layers in the polymer matrix²⁴.

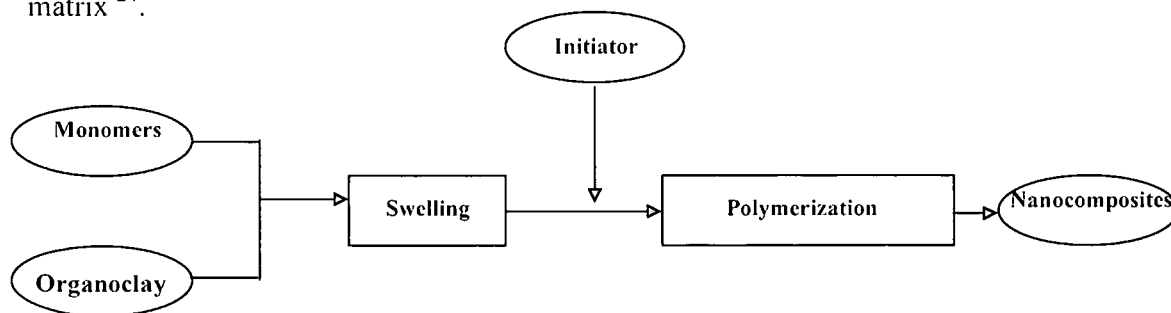


Fig. 3.3: Schematic representation of the preparation of nanocomposites via in-situ polymerization.

In the case of using a monomer solution, the polarity of the solvent has a significant effect. In order to ensure a high monomer concentration inside the clay galleries, the solvent should have the ability to interact with the polar surface of the clay. Akelah and Moet³³ modified Na⁺-MMT and Ca²⁺-MMT using (vinyl benzyl) trimethyl ammonium chloride, then the modified clay was dispersed in three different solvents, acetonitrile, acetonitrile/toluene and acetonitrile/THF. Styrene was added to the dispersed clay and polymerized. They obtained an intercalated structure with different interlayer distances,

Theoretical background

depending on the solvent used. Acetonitrile was found to be the best solvent.

Wang *et al.*³⁴ prepared polymer-clay nanocomposites of styrene and methyl methacrylate via bulk, solution, suspension and emulsion polymerizations. They then characterized them to determine what, if any, effects there were on the nanocomposites structures for each mode of preparation. Two organic compounds were used to modify the clay: one contained a double bond and the other had no double bond. When the organic treatment applied to the clay incorporated a polymerizable double bond, the possibility to obtain an exfoliated structure increased. The technique used to synthesize nanocomposites has a large effect on the type of materials that may be obtained. Solution polymerization of both styrene and methyl methacrylate in the presence of clay containing a double bond or one without a double bond yields only an intercalated structure. Emulsion, suspension and bulk polymerization can yield both intercalated and exfoliated nanocomposites depending on the organic compounds used to modify the clay³⁴.

3.2.4.1 Preparation of nanocomposites using emulsion free radical polymerization

Emulsion polymerization has been successfully used for the synthesis of nanocomposites for many polymers, such as polystyrene^{30,31,35,36}, poly(methyl methacrylate)^{36,37}, polyacrylonitrile, epoxy³⁸, poly(styrene-co-methyl methacrylate)³⁹, poly(n-butyl acrylate-co-methyl methacrylate)⁴⁰ and poly(n-butyl acrylate-co-styrene)⁴⁰.

Use of an emulsion polymerization technique to prepare polymer-clay nanocomposites has several advantages^{31,39}. One of the most important advantages is that water is used as the dispersion medium. Water makes the galleries of layered silicates wide without any chemical treatment³⁹. Na⁺-MMT clay swells due to the presence of hydration water molecules around the inorganic cations (Na⁺)⁴¹, and this leads to insertion of micelles into the galleries of the layered silicate³¹. However, in the presence of a limited amount of water, Na⁺-MMT forms gels that contain isolated silicate layers and aggregates of several layers. Therefore, reducing the size of aggregated Na⁺-MMT before the polymerization reaction is an essential requirement to allow the homogeneous dispersion of clay particles in the aqueous medium of an emulsion system³¹.

The polarity of monomers has a large effect on the final nanocomposite products⁴². Choi

Theoretical background

and Chung⁴⁰ studied the effect of a monomer's polarity on the basal spacing of silicate layers and on the morphology of the final nanocomposite products. They synthesised poly(n-butylacrylate-co-methyl methacrylate) [P(BA-co-MMA)]/silicate nanocomposites and poly(n-butylacrylate-co-styrene) [P(BA-co-ST)]/silicate nanocomposites by conventional emulsion polymerization. The [P(BA-co-MMA)] nanocomposites showed an exfoliated structure, while the [P(BA-co-ST)] nanocomposites had the intercalated structure. This could be due to the higher polarity of both of the BA/MMA comonomers compared to that of the BA/ST comonomers. The monomer with high polarity makes the basal spacing of silicate layers wide, and the degree of expansion of the silicate layer space by monomers affects the resultant morphology of the copolymer/silicate nanocomposite, causing the exfoliated structure of P(BA-co-MMT) and the intercalated structure of P(BA-co-ST).

Expansion of basal spacing of silicate layers is important for polymer/silicate nanocomposites prepared by in-situ polymerization, since at least two polymerization sites will consume monomers competitively: one is inside the silicate layers including the surface, and the second is outside silicate layers (reaction medium). If the polymerization rate outside the silicate layers is so fast so as to cause most of the monomer to be consumed, then the polymerization rate inside the silicate layers will decrease because the polymerization rate is proportional to the monomer concentration. The monomer concentration inside clay galleries depends on the degree of expansion of basal spacing of silicate; as the expansion of basal spacing was high; the concentration of monomers inside clay galleries becomes high. In this case more polymerization occurs inside clay galleries, and improves the chance of obtaining exfoliated nanocomposites. The basal spacing of silicate before polymerization is therefore an important parameter for predicting the structure of nanocomposites materials⁴⁰.

In addition to the effect of monomer polarity on the morphology of nanocomposites, the monomer composition could play an important role in the synthesis of exfoliated structures by in-situ polymerization. Choi *et al.*⁴³ investigated the relationship between the composition of monomers and the resultant morphology of the composites using Na⁺-MMT. They synthesized two types of poly(styrene-co-acrylonitrile), SAN (I) and

Theoretical background

SAN (II) /silicate nanocomposites, via emulsion polymerization. SAN (I) was synthesized with acrylonitrile in the initial stage, after which a mixture of styrene and acrylonitrile was added in the second stage, while SAN (II) was prepared with a mixture of styrene and acrylonitrile in a polymerization reaction. An exfoliated structure was obtained with SAN (I), while an intercalated structure was achieved with SAN (II).

In general in-situ intercalative polymerization relies on a suitable choice of the organic modifier and the type of clay. The practical advantages of this method are that the silicate can be used without modification⁴³ and it is simple to vary the silicate loading.

The low viscosity and small size of the monomers, compared to polymers, makes them penetrate more easily inside the galleries of silicate layers. Another advantage of in-situ intercalative polymerization, is that the silicate is combined with polymer at room temperature⁴⁴, which reduces the problem of polymer degradation during the process, and no decomposition of surfactants takes place. Minimal quantities of solvents are used (in cases where monomer solutions are used) as opposed to very dilute solutions used for the solution technique⁴⁵.

3.3 Characterization of the structure of the nanocomposites

Three different nanocomposites structures can be distinguished, depending on the ordering and the dispersion of clay layers inside the polymer matrix, namely conventional, intercalated and exfoliated³⁹.

The techniques most commonly used for characterization of the nanocomposite structures are X-ray diffraction and transmission electron microscopy⁴⁶.

3.3.1 X-ray diffraction

X-ray diffraction allows the determination of the space between structural layers of silicate (the distance between the basal layers of the MMT clay, or of any layered material) by using Bragg's law

$$n\lambda = 2d \sin \theta \quad 3.1$$

where λ corresponds to the wavelength of the X-ray radiation used in the diffraction

Theoretical background

experiment, d is the spacing between diffractive lattice planes and θ is the measured diffraction angle⁴⁷.

Intercalation and exfoliation change the dimensions of gaps between the silicate layers, so an increase in layer distance indicates that a nanocomposite has formed. A reduction in diffraction angle value corresponds to an increase in the silicate layer distance⁴⁸. X-ray diffraction has been used to look at changes in d -spacings when nanocomposite materials are prepared. The d -spacing observed by XRD for nanocomposite materials has been used to describe the nanoscale dispersion of the clay in the polymer⁴⁹. Fig. 3.4 below shows X-ray patterns of three layered silicate structures³.

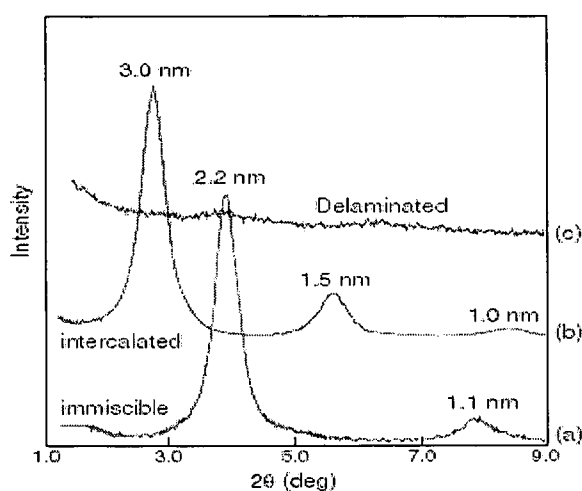


Fig. 3.4: X-Ray patterns of three layered silicates structures: (a) conventional, (b) intercalated, (c) exfoliated³.

Conventional (immiscible) materials exhibit no change in d -spacing, meaning that no polymer has entered the gallery and that the spacing between clay layers is unchanged. *Intercalated* nanocomposites have an increased d -spacing, indicating that polymer has entered the gallery, expanding the layers. *Exfoliated* (delaminated) materials show no XRD peak, suggesting that a great amount of polymer has entered the gallery space and disorder of plates^{2,16,35,39,49}.

Although XRD is a most useful technique for measuring the d -spacing of ordered immiscible and ordered intercalated nanocomposites^{2,50} it may be insufficient for the measurement of disordered and exfoliated materials that give no XRD peaks. More specifically, the absence of a peak may be misinterpreted in cases where no

Theoretical background

peak is seen ^{46,50}.

Many factors, such as concentration and order of the clay, can influence the XRD patterns of layered silicates ⁵⁰. For example, samples in which the clay is not well ordered will fail to produce a Bragg diffraction peak, and that is an incorrect conclusion of the data. It is not the fault of the technique that leads to the incorrect conclusion of a nanocomposite being exfoliated when in reality it is highly disordered. Therefore, the lack of a peak obtained during XRD analysis does not prove, or disprove, the existence of exfoliated clay plates in the nanocomposite. More specifically, XRD only describes the relationship between clay layers in the polymer, not the relationship of the clay to the polymer ¹⁶.

3.3.2 Transmission electron microscopy

TEM is a very powerful tool for the analysis of polymer-clay nanocomposites as it can qualitatively describe how the layered silicate is dispersed in the polymer. When nanocomposites have formed, the intersections of the silicate sheets are seen as dark lines, which are the cross-sections of the silicate layers ^{2,3,16}.

Although TEM is a technique that gives a clear picture of the morphology of the nanocomposite, good sample preparation techniques for TEM are important. Very thin cross-sections (40-50 nm) of the nanocomposite are required to get a good quality image. For this reason the nanocomposite needs to be microtomed. There are also problems with TEM micrographs when the arrangement of silicate layers are not in the edge-on position; the comparison between adjacent silicate layers is altered, and thus the silicate layers can not be properly distinguished by TEM ⁴⁶.

3.4 Determination of the properties of nanocomposites

The incorporation of layered silicates in a polymer matrix has lead to improvements in the properties of polymers in which they are dispersed ^{2,3,32}. Amongst those properties, an expected large increase in modulus (tensile or Young's modulus and flexural modulus) of nanocomposites with filler contents sometimes as low as 1 wt% has drawn much attention ^{51,52}. Improvements in thermal stability and fire retardancy are other interesting

Theoretical background

properties displayed by nanocomposites. PCNs have also been studied and used for their superior barrier properties against gas and vapour transmission. Finally, depending on the type of polymeric materials, nanocomposites can also display interesting properties in the terms of ionic conductivity or thermal expansion.

The following sections describe how the presence of clay particles in a polymer matrix can affect the thermal and mechanical properties of polymers.

3.4.1 Thermal stability

Thermogravimetric analysis is used primarily for determining the thermal stability of a polymer. TGA is an old technique but has been applied to polymers only since the 1960s⁵³. The most widely used TGA method is based on continuous measurement of weight on a sensitive balance (thermobalance) as the sample temperature is increased in air or an inert atmosphere. This is referred as non-isothermal TGA. Data are recorded as thermograms of weight versus temperature.

Weight loss may arise from evaporation of residual moisture or solvent, but at higher temperatures it results from polymer decomposition. Besides providing information on thermal stability, TGA may be used to characterize polymers through loss of a known entity, such as HCl from vinyl chloride. TGA is also useful for determining volatilities of plasticizers and other additives⁵³.

In general, PCNs show improved thermal stability relative to the pristine polymers, regardless of the experimental environment^{53,54}. Generally, the incorporation of silicate in the polymer matrix enhances the thermal stability by acting as a superior insulator and mass transport barrier to the volatile products generated during decomposition⁴.

The improvement in thermal stability of polymer clay nanocomposites was first reported by Blumstein⁵⁵ when he studied the thermal stability of polymethylmethacrylate (PMMA) and montmorillonite clay. He showed that when PMMA was inserted between lamellae of montmorillonite clay the thermal degradation was increased under conditions that would otherwise degrade pure PMMA. He proposed that the stability of the PMMA-nanocomposites is due not only to its structure, but also to restricted thermal

Theoretical background

motion of the PMMA in the gallery. Very small amounts of clay are required for an improvement in thermal stability relative to the pristine polymers⁵⁶.

Doh and Cho⁵⁷ observed that the maximum thermal stability of their intercalated polystyrene-clay nanocomposites was achieved when only 0.3 wt% clay was used. They used dimethylbenzyl octadecyl ammonium-modified MMT clay.

Xu *et al.*³⁹ synthesized poly(styrene-co-methylmethacrylate) using 2-acrylamido-2-methyl-1-propanesulphonic acid (AMPS) as clay modifier. TGA results showed that as the clay content increased, the onset temperature of thermal decomposition of the nanocomposite moved slightly towards a higher temperature. They also found that the exfoliated nanocomposite with 3 wt% silicate showed a 7°C increase in decomposition temperature at 20% weight loss. This may result from the thermal barrier property of the clay plates.

TGA results were found to be environment dependent. Poly(ethylene-co-vinyl acetate) synthesized by melt intercalation showed better thermal stability in a nitrogen environment relative to air, and the thermal stability increased with an increasing amount of clay. In air, the nanocomposites showed a significant delay of weight loss, maybe due to the barrier effect to diffusion of both the volatile thermo-oxidation products and oxygen from the gas phase to polymer⁴.

When nanocomposites are utilized in high-temperature applications, the low thermal stability of the surfactants, which are usually used to render the layered silicates organophilic, can be a limiting factor. Zhang *et al.*⁵⁸ used three surfmer-modified clays and a non-reactive surfactant-modified clay to prepare polystyrene-clay nanocomposites and discovered that surfmer-based nanocomposites had superior thermal stability relative to non-reactive surfactant-based nanocomposites.

The organoclay has two opposing functions affecting the thermal stability of the polymer-clay nanocomposite. One is its barrier effect, which should improve the thermal stability, and the other is the catalytic effect towards the degradation of the polymer matrix which decreases the thermal stability. When adding a low fraction of clay to the polymer matrix, the clay layers should be well dispersed. The barrier effect is predominant, but with

Theoretical background

increasing loading the catalyzing effect rapidly increases and becomes dominant, so that the thermal stability of the nanocomposite decreases⁵⁸.

The clay acts as a heat barrier, which enhances the overall thermal stability of the system, as well as assists in the formation of char after thermal decomposition. In the early stages of thermal decomposition the clay shifts the decomposition to higher temperatures. After that, this heat barrier effect results in a reverse thermal stability. In other words, the stacked silicate layers can hold accumulated heat, which can be used as a heat source to accelerate the decomposition process, in conjunction with the heat flow supplied by the outside heat source^{4,32}.

Exfoliated structures have hugely improved thermal properties compared to conventional and intercalated materials, due to the homogeneous dispersion of the clay layers through the polymer matrix and the high surface area of clay layers⁵⁹.

3.4.2 Dynamic mechanical analysis

Dynamic mechanical analysis measures the response of a material to cyclic deformation as a function of temperature. There are three main parameters that are used to express DMA results: (i) the storage modulus (G^I), which is a measure of elastic response to the deformation; (ii) the loss modulus (G^{II}), which is a measure of the plastic response, and (iii) $\tan \delta$, i.e. the ratio of G^{II}/G^I . $\tan \delta$ can be used for the determination of energy absorption through molecular mobility after the glass transition temperature (T_g)³², which can be measured.

DMA not only measures the dynamic mechanical properties of a material, but also detects changes in the viscoelastic behaviour of a polymer after it is compounded with other materials. It is well known that the T_g of a polymer depends on the onset of the mobility of chain segments of the polymer molecules⁶⁰.

If the molecular chain is restricted then the motion or relaxation of the chain segment becomes difficult at the original glass transition temperature but becomes possible at higher temperatures. When the polymer molecules are intercalated in the silicate gallery or the silicate layer is partially exfoliated in the polymer matrix, the chain conformations

Theoretical background

of the polymer molecules will not readily change because of geometric constraints and hence the interactions between the polymer and the surface of the silicate layers become stronger. Therefore, the dynamic behaviour of PCNs is different from that of pure polymer. Sluggish motions of chain segments of polymer molecules increase the T_g of nanocomposites, which means that the systems become similar to cross-linked polymer systems⁶¹.

The interaction between polymer and silicate layers at the interface of layers and the polymer matrix can suppress the mobility in the polymer segments in or near the interface, leading to improved mechanical properties. In general, higher G' values for nanocomposites below the T_g (i.e. glassy state) and in the rubbery region, relative to pristine polymers and conventional composites, are obtained. This can be attributed to the large aspect ratio of the structural hierarchy on the nanoscale level. The incorporation of small quantities of polar comonomers during the synthesis of PCNs not only affects the resultant nanocomposite structure, but the mechanical properties as well^{32,62}.

Choi *et al.*⁴³ synthesized exfoliated and intercalated poly(styrene-co-acrylonitrile) copolymer nanocomposites using AMPS as clay modifier. They found interesting results in terms of mechanical properties of nanocomposites. The exfoliated poly(styrene-co-acrylonitrile) has higher storage modulus than the intercalated structure. They also found that the T_g values for exfoliated nanocomposites increased with the content of silicate, but the intercalated nanocomposites had lower T_g values than pure poly(styrene-co-acrylonitrile). They suggested that the decrease in glass transition temperature for intercalated structures was related to the molecular weight distribution of the polymer matrix. A polymer with broad molecular weight distribution may contain a low molecular weight portion, and the low molecular weight materials will reduce the glass transition temperature in a manner like plasticizers or lubricants.

Qutubuddin and Fu⁶³ synthesized fully exfoliated polystyrene using vinylbenzyltrimethylammonium as clay modifier. They found a decrease in T_g from 100°C in the pure polymer to 94°C in the polystyrene nanocomposite containing 7.6% clay. They interpreted this decrease in T_g to be related to a decrease in molecular weight resulting from hindered diffusion of the polymerization initiator (hindered by the

Theoretical background

high viscosity of the styrene-swelled clay), giving faster termination, as well as the restricted propagation of styrene chains by the impervious clay platelets.

Xu *et al.*⁵⁹ synthesized exfoliated poly(methyl methacrylate-co-acrylonitrile) nanocomposites via emulsion polymerization using AMPS as clay modifier. They found that nanocomposites with 20 wt% clay showed up to 163% increase in storage modulus relative to the neat copolymer. The Young's modulus of nanocomposites was also higher than that of the neat copolymer. Young's modulus increased steadily as the silicate content increased, due to the exfoliated structure at high clay content.

3.5 References

- (1) Yano, K.; Usuki, A.; Okada, A.; Kurachi, T.; Kamigaito, O. *Journal of Polymer Science: Part A: Polymer Chemistry* **1993**, *31*, 2493 - 2498.
- (2) Ray, S.; Okamoto, M. *Progress in Polymer Science* **2003**, *28*, 1539 - 1641.
- (3) Alexandre, M.; Dubois, P. *Materials Science and Engineering*, **2000**, *28*, 1 - 63.
- (4) Okamoto, M. *Rapra review reports* **2003**, *14*, 1 - 40.
- (5) Strawhecker, K.; Manias, E. *Chemistry of Materials* **2000**, *12*, 2943 - 2949.
- (6) Jeon, H.; Jung, H.; Hudson, S. *Polymer Bulletin* **1998**, *41*, 107 - 113.
- (7) Lan, T.; Admananda, D. P.; Kaviratna, P. D.; Pinnavaia, T. J. *Chemistry of Materials* **1994**, *6*, 573 - 575.
- (8) Carrado, K. A.; Xu, L. *Chemistry of Materials* **1998**, *10*, 1440 - 1445.
- (9) Manias, E.; Chen, H.; Krishnamooti, R.; Genzer, J.; Kramer, E. J.; Giannelis, E. *P. Macromolecules* **2000**, *33*, 7955 - 7966.
- (10) Lebaron, P. C.; Wang, Z.; Pinnavaia, T. J. *Applied Clay Science* **1999**, *15*, 11 - 29.
- (11) Vaia, R.; Jandt, K. D.; Kramer, E. J.; Giannelis, E. P. *Chemistry of Materials* **1996**, *8*, 2628 - 2635.
- (12) Giannelis, P. E. *Advanced Materials* **1996**, *8*, 29 - 40.
- (13) Fornes, T. D.; Yoon, P. J.; Hunter, D. L.; Keskkula, H.; Paul, D. R. *Polymer* **2002**, *43*, 5915 - 5933.
- (14) Huang, J.; Zhu, Z.; Yin, J.; Qian, X.; Sun, Y. *Polymer* **2001**, *42*, 873 - 877.
- (15) Vaia, R.; Ishii, H.; Giannelis, E. P. *Chemistry of Materials* **1993**, *5*, 1694 - 1696.
- (16) Morgan, A. B.; Gilman, J. W. *Journal of Applied Polymer Science*, **2002**, *87*, 1329 - 1338.
- (17) Vaia, R. A.; Jandt, K. D.; Kramer, E. J.; Giannelis, E. P. *Chemistry of Materials* **1996**, *8*, 2628 - 2635.
- (18) Hasegawa, N.; Okamoto, H.; Kawasumi, M.; Usuki, A. *Journal of Applied Polymer Science* **1999**, *74*, 3359 - 3364.
- (19) Kaempfer, D.; Thomann, R.; Mulhaupt, R. *Polymer* **2002**, *43*, 2909 - 2916.
- (20) Kawasumi, M.; Hasegawa, N.; Kato, K.; Usuki, A.; Okada, A. *Macromolecules*

Theoretical background

- 1997, 30, 6333 - 6338.
- (21) Huang, X.; Lewis, S.; Brittain, W. J. *Macromolecules* **2000**, 33, 2000 - 2004.
- (22) Liu, X.; Wu, Q. *Polymer* **2001**, 42, 10013 - 10019.
- (23) Usuki, A.; Okada, A.; Kurachi, T. *Journal of Applied Polymer Science* **1997**, 63, 137 -139.
- (24) Nam, P. H.; Maiti, P.; Okamoto, M.; Kotaka, T.; Hasegawa, N.; Usuki, A. *Polymer* **2001**, 42, 9633 - 9640.
- (25) Gilman, J.; Awad, W.; Davis, R.; Shields, J.; Harris, R.; Davis, C.; Morgan, A.; Sutto, T.; Callahan, J.; Trulove, P.; Delong, H. *Chemistry of Materials* **2002**, 14, 3776 - 3785.
- (26) Xie, W.; Xie, R.; Pan, W.; Hunter, D.; Koene, B.; Tan, L.; Vaia, R. *Chemistry of Materials* **2002**, 14, 4837 - 4845.
- (27) Park, C. I.; Park, O. O.; Lim, J. G.; Kim, H. J. *Polymer* **2001**, 42, 7465 -7475.
- (28) Gilman, J. W. *Applied Clay Science* **1999**, 15, 31 - 49.
- (29) Rosorff, M. In *Nano Surface Chemistry*; Marcel Dekker Inc: New York and Basel, 2002; pp 653 - 673.
- (30) Qutubuddin, S.; Tajuddin, Y. *Polymer Bulletin* **2002**, 48, 143 -149.
- (31) Noh, M. W.; Lee, D. C. *Polymer Bulletin* **1999**, 42, 619 - 626.
- (32) Nalwa, H. S. In *Encyclopedia of Nanoscience and Nanotechnology*; American Scientific Publishers: California, 2004; Vol. 8, pp 791 - 843.
- (33) Akelah, A.; Moet, A. *Journal of Materials Science* **1996**, 31, 3589 - 3596.
- (34) Wang, D.; Zhu, J.; Yao, Q.; Wilkie, C. A. *Chemistry of Materials* **2002**, 14, 3837 - 3843.
- (35) Kim, Y. K.; Choi, Y. S.; Wang, K. H.; Chung, I. J. *Chemistry of Materials* **2002**, 14, 4990 - 4995.
- (36) Zeng, C.; Lee, L. J. *Macromolecules* **2001**, 34, 4098 - 4103.
- (37) Huang, X.; Brittain, W. J. *Macromolecules* **2001**, 34, 3255 - 3260.
- (38) Lee, D. C.; Jang, L. W. *Journal of Applied Polymer Science* **1997**, 68, 1997-2005.
- (39) Xu, M.; Choi, Y. S.; Kim, Y. K.; Wang, K. H.; Chung, I. J. *Polymer* **2003**, 44, 6387 - 6395.
- (40) Choi, Y. S.; Chung, I. J. *Macromolecules Research* **2003**, 11, 425 - 430.

Theoretical background

- (41) Yariv, S.; Cross, H. *Organo-Clay Complexes and Interactions*; Marcel Dekker, Inc: New York and Basel, 2002.
- (42) Jang, B. N.; Wang, D.; Wilkie, C. A. *Macromolecules* **2005**, *38*, 6533 - 6543.
- (43) Choi, Y. S.; Xu, M.; Chung, I. J. *Polymer* **2003**, *44*, 6989 - 6994.
- (44) Choi, Y. S.; Ham, H. T.; Chung, I. J. *Polymer* **2003**, *44*, 8147 - 8154.
- (45) Sadhu, S.; Bhowmick, A. K. *Journal of Applied Polymer Science* **2004**, *92*, 698 - 709.
- (46) Causin, V.; Mareigo, C.; Ferrara, G. *Polymer* **2005**, *46*, 9533 - 9537.
- (47) Ginnelis, P. E. *Advanced Materials* **1996**, *8*, 29 - 40.
- (48) Poreter, D.; Metcalfe, E.; Tomas, M. J. K. *Fire and Materials* **2000**, *24*, 45 - 52.
- (49) Haraguchi, K.; Jun, H.; Matsuda, K.; Takehisa, T.; Elliott, E. *Macromolecules* **2005**, *38*, 3482 - 3490.
- (50) Morgan, A. B.; Gilman, J. W. *Journal of Applied Polymer Science* **2003**, *87*, 1329 - 1338.
- (51) Wang, H.; Chang, K.; Chu, H. *Polymer International* **2005**, *54*, 114 - 119.
- (52) Luckham, P. F.; Rossi, S. *Advances in Colloid and Interface Science* **1999**, *82*, 43 - 92.
- (53) Stevens, M. P. *Polymer chemistry : An introduction*; Oxford University Press: New York, 1990.
- (54) Jang, B. N.; Wilkie, C. A. *Polymer* **2005**, *46*, 9702 - 9713.
- (55) Blumstein, A. *Journal of Polymer Science: Part A: Polymer Chemistry* **1965**, *3*, 2653 - 2661.
- (56) Gilman, J. W.; Jackson, C. L.; Morgan, A. B.; Harris, R. *Chemistry of Materials* **2000**, *12*, 1866 - 1873.
- (57) Doh, J. H.; Cho, I. *Polymer Bulletin* **1998**, *41*, 511 - 519.
- (58) Zhang, W. A.; Chen, D. Z.; Xu, H. Y.; Chen, X. F.; Fang, Y. E. *European Polymer Journal* **2003**, *39*, 2323 - 2328.
- (59) Xu, M.; Choi, Y. S.; Wang, K. H.; Kim, J. H.; Chung, I. *Macromolecules Research* **2003**, *11*, 410 - 417.
- (60) Kanapitsas, A.; Pissip, P.; Kotsilkova, R. *Journal of Non-Crystalline Solids* **2002**, *305*, 204 - 211.

Theoretical background

- (61) Zhang, Y.; Lee, J.; Jang, H.; Nah, C. *Composites: Part B* **2004**, *35*, 133 - 138.
- (62) Manias, E.; Chen, H.; Krishnamooti, R.; Genzer, J.; Kramer, E. J.; Giannelis, E. *P. Macromolecules* **2002**, *33*, 7955 - 7966.
- (63) Qutubuddin, S.; Fu, X. *Polymer* **2001**, *42*, 807 - 813.

Experimental

4.1 Introduction

This chapter is divided to two parts. The first part describes the treatment of the surface of Na⁺-MMT with the following four different organic compounds to form organoclays: 2-Acrylamido-2-methyl-1-propanesulphonic acid, sodium 1-allyloxy-2-hydroxypropyl sulphonate (Cops), N-isopropylacrylamide (NIPA), and methacryloyloxyundecan-1-yl sulphate (MET).

The various organoclays were characterized using FT-IR, SAXS, and TGA.

The second part of this chapter describes the synthesis of poly(styrene-co-butylacrylate) nanocomposites by batch and semi-batch free radical polymerization in emulsion.

The structures and properties of the nanocomposite were characterized using SAXS, TEM, SEM, TGA, DMA and GPC.

4.2 Materials

The following materials were used to treat the surface of Na⁺-MMT and for the synthesis of poly(styrene-co-butylacrylate) nanocomposites.

Sodium montmorillonite clay (Na⁺-MMT) was obtained from Southern Clay Products, Inc. (U.S.A). It is a fine powder with an average particle size of less than 13 μm³ by volume in the dry state, and has a cation exchange capacity of 92.6-meq/100g clay. 2-acrylamido-2-methyl-1-propanesulphonic acid was obtained from Aldrich. Sodium 1-allyloxy-2-hydroxypropyl sulphonate was obtained from Rhodia. N-isopropylacrylamide was obtained from Aldrich.

Stabilized styrene and butylacrylate monomers were obtained from Aldrich. The stabilizers were removed from these monomers by washing three times with 3% potassium hydroxide solution and then purifying by distillation under reduced pressure at

Experimental

30°C. Sodium dodecyl benzenesulphonate (SDBS), and 4,4-azobis (4-cyanovaleric acid) were obtained from Fluka and used as received.

4.3 Modification of Na⁺-MMT with various compounds

Modification of Na⁺-MMT by AMPS

Na⁺-MMT (2 g) was introduced to a 250-ml flask containing 150 g deionised water. The mixture was stirred at room temperature until the aggregation of the clay in the deionised water was no longer observed. Various quantities of AMPS (0.945, 0.383, 0.287, 0.191 and 0.095g) were added to the mixture, which most then stirred for an additional 24 h, because after 24h of stirring, the most AMPS would enter onto clay even if the mixture was stirred more then 24h ((see Appendix A: Fig. 1 (A)).

AMPS-MMT samples were separated from the water by centrifugation of the mixture at 4400 rpm (for 30 min). They were redispersed in 100 ml of deionised water to remove any unadsorbed AMPS. This procedure was repeated five times, until the washing water was free of AMPS. This was confirmed by measuring the pH of the centrifuged water. After the washing, the pH was found to be similar to that of the dispersion clay without AMPS, i.e.10.5. The silicate cakes were dried in a vacuum oven for three days at 85°C.

The modifications of Na⁺-MMT using Cops, NIPA and MET were carried out under similar conditions used to modify the clay using AMPS.

4.4 Functionalization of Na⁺-MMT by AMPS at different pH values

Keeping all the other parameters constant, the modification of Na⁺-MMT using AMPS was then carried out at room temperature at different pH values, namely 0.63, 1.18, 2.8, 3.5 and 6.0. This enabled the author to investigate the effect of pH on the interaction between AMPS and Na⁺-MMT. Different samples of AMPS-MMT were prepared with the same amounts of clay and the same amounts of AMPS, at different pH values. Na⁺-MMT (2 g) was dispersed in 150 ml deionised water, and the dispersion was stirred vigorously overnight. AMPS (25% relative to CEC of the clay) was dissolved in 50 ml deionised water, and the AMPS solution was added slowly to the clay suspension. The pH of the mixture was 2.8. Samples with pH below 2.8 were prepared by adding 0.1 M

Experimental

HCl, while the samples with pH above the 2.8 were prepared using 0.1 M NaOH solution. The mixtures were stirred for 24 h at room temperature. The modified clay was then filtered, and thoroughly washed with water, followed by drying at 55°C in a vacuum oven.

4.5 Characterization of organoclays

4.5.1 FT-IR spectroscopy

Fourier-transform infrared spectroscopy (FT-IR) was used to qualitatively prove that the organic modifiers had interacted with the clay minerals by the formation of some kind of new bond. FT-IR spectroscopy was used to detect shifts in vibrational bands due to specific interaction between clay and the organic modifiers.

Infrared spectra were obtained with Perkin Elmer 1650 transform infrared spectrophotometer, and recorded by averaging 32 scans.

4.5.2 Small angle X-ray scattering

SAXS measurements were performed at 298 K. SAXS diffraction measurements were carried out in a transmission configuration. A copper rotating anode X-ray source (functioning at 4 kW) with a multilayer focusing “Osmic” monochromator giving high flux (10^8 photons/sec) and punctual collimation was used. An “image plate” 2D detector was used. Diffraction curves were obtained, giving diffracted intensity as a function of the wave vector q .

For crystalline compounds, the d spacing d_{hkl} between reticular planes hkl can be determined from the position of corresponding Bragg peaks observed on the diffraction curve. The d_{hkl} was calculated from Bragg’s law:

$$2d_{hkl}\sin\theta = \lambda \quad 4.1$$

where 2θ is the diffraction angle and $\lambda_{Cu} = 1.54 \text{ \AA}$

$$q = \frac{4\pi\sin\theta}{\lambda} \quad 4.2$$

Experimental

From relations (4.1) and (4.2), the following can be deduced:

$$d_{hkl} = \frac{2\pi}{q_{hkl}} \quad 4.3$$

where q_{hkl} is the q value corresponding to the associated Bragg peak position.

4.5.3 Thermogravimetric analysis (TGA)

TGA analyses of the organoclay and nanocomposites were carried out using a TGA-50 SHIMADZU thermogravimetric instrument, with a TA-50 WSI thermal analyzer connected to a computer. Samples (10-15 mg) were degraded in nitrogen (flow rate 50 ml/min) at a heating rate of 2.5-10°C/min.

4.6 Synthesis of poly(styrene-co-butylacrylate) nanocomposites

All nanocomposites were synthesized via emulsion polymerization. However, two different synthesis strategies were employed. In *semi-batch emulsion polymerization* the monomers and initiator were added to the reactor at different stages in the presence of Na⁺-MMT. In *batch emulsion polymerization* all monomers, initiator and surfactant were added together. These two methods are described below.

4.6.1 Synthesis of poly (styrene-co-butylacrylate) nanocomposites by batch emulsion polymerization

In a 250-ml flask, different amounts of Na⁺-MMT as shown in Table 4.1 were dispersed in deionised water (150 g). The mixture was stirred for 1 h, then different quantities of AMPS (i.e. the ratio of AMPS to clay was 100% CEC of clay) were added to the mixture and stirred at room temperature for an additional 24 h.

*Experimental***Table 4. 1: Formulations for the preparation of nanocomposites using AMPS**

Styrene / butylacrylate	The amount of clay		The amount of AMPS (g)*
	% clay relative to monomers	(g)	
11/9	1	0.2	0.04
11/9	3	0.6	0.12
11/9	5	1	0.20
11/9	7	1.4	0.27
11/9	10	2	0.40

* The ratio of AMPS to clay is 100% CEC of clay

Styrene (11 g) and butylacrylate (9 g) were added and the mixture was stirred for 30 min. At this point SDBS (0.4 g) was added and the mixture was stirred for an additional 1 h. Then the mixture was sonicated at 90% amplitude with a Sonics & Materials Inc, the total energy was in the range of 70 to 73 kJ, Vibracell VCX 750 ultrasonicator, at 30°C for 15 min. The above mixture was transferred into a three-neck round-bottom flask equipped with a mechanical stirrer, a reflux condenser, a nitrogen inlet and a rubber septum.

The Initiator 4,4-Azobis (4-cyanovaleric acid) (0.04 g) was added to the reactor. The mixture was stirred at room temperature for 1 h under nitrogen atmosphere. Then the flask containing the mixture was transferred to an oil bath at 85°C, and the mixture stirred for an additional 6 h. At the end of the polymerization the oil bath and hotplate were removed, and the reaction was chilled with ice water for 10 min. Small amounts of polymer latex were dried in a vacuum oven at 25°C for 24 h and analyzed by SAXS, TEM, TGA and DMA.

Experimental

The other series of poly(styrene-co-butylacrylate) nanocomposites were synthesized under similar conditions using the other clay modifiers, Cops, NIPA and MET.

4.6.2 Synthesis of poly(styrene-co-butylacrylate) nanocomposites by semi-batch emulsion polymerization

Pristine Na⁺-MMT was dispersed in deionised water (from 1% to 10%, relative to weight of monomers used as shown in table 4.1). AMPS (the ratio of AMPS was 100% CEC of clay) was added and the mixture stirred at room temperature for 24 h.

Styrene (1.27 g) and butylacrylate (1.13 g) were added to the above mixture placed in a 1-L four-neck, round-bottom flask. The flask was equipped with a baffle stirrer, a reflux condenser, a nitrogen inlet, and a rubber septum. Initiator in aqueous solution (0.01 g 4,4-Azobis (4-cyanovaleric acid)) was injected into the flask through a rubber septum using a glass syringe. The mixture was first stirred at 200 rpm for 1 h under a nitrogen atmosphere at room temperature and then the temperature was increased to 65 °C. A 10% aqueous solution of SDBS (0.4 g) was added to stabilize the polymer particles in order to obtain high conversion.

After the initial polymerization was completed, styrene (9.73 g) and butylacrylate (7.87 g) were mixed and fed (for around 3 h at a flow of 0.12 cm³/min) into the flask through a septum. 0.03g of initiator was added during feeding of the monomers at the rate of 10mg/h. After all monomers had been added, additional initiator (0.01 g) was added. The mixture was stirred for an additional 4 h at 65°C, and then the polymerization temperature was raised to 85°C for an additional 2 h.

4.7 Synthesis of poly(styrene-co-butylacrylate)

For comparison of the changes in thermal and mechanical properties of poly(styrene-co-butylacrylate) due to the presence of clay filler, a pure poly(styrene-co-butylacrylate) standard was prepared under conditions similar to those employed for the preparation of nanocomposites (see Section 4.6.1).

4.8 Characterization of poly(styrene-co-butylacrylate) nanocomposites

Experimental

The structures of the nanocomposites were characterized using SAXS and TEM, while the properties of the nanocomposites were investigated by TGA, DMA, and GPC.

4.8.1 Small angle X-ray scattering

Refer to Section 3.6.1, and Section 4.5.2.

4.8.2 Transmission electron microscopy

TEM was used to monitor the distribution of clay particles in poly(styrene-co-butylacrylate) nanocomposites at the nanometer scale. Bright field TEM images were recorded on a JEM 200CX (JEOL Tokyo, Japan) TEM at an accelerating voltage of 120 kV. Prior to analysis, samples were stained with OsO₄, then embedded in epoxy resin and cured for 24 h at 60°C. The embedded samples were then ultramicrotomed with a glass knife on a Reichert Ultracut S ultra microtome at room temperature. This resulted in sections with a nominal thickness of ~ 100 nm. The sections were transferred from water at room temperature to 300-mesh copper grids, which were then transferred to the TEM apparatus.

4.8.3 Scanning electron microscopy

Scanning electron microscopy (SEM) was used to look at the surfaces of the nanocomposite samples. Imaging of the surfaces of the samples was accomplished using a Leo® 1430VP scanning electron microscope. Prior to imaging, the samples were sputter-coated with gold. Samples were quantified by EDS analysis using an Oxford Instruments® 133keV detector and Oxford INCA software.

4.8.4 Dynamic mechanical analysis

A Perkin Elmer DMA 7e instrument was used for dynamic mechanical analysis, using thin-film mode. Samples were prepared by pressing the polymer into thin discs using a hydraulic press. Samples were brought to 50°C and held there for a minute before being heated to 175 °C at a heating rate of 5°C/min and the frequency was 1 Hz.

4.8.5 Gel permeation chromatography

GPC was performed using a Waters 600E system controller equipped with a Waters 610

Experimental

fluid unit pump, a Waters 410 differential refractometer as detector, and a column set of a PLgel 5 mm guard 50×7.5 mm and a PLgel 5 mm mixed-C 300×7.5 mm column (Polymer Laboratories). Measurements were carried out at 30°C, using a flow rate of 1 ml/min, and THF as eluent. The GPC column was first calibrated with 10 samples of polystyrene standards, prior to analysis; samples were vigorously stirred in THF for a week (to ensure all components were in solution). The samples were then filtered through a 0.45- μ m-filter membrane, five times, thus only the THF soluble components were analyzed.

4.8.6 Thermogravimetric analysis

Refer to Section 3.6.2.

4.9 References

- (1) Stevens, M. P. *Polymer Chemistry : An Introduction*; Oxford University Press: New York, 1990.

The interaction mechanism of AMPS with clay

5.1 Introduction

Sodium montmorillonite is the most common clay used to synthesize nanocomposite materials due to its availability and high aspect ratio relative to other types of clay¹. The presence of exchangeable Na⁺ in the clay interlayer makes the clay surface completely hydrophilic and incompatible with hydrophobic polymers¹⁻⁴. Furthermore, the clay platelets are bound to each other by Van der Waals force, which makes the clay interlayer very narrow. This makes the penetration of most polymers or monomers into the clay galleries extremely difficult⁵. The hydrophilicity of the clay surface can be changed by surface modification using compounds that can attach to the surface in different ways⁶.

The ion exchange reaction is the most common method for the treatment of a clay surface⁷. Alkyl ammonium cations are usually used as clay modifiers to replace the interlayer cations and to widen the interlayer spaces^{3,6-9}. Organic molecules can also adsorb to clay¹⁰ in different ways, such as: by formation of hydrogen bonds between the hydroxyl groups of the clay surface and some functional groups of organic modifiers, or by ion-dipole interactions between exchangeable cations and organic molecules. The latter type of interaction can be directly between exchangeable cations and organic modifiers, or organic modifiers and cations linked indirectly through water bridges¹¹.

In this study four different compounds were used to modify Na⁺-MMT, namely 2-acrylamido-2-methyl-1-propanesulphonic acid (AMPS), sodium 1-allyloxy-2-hydroxypropyl sulphonate (Cops), N-isopropylacrylamide (NIPA), and methacryloyloxyundecan-1-yl sulphate (MET). Besides using Cops, NIPA and MET as clay modifiers to synthesize nanocomposites, they were also used to study how AMPS itself can interact with the clay (see Section 5.4).

The chemical structures of the above compounds are shown in Table 5.1. The treatment

Results and discussions

of Na⁺-MMT by these compounds was explained in Section 4.3.

Some work has reported on the preparation of polymer nanocomposites by emulsion polymerization using AMPS as a clay modifier^{12,13}. The use of a low percentage of AMPS as a specialty monomer seems to play a major role in achieving a successful exfoliation of clay. However, the mechanism by which AMPS interacts with clay, as well as by which AMPS promotes exfoliation of clay in emulsion polymerization, has not been resolved yet.

Table 5.1: Clay modifiers used in this study

Clay modifier	Code	Structure
2-acrylamido-2-methyl-1-propanesulphonic acid	AMPS	$\text{H}_2\text{C}=\text{CH}-\overset{\text{O}}{\parallel}{\text{C}}-\text{NH}-\overset{\text{CH}_3}{\underset{\text{CH}_3}{\text{C}}}-\overset{\text{H}}{\text{C}}-\overset{\text{O}}{\parallel}{\text{S}}(\text{OH})_2$
Sodium 1-allyloxy-2-hydroxypropyl sulphonate	Cops	$\text{H}_2\text{C}=\text{CH}-\overset{\text{H}}{\underset{\text{H}}{\text{C}}}-\text{O}-\overset{\text{H}}{\underset{\text{H}}{\text{C}}}-\overset{\text{OH}}{\text{CH}}-\overset{\text{H}}{\underset{\text{H}}{\text{C}}}-\overset{\text{H}}{\underset{\text{H}}{\text{C}}}-\overset{\text{O}}{\parallel}{\text{S}}(\text{O}^-)\text{Na}^+$
N-Isopropylacrylamide	NIPA	$\text{H}_2\text{C}=\overset{\text{H}}{\text{C}}-\overset{\text{O}}{\parallel}{\text{C}}-\text{N}-\overset{\text{H}}{\text{CH}}-\overset{\text{CH}_3}{\underset{\text{CH}_3}{\text{C}}}$
Methacryloyloxyundecan-1-yl sulphate	MET	$\text{H}_2\text{C}=\overset{\text{CH}_3}{\text{C}}-\overset{\text{O}}{\parallel}{\text{C}}-\text{O}-(\text{CH}_2)_{11}-\text{SO}_3\text{Na}^+$

The main objective of this study described in this chapter is to understand how AMPS interacts with clay. Investigations were carried out to try to determine the interaction mechanism between AMPS and Na⁺-MMT (i.e. ion exchange or adsorption). Furthermore the effects of pH on the interaction between AMPS and Na⁺-MMT were studied. The use of AMPS as clay modifier to synthesize nanocomposites has been reported in the literature¹²⁻¹⁷, but no mention could be found of using Cops, NIPA or MET as clay modifiers to synthesize nanocomposites materials.

The organoclays were characterized using different analytical techniques. FT-IR was

Results and discussions

used to confirm the presence of organic modifiers in a clay by recording the appearance of new IR bands related to those compounds¹⁸. SAXS analysis was also used to study changes of the spacing of interlayer silicates as a result of the insertion of organic compounds into the clay galleries^{10,18,19}. TGA was used to determine the quantities of organic compounds inside the clay galleries¹⁸.

5.2 Clay surface modification by AMPS

The modification of the clay by AMPS was carried out according to the procedure described in Section 4.3. Clay was modified with different AMPS concentrations. Although AMPS was not expected to ion-exchange with the Na⁺ cation of the clay surface, the concentration of AMPS was correlated to the CEC of clay to give an element of comparison with cationic surfactants generally used to prepare modified clay.

The CEC of Na⁺-montmorillonite is 92.6 meq/100g. The concentration of organic modifier (e.g. AMPS) is given in % CEC. This unit relates to the theoretical concentration of any cationic surfactant necessary to ion exchange all of the exchangeable cations (i.e. 92.6 meq/100g of clay in the cases of Na⁺-montmorillonite).

In order to remove all un-adsorbed AMPS from the external clay surface, the AMPS-MMT samples were washed using deionised water and centrifuged to separate the AMPS-MMT from the water. This procedure was repeated until the washing water was found to be free of AMPS, as confirmed by measuring the pH of the washing water. The pH should be similar to that of the dispersion clay without AMPS (about 10.5). Fig. 5.1 shows the change of pH of the water after washing as a function of the number of washings.

Results and discussions

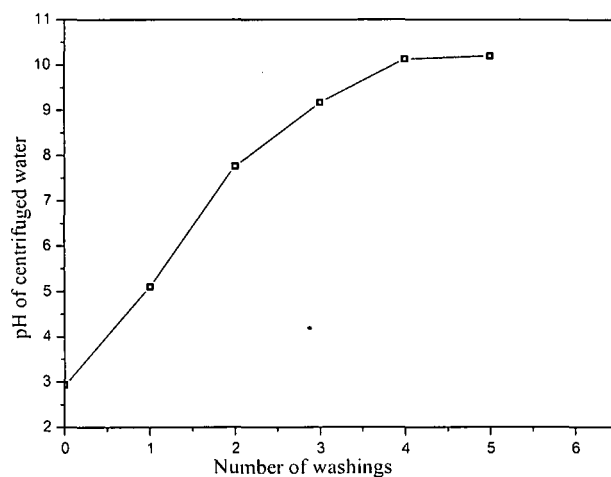


Fig. 5.1: pH values of centrifuged water vs. the number of washings for 100% CEC AMPS.

The pH value of the dispersion clay (without AMPS) in water was 10.5. When AMPS was added (100% CEC) the pH value of the water after washing was found to be low (2.94). Then this pH value increased with subsequent washings until it became constant after washing the modified clay 4 -5 times. The change in pH value is due to the removal of unadsorbed AMPS molecules from the external surface of the clay. Therefore the characterization of AMPS-MMT by other analytical methods will be only related to the AMPS localized inside the clay galleries. The AMPS-MMT samples were characterized using SAXS, TGA and FT-IR, as described in the following sections.

5.2.1 Determination of the amount of AMPS adsorbed in the clay galleries

The presence of an excess amount of AMPS could have an effect on the polymerization rate¹² when the AMPS-MMT is later used to synthesise polymer-clay nanocomposites (see Section 4.7), therefore the determination of the specific amount of AMPS that enters into the clay galleries is necessary.

Thermogravimetric analysis (TGA) was used to determine the amount of AMPS inside the clay galleries^{5,12,18}. Various amounts of AMPS were used to modify the clay surface (25%, 50%, 75%, 100% and 130% relative to CEC of the clay) using fixed amounts of clay. The amount of AMPS loaded in the clay was determined from the difference between the residual weight difference between clay with AMPS and pristine clay at 600°C, as seen in Fig. 5.2(a-e). Clay minerals are relatively thermally stable compared to

Results and discussions

organic molecules. These minerals will begin to lose structural hydroxyl groups at 600°C but will maintain the layer structure up to 800°C²⁰. The decomposition behaviour of pure, dried AMPS is included in the figure. The AMPS starts to decompose at about 185°C and its residue at 800°C is 7.6%.

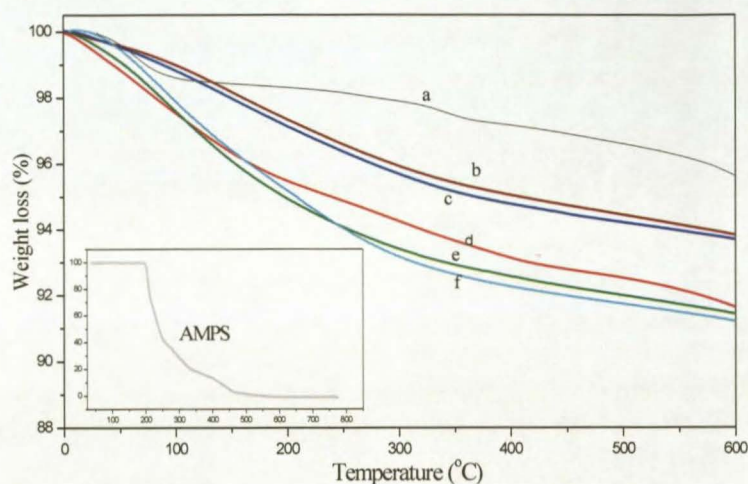


Fig. 5.2: Thermal gravimetric curves of: (a) pristine Na⁺-MMT and Na⁺-MMT with different AMPS concentrations: (b) 25% CEC (c) 50%CEC (d) 75% CEC (e) 100% CEC (f) 130% CEC. (The insert shows thermal decomposition of dried AMPS.)

The weight loss of pure clay between 20°C and 100°C corresponds to the removal of water from the interlayer coordinated to Na⁺. The weight loss of Na⁺-MMT in the temperature range of 100°C to 600°C is about 2.6%, and can be attributed to the decomposition of hydrogen-bonded water molecules and some of the hydroxyl groups from tetrahedral sheets of the clay^{21,22}.

Table 5.2 summarizes the amounts of AMPS used in the modification process, and the amounts of AMPS inside the clay galleries determined from the weight loss by TGA at 600°C. If all CEC sites of the clay were exchanged with AMPS, then the mass of AMPS in clay galleries would be closer to the theoretical mass fraction of AMPS in AMPS-MMT²³. The theoretical mass here is the initial quantity of AMPS added. The amounts of AMPS found inside the clay galleries were very low compared to the initial quantity of AMPS over the entire experimental concentration range. For example, in the case of 25% CEC, the initial quantity of AMPS was 0.095 g. However, less than half of

Results and discussions

this amount (0.002 g) entered inside the clay galleries, meaning that around 0.093 g of AMPS was lost during the process. In the case of 100% CEC, the initial quantity of AMPS was 0.383 g while the amount of AMPS inside the clay galleries was found to be only 0.023g.

Table 5.2: Initial AMPS concentrations and the quantities of AMPS inside clay galleries

Initial concentration of AMPS		Weight loss (%) at 600°C	Quantities of AMPS in clay galleries	
% CEC of clay	mass (g)		% mass	mass (g)
0%	0.00	4.02	0.00	0.00
25% CEC	0.095	6.15	2.13	0.002
50% CEC	0.191	6.32	2.30	0.004
75% CEC	0.287	8.42	4.41	0.014
100% CEC	0.383	8.60	4.60	0.019
130% CEC	0.495	8.81	4.84	0.023

Initially it was expected that when the initial concentration of AMPS is low (e.g. 25% CEC) all the AMPS would enter inside the clay galleries, but the results that were obtained were quite different. Furthermore, when 50%, 75%, 100% and 130% AMPS was used; only a fraction of AMPS was to be found effectively included in the clay galleries (see Table 5.2). This is difficult to explain since no more AMPS should have entered the clay galleries than in the case of the 25%. This could be related to the nature of the AMPS molecule; AMPS is uncharged, and therefore might not interact with the clay according to the ion exchange model. Indeed, in order for any molecule to replace the Na^+ from the clay galleries the molecule must be positively charged^{18,24,25}. Thus, interaction between molecules like AMPS and clay by ion exchange seems not to be occurring. The attachment of AMPS to the clay might occur by the formation of hydrogen bonding between amide groups of AMPS molecules and the hydroxyl groups on the clay surface²⁶, or it could be due to the formation of complexes between the sulphate group of AMPS and the water molecules that surround the sodium cations^{18,26}. These bonds are relatively weak and reversible, the bond energy usually ranges from

Results and discussions

1 kcal/mol to 5 kcal/mol²⁶, thus they may break upon being washed five times with water, leading to the loss of a relatively large quantity of adsorbed AMPS during the process. On the other hand, if AMPS ion exchanged with Na⁺ in the clay galleries, the initial amount of AMPS would be equal to the amount of AMPS inserted inside the clay galleries, especially for AMPS concentrations below 100% CEC. This behaviour of AMPS is completely different from the behaviour of cationic surfactants. For instance, Biasci *et al.*²⁷ found that cetyltrimethylammonium bromide (CTAB) was ion exchanging with clay, without loss, meaning that most of the surfactant entered into the clay galleries and effectively ion-exchanged.

5.2.2 The organization of AMPS in the clay galleries

X-ray diffraction has been used to study the changes in the basal spacing of montmorillonite before and after modification²⁸, i.e. the changes in the interlayer distance caused by the insertion of surfactant could be monitored by SAXS measurements. Variation in the *d* spacing (interlayer distance) was found to be a step function of the surfactant concentration²⁹. The *d* spacing could be calculated according to Bragg's law: $d = 2\pi/q$ (where *q* is a wave vector and its value corresponds to the associated Bragg peak position)⁵.

In order to monitor the change in basal spacing of clay as a function of AMPS concentration, fixed amounts of clay (1 g) were modified using different AMPS concentrations. The quantities of AMPS that were used to modify the clay surface were calculated relative to the cation exchange capacity of the Na⁺-MMT that was used (i.e. 92.6 meq/100 mg). Unmodified clay was used as a reference.

The SAXS pattern of pristine Na⁺-MMT Fig. 5.3(a) shows that the pristine Na⁺-MMT has an interlayer spacing of $d = 1.14$ nm, which is in agreement with the literature^{12,30}. Clearly the SAXS patterns of AMPS-MMT samples Fig. 5.3(b-h) show that the XRD peak position shifted toward the small (*q*) value, and according to Bragg's law the interlayer spacing of AMPS-MMT samples was increased compared to that of pristine Na⁺-MMT.

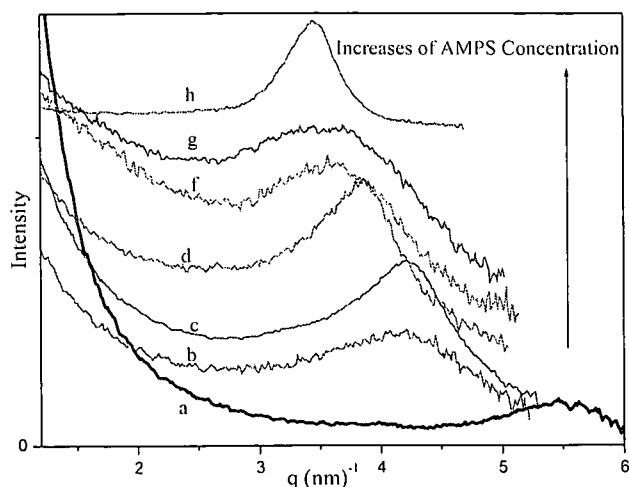
Results and discussions

Fig. 5.3: SAXS patterns of (a) pristine Na⁺-MMT, and AMPS-MMT samples with different AMPS concentrations b) 10%, c) 25%, d) 50%, f) 75%, g) 100% and h) 130% CEC of clay.

The increases in the interlayer distance of AMPS-MMT samples confirm the insertion of AMPS molecules into the clay galleries as observed by TGA (see Section 5.2.1). Furthermore, AMPS molecules can widen the clay galleries, thus AMPS can facilitate the insertion of polymers or monomers¹⁴. The *d*-spacing reached a maximum (1.82 nm) when the concentration of AMPS was between 75 and 130% CEC Fig. 5.3(f-h). Xu *et al.*¹² found that the AMPS molecule successfully enlarged the *d* spacing of clay; they found the maximum *d*-spacing of the interlayer was 2.1 nm when the concentration of AMPS was 100% CEC. However, in their case the modified clay was not washed to its initial pH.

AMPS has an amide group and sulphuric acid group in the molecule. Therefore AMPS may be linked to the silicate layers due to strong interaction of amide groups with pristine Na⁺-MMT^{12,14}. The interaction mechanism between AMPS and pristine Na⁺-MMT is discussed in more detail in Section 5.3.

Fig. 5.4 shows the changes of interlayer distance as a function of AMPS concentration. All *d*-spacing values were determined from the SAXS results of Fig. 5.3 and then calculated according to Bragg's law.

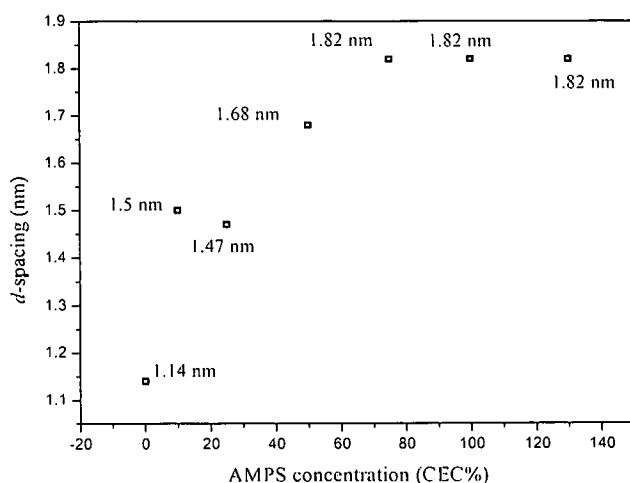
Results and discussions

Fig. 5.4: Interlayer distances of Na⁺-MMT and AMPS-MMT vs. AMPS concentration.

Clearly, from the SAXS patterns of modified clay the interlayer distance was found to be a function of AMPS concentration; as the AMPS concentration increased so the peaks are shifted to low q values (i.e. greater interlayer distance). However, Fig. 5.3 and Fig. 5.4 illustrate that the interlayer distance for 10% CEC is slightly larger than that for 25%. This could be explained by the fact that the concentration of AMPS in the case of 10% CEC is very low; therefore there is still a large amount of exchangeable Na⁺ which can adsorb water. The high hydration energy of Na⁺ cations could therefore make the basal spacing of 10% CEC (1.52 nm) higher than that for 25% CEC (1.46 nm)²⁹. A change in the interlayer distance is very pronounced at AMPS concentrations between 10% and 75% CEC. On the other hand, no further change in the interlayer distance is observed at higher AMPS loading (i.e. 75% to 130% CEC), where the interlayer distances is around 1.82 nm. This means that there is a limited amount of AMPS that can enter into the clay galleries even if an excess amount of AMPS is added. This is consistent with the TGA results (see Section 5.2.1), which showed that the clay surface reached a maximum coverage by AMPS molecules when the concentration of AMPS was between 75% and 100% of the CEC of clay.

The change in interlayer distance as a function of AMPS concentration could result from a change in the conformation of AMPS molecules inside the clay galleries. The arrangement of organic modifiers inside clay galleries depends on the concentration of organic modifiers, chain length, and temperature^{5,31}. Here the temperature and

Results and discussions

chain length were similar for all samples, but the concentration of AMPS was different and the d -spacing increased as the AMPS concentration that was used increased. Therefore the arrangement of AMPS inside the clay galleries is likely to change as more AMPS molecules enter inside the galleries. Fig. 5.5 shows the possibilities of AMPS arrangements inside clay galleries as a function of AMPS concentration, as proposed by Vaia *et al.*³¹ (they described the arrangement of alkylammonium inside clay galleries).

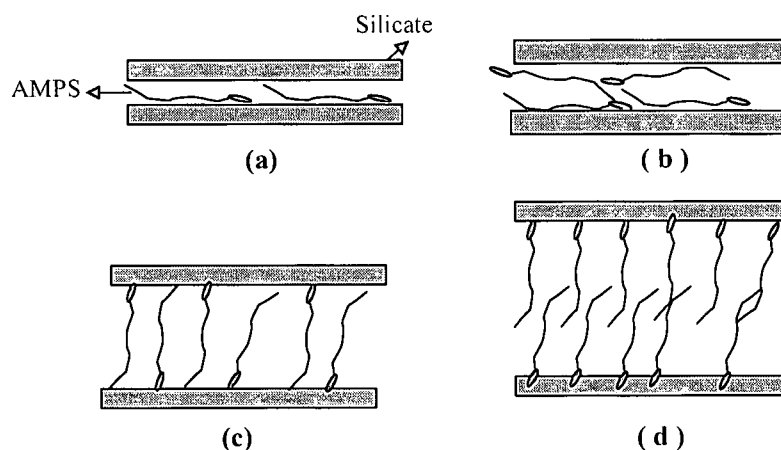


Fig. 5.5: Schematic representation of the arrangement of AMPS molecules inside silicate layers: (a) mono-layer, (b) bi-layer, (c) paraffin-type mono-layer and (d) paraffin-type bi-layer³¹.

The AMPS molecules might arrange themselves in the different ways into clay galleries depending on their concentrations. When the quantity of AMPS inside the clay galleries is very low the molecules might take on a mono-layer arrangement, as shown in Fig. 5.5(a). A bi-layer arrangement with molecules aligned parallel to the clay surface could take place as the concentration of AMPS increased, as shown in Fig. 5.5(b). As the concentration of AMPS becomes very high, the molecules may arrange themselves as a paraffin-type mono-layer and a bi-layer, as seen in Fig. 5.5(c and d) respectively. Thus, this could explain why the d -spacing of clay is wide when the amount of AMPS that is used is high. Furthermore, the abrupt increase in d -spacing at 75% CEC in Fig. 5.4, could be due to transition of the mono-layer type to the paraffin-type. This is further supported by the changes in the shape of diffraction peaks with AMPS concentrations (see Fig. 5.3). A narrow peak indicates that clay platelets are regularly packed while broad peaks show heterogeneity of packing, with a relatively undefined d spacing³². In other words this means that the two relatively narrow peaks observed with 50% and 130% CEC indicate a regular packing of AMPS on the clay surface, respectively a paraffin type

Results and discussions

mono-layer and bi-layer Fig. 5.5(c and d). The broad peak for intermediate concentrations of AMPS in Fig. 5.3(f and g) shows a relative disorder existing during the transition between these two modes of packing (i.e. some galleries still in mono-layer and others in bi-layer packing). Although SAXS measurement can provide an indication of whether the clay modifier intercalated inside clay galleries^{10,29}, by measuring the changes in d spacing after the modification process²⁹, this technique does not fully indicate the types of interactions that could be occurring between AMPS and the clay.

5.3 Determination of types of interaction between AMPS and clay

The types of interaction that could occur between AMPS and clay are discussed here. Xu *et al.*¹² used AMPS as a clay modifier and suggested that AMPS and clay interact via an ion-exchange reaction. On the other hand the adsorption of AMPS onto clay seems to be possible because of the chemical nature of AMPS^{18,26}.

As mentioned in Sections 5.2.2 and 5.2.1 TGA and SAXS measurements proved that interaction between AMPS and clay does take place, but these two analytical methods do not allow the type of interaction between AMPS and clay to be identified. FT-IR is an alternative method that can be used to analyse AMPS-MMT, and provide information in terms of chemical interaction between AMPS and clay.

5.3.1 Characterization of AMPS-MMT by FT-IR

FT-IR analysis was used to characterize AMPS-MMT, to determine the type of interaction between AMPS and clay. FT-IR spectra of neat Na⁺-MMT and Na⁺-MMT modified with AMPS were recorded and compared (see Appendix B: Fig.1(A)). The FT-IR spectrum of Na⁺-MMT shows absorption bands at 3432, 3630 and 1640 cm⁻¹ (see Table 5.3 below) corresponding to the OH stretching of silicate layers¹². The very sharp band at 1043 cm⁻¹ is related to the stretching of Si-O bonds of the silicate layer^{12,15}. The band at 620 cm⁻¹ is related to the Al-O of the silicate layers. The appearance of new bands in the FT-IR spectrum of clay modified by AMPS (see Appendix B: Fig. 1 (A)) indicates the presence of AMPS in the clay. The bands at 2947 and 2850 cm⁻¹, are related to C-H stretching of AMPS molecules. Other new bands in the FT-IR spectrum of AMPS-MMT can be seen at 1540 cm⁻¹, corresponds to NH bending, and 1372 cm⁻¹ related to S=O of

Results and discussions

AMPS. The FT-IR spectrum of AMPS-MMT was found to be similar with that reported in literature ^{12,17}.

Table 5.3: FT-IR results for Na⁺-MMT and AMPS-MMT

	AMPS	Na ⁺ -MMT	AMPS-MMT
Assigned groups	Wavelength (cm ⁻¹)	Wavelength (cm ⁻¹)	Wavelength (cm ⁻¹)
Al-O		620	620
Si-O		526, 463, 1043	520, 460, 1040
N-H	3235, 1542		1543, 3250
C-H	2950, 2848		2850, 2947
S=O	1372		1372
O-H		1640, 3432, 3630	3434, 3631, 1650

The determination of the type of interaction between clay and AMPS is hard to achieve using FT-IR; this was due to the following reasons:

- Very small amounts of AMPS (relative to the amount of clay) were used to modify the clay, since the amount of AMPS used was calculated relative to the cation exchange capacity of the clay (CEC). This amount of AMPS is about 100% CEC of clay, which is the same amount of AMPS used later to synthesis nanocomposites (see Section 4.3). In fact not all of the AMPS used enters inside the clay galleries ¹². Only a specific amount of AMPS entered into the clay galleries ^{12,13} while the remaining amount (i.e. unreacted AMPS) was removed by washing by deionised water five times (see Section 4.2.1). The amount of adsorbed AMPS was determined by using TGA (see Section 5.2.3).
- Na⁺-MMT itself has a very complicated FT-IR spectrum ¹⁸. This results in overlapping between bands originating from both clay and AMPS. Therefore, the characteristic absorption bands of the functional AMPS groups cannot be easily seen in the presence of the bands of clay minerals ¹⁸.

The occurrence of interaction of the AMPS molecule within the clay galleries was confirmed by TGA, SAXS and FT-IR. However, the types of interactions involved

Results and discussions

are still not understood. Xu *et al*¹² proposed the mechanism of the interaction via an ion-exchange mechanism, Furthermore, the chemical nature of AMPS enables it to adsorb onto clay, as will be discussed in Section 5.3.4.

5.3.2 Investigation into the interaction between AMPS and clay via ion exchange

As mentioned in Section 5.2.1 the amount of AMPS inside the clay galleries was calculated from TGA thermograms, showing that the AMPS might interact with clay via weak bonds, rather than ion exchange. However, this is not in agreement with Xu *et al.*^{12,14} who suggested that AMPS molecules can ion exchange with the Na⁺ on the surface of clay. They proposed that, in an aqueous medium, a proton dissociates from the sulphuric acid group of the AMPS, the proton then moves to nitrogen to form a protonated amide group which exchanges with the sodium cations. The sodium dissociated from silicates will associate with the sulphate ion of AMPS to form sulphuric acid sodium salts. The AMPS would move to the surface of the silicate layers due to the dipolar interaction.

According to Xu *et al.*¹², the nitrogen of the amide group of AMPS molecule can be protonated by the labile proton of the sulphate group, forming zwitterions. However, the amides in fact are very weak bases. Amide groups have a pKa (Acid dissociation constant) around -0.5. Therefore amides do not have clearly noticeable acid-base properties in water³³. Therefore at this point the Xu theory is questionable since amide groups of AMPS are not protonated in an aqueous medium, and this indicated that the AMPS can not be ion exchanged with the clay.

The question that now needs to be answered is: Does the pH of the medium affect the interaction between AMPS and clay? This will be addressed in Section 5.3.3

5.3.3 pH dependence of Na⁺-MMT surface modified using AMPS

By treatment of the clay with AMPS at low pH values (high H⁺ concentration), the possibility to protonate the amide group of AMPS should increase (according to the mechanism proposed by Xu). This would make AMPS positively charged, allowing AMPS to interact with the clay via an ion exchange reaction. This has been successfully

Results and discussions

done by others with some amino acids such as aminoundecanoic acid³⁴ and glycine^{18,26}.

The treatment of the clay surface using AMPS was then carried out at different pH conditions, namely 0.63, 1.18, 2.8, 3.5, and 6.0. The amounts of AMPS and the amounts of clay were similar for all samples (see Section 4.2.3).

The amount of AMPS that could be inserted inside the clay galleries was determined using TGA analysis as shown in Fig. 5.6.

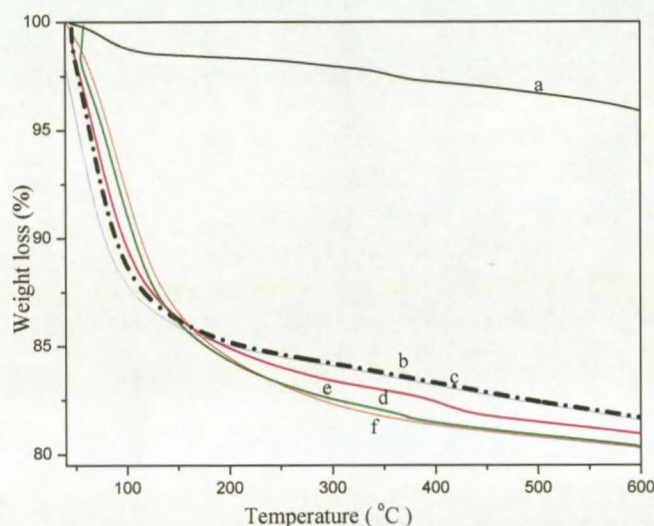


Fig. 5.6: Thermal gravimetric curves of (a) Na⁺-MMT, and AMPS-MMT at different pH values: (b) 0.63 (c) 1.81 (d) 2.8 (e) 3.5 and (f) 6.0.

The weight loss at around 105°C refers to the loss of the water inside the clay galleries¹². The difference in the weight loss between the pristine clay curve Fig. 5.6(a) and other curves are related to the amount of AMPS plus some water molecules inside clay galleries. Fig. 5.6(c-f) illustrates that the amount of AMPS inserted into clay galleries was not significantly affected by the pH value. (The slight differences in the weight loss between some samples may be attributed to experimental errors).

Some overlapping of TGA curves can be seen in Fig. 5.6. This means that those samples had the same AMPS amounts whatever the pH conditions. This result indicates that the amide group of AMPS is unable to protonate even when the pH values were low (i.e. the concentration of H⁺ in solution was high)³⁵. This confirms that the attachment between the AMPS molecules and clay surface does not occur by an ion-exchange reaction. On the other hand the pH value has a significant effect on the interaction between an amino

Results and discussions

acid and clay. Li et al.³⁴ found that the aminoundecanoic acid interacted with clay by an ion-exchange reaction only when the pH was adjusted to 3, this means that aminoundecanoic acid become positively charged at pH 3, and thus it can easily interact with clay via ion-exchange. Glycine is another example; this molecule was found to be adsorbed by clay via an ion exchange reaction in the acid medium, but it does not interact with clay under normal conditions²⁶.

The changes in basal spacing of clay galleries according to change of the pH values were monitored by SAXS measurements. The AMPS concentration was the same for all samples (i.e. 25% CEC). The basal spacing was determined by SAXS and the results are shown in Fig. 5.7.

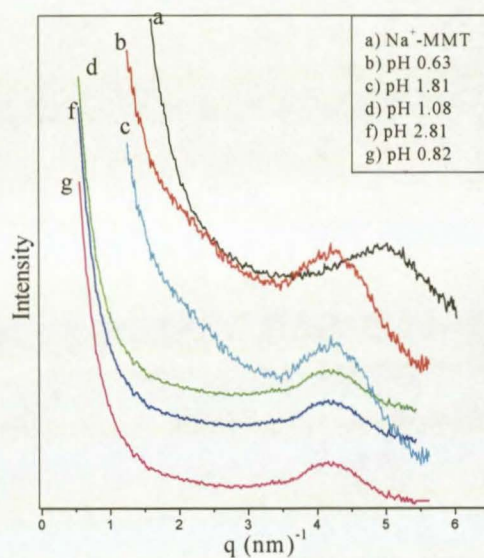


Fig. 5.7: SAXS traces for AMPS-MMT prepared at different pH values.

Fig. 5.7 clearly shows that the positions of SAXS traces for all AMPS-MMT are quite similar. This indicates that there is no change in the basal spacing of samples of AMPS-MMT whatever the pH conditions of preparation (the *d*-spacing of all samples was about 1.48 nm), hence the pH values do not affect the amount of AMPS entering the clay galleries.

5.4 Investigation into the interaction between AMPS and clay via adsorption

Analysis of AMPS-MMT samples by FT-IR did not give evidence of specific interactions occurring between AMPS and clay. Furthermore, the results described in Sections 5.2.1 and 5.3.2, indicated that ion exchange cannot occur between AMPS and clay. Thus in order to determine which chemical group is the driving force leading to adsorption of AMPS inside the clay galleries, an alternative method was required. This method involved the comparison of adsorption behaviours of molecules similar to AMPS in terms of structure and chemical groups. The compounds selected were Cops, NIPA and MET (see Table 5.1). The treatment of clay surfaces with these three alternatives compounds was carried out using a similar procedure to that used with AMPS (see Section 4.2.1.).

MET and Cops both bear a SO_3H group (similar to AMPS), but no amide group. The comparison of adsorption behaviour of Cops and MET with AMPS, could be useful in terms of understanding whether adsorption of AMPS into the clay galleries is due to sulphate group or not.

On the other hand, NIPA has an amide group, but no sulphate group. NIPA is an uncharged molecule; hence an ion-exchange reaction between NIPA and the clay surface is impossible. Therefore if NIPA interacts by formation of hydrogen bonds with clay, it would show that a similar interaction occurs between AMPS and clay by its amide group.

At this point the choice of NIPA, MET, and Cops could be helpful to investigate the possibilities of the interaction between AMPS and clay. Hence there are two possible interactions that will be discussed:

- Adsorption via a sulphate group.
- Adsorption via amide group.

Cops-MMT, NIPA-MMT and MET-MMT were characterized using different techniques, (FT-IR, TGA and SAXS). Results were compared with similar results for AMPS-MMT, as described in the following sections.

Results and discussions

5.4.1 Adsorption via sulphate groups

In order to study the possible occurrence of interaction between AMPS and clay via a sulphate group, MET and Cops were also used to modify the clay surface.

5.4.1.1 FT-IR characterization of Cops-MMT and MET-MMT

The FT-IR spectrum of MET, Na⁺-MMT and MET-MMT are shown in Appendix B: Fig 1 (D). The FT-IR spectrum of MET-MMT was compared to that for Na⁺-MMT, the FT-IR spectrum of Na⁺-MMT was discussed previously in section 5.3.1. New strong bands appeared at 2930 cm⁻¹ and 2848 cm⁻¹ in the FT-IR spectrum of MET-MMT, both are related to CH bands of MET. Another new band appeared at 1714 cm⁻¹, due to the C=O group of MET. In Appendix B: Fig. 1 (D) an absorbance band assigned to the O-H stretching in silicate lattices shifts to 3425 cm⁻¹ from its original wavenumber at 3438 cm⁻¹. The interaction between hydroxyl group of silicate and sulphate group of MET may cause the shift of absorbance bands, and the absorbance band shift indicates that the silicate may absorb the MET through hydrogen bonding.

The FT-IR spectrum of Cops-MMT (Appendix B: Fig. 1 (C)) showed some new bands (with respect to the spectrum of Na⁺-MMT). The new band at 2920 cm⁻¹ corresponds to C-H of Cops. The O-H band of silicate at 3436 cm⁻¹ become broader and shifted to 3424 cm⁻¹ when the clay was modified by Cops, this indicated that silicate layers linked to Cops molecules.

The absence of other new peaks that were expected to be seen in FT-IR spectra of Cops-MMT and MET-MMT is due to highly complicated FT-IR spectra of the clay itself, overlapping with the peaks of modifiers¹⁸. However, the appearance of the new bands in the FT-IR spectra of the modified clays at least indicates that Cops and MET indeed interacted with clay. For MET, the interaction indeed occurred via the sulphate group and this is in agreement with the finding of Choi and Chang³⁶. They suggested the ability of adsorption of potassium persulphate (KPS) into clay is via the interaction between the hydroxyl groups of the silicates and the sulphuric ions of KPS. However, in the case of Cops, its hydroxyl group could be the other group that can help Cops to interact with clay

Results and discussions

together with the sulphate group.

5.4.1.2 Amounts of Cops and MET inside the clay galleries

TGA was used to determine the total amount of organic compounds that could enter into the clay galleries. Fig. 5.8 shows the TGA thermograms of unmodified clay and clay modified with different organic modifiers. The quantities of AMPS, Cops and MET inside the clay galleries, determined from TGA at 600°C, are summarized in Table 5.4.

The quantities of compounds inside the clay galleries was determined from the difference in the weight loss found between unmodified clay and modified clay at 600°C. The weight loss of Na⁺-MMT in Fig. 5.8(a) is due to the loss of adsorbed water. The weight loss measured for the modified clays Fig. 5.8(b-d) is due to the decomposition of the clay modifiers in addition to loss of adsorbed water in the clay.

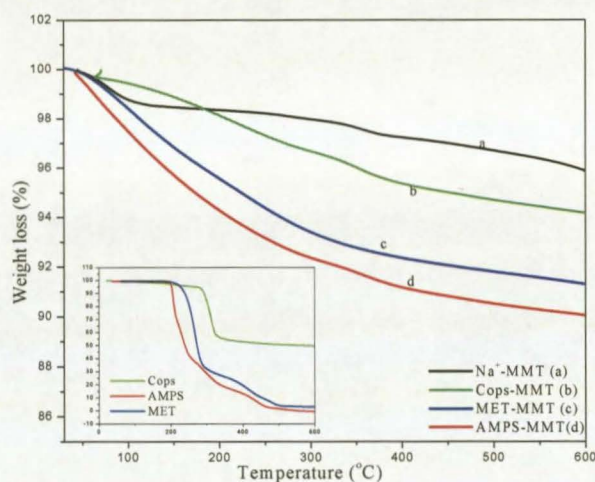


Fig. 5.8: TGA thermograms of (a) Na⁺-MMT, (b) Cops-MMT, (c) MET-MMT, and (d) AMPS-MMT. (The insert shows thermal decomposition of dried Cops, MET and AMPS).

Table 5.4 shows that the quantities of the different organic modifiers inside the clay galleries differ. This could be due to the different masses of clay modifiers that were used; each of the initial organic modifiers was used in the same molar ratios (i.e. 100% CEC), and thus a different mass of each was used depending on its own molecular weight. Also, the difference in the thermal degradation of the clay modifiers could lead to a difference in the thermal behaviour of each of the organoclays. The degradation of the

Results and discussions

organic modifiers themselves may have an influence on the thermal stability of the organoclays. The decomposition behaviours of pure dried AMPS, Cops and MET are included in Fig. 5.8.

Table 5.4: Quantities of organic modifiers inside the clay galleries

Organic modifiers	% Weight loss at 600°C	Quantities of organic modifiers in clay galleries	
		% mass	mass (g)
Na ⁺ -MMT	4.03	0.00	0.00
Cops-MMT	5.86	1.66	0.003
AMPS-MMT	8.60	4.60	0.019
MET-MMT	7.95	3.92	0.012

TGA results showed that Cops and MET can interact with clay surfaces, as did the FT-IR results. In the case of Cops and MET the interaction could occur via hydrogen bonding between hydroxyl groups in the Na⁺-MMT lattice and the sulphate group of Cops and MET. This is consistent with the results of work done by Choi and Chung³⁶ who found that potassium persulphate can adsorb onto the clay surface by the formation of hydrogen bonds between the sulphate group of potassium persulphate and the hydroxyl group of the clay surface.

Since the sulphate group has the ability to interact with the clay surface, as is occurring in the case of MET and Cops, hence, AMPS also can interact with the clay surface by formation of hydrogen bonding between sulphate groups of AMPS and hydroxyl groups of the clay surface. Again, this shows that AMPS adsorbs onto clay without an ion-exchange reaction. This in agreement with results obtained in Sections 5.3.2 and 5.3.3.

Table 5.4 also shows that the amount of AMPS inside clay galleries is greater than the amount of Cops and MET. This could be related to the fact that AMPS adsorb more readily onto clay, via both functional groups (i.e. amide and sulphate) simultaneously. Again this shows that AMPS adsorbs onto clay without an ion exchange reaction. This is in agreement with results presented in Sections 5.3.2 and 5.3.3.

Results and discussions

5.4.1.3 Study of d-spacing of AMPS-MMT, MET-MMT and Cops-MMT by SAXS

SAXS measurements allow us to see the changes in the basal spacing of clay, as the organic molecules insert inside the clay galleries. The changes in interlayer distance have been found to be dependent on the chemical structure of the organic clay modifier³⁷. The d spacing (interlayer distance) of clay was calculated as described in Section 5.2.2.

SAXS measurements were used to compare the basal spacing of three types of organoclay. These three different organoclays were prepared under similar conditions using the same ratio of organic modifiers relative to the clay (i.e. 100% CEC of clay). Fig. 5.9 below shows the SAXS patterns of unmodified clay, and clay modified with different organic modifiers.

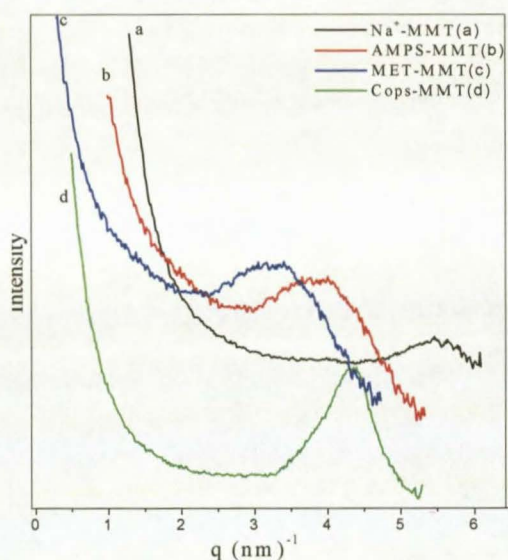


Fig. 5.9: SAXS patterns for (a) Na⁺-MMT, (b) AMPS-MMT, (c) MET-MMT and (d) Cops-MMT

Fig 5.9 shows that the SAXS diffraction peak position of modified clay shifted towards lower (q) values (i.e. high interlayer distance, as calculated using Bragg's law) when compared to pristine clay. The significant increases in the d-spacing of modified clay in Fig. 5.9(b-c), relative to that for pure clay in Fig. 5.9(a), confirmed that the three different compounds inserted inside the clay galleries were not just adsorbed on the external surface²⁰. SAXS results in Fig. 5.9 also illustrate that the galleries of silicate layers undergo greater expansion when MET was used than when Cops and AMPS were used.

Results and discussions

The *d*-spacing of MET-MMT was found to be about 1.97 nm while the *d*-spacing was 1.82 and 1.45 nm for AMPS-MMT and Cops-MMT respectively. This is due to the longer chain length of MET relative to AMPS and Cops. This was expected, according to the finding of Kalendova et al.³⁸ and Memut and Lagaly³⁹ who found that the interlayer distance of the clay increases as the chain length of the clay modifier increases.

In general, the interlayer distance depends on the charge density of the clay⁴⁰, and on the chain length of clay modifier⁴¹. Here the charge density of clay is the same because the same clay was used; the difference is only in the chemical structure of the organic modifier. Although Cops molecules have a slightly longer chain length (7 carbon atoms) relative to that of the AMPS chain (5 carbon atoms), the *d*-spacing of AMPS-MMT (1.82 nm) is greater than the *d*-spacing obtained for Cops-MMT (1.45 nm). In this case the difference in chain length between Cops and AMPS is small, and therefore negligible. This is in accordance with the finding of Usuki *et al*⁴¹, who showed that swelling of montmorillonite modified with an ω -amino acid increased significantly when the carbon number of the amino acid was greater than 8 atoms, whereas the effect of the chain length of organic modifiers is not significant when the chain is less than seven carbon atoms.

The treatment of clay by AMPS exhibited higher *d*-spacing relative to that when Cops was used. This is because AMPS molecules can interact with the clay by both sulphate and probably the amide group. This allows greater amounts of AMPS to adsorb onto clay surface inside the galleries, compared to Cops (which can adsorb into clay only via sulphate groups). This is consistent with TGA results, which showed that the amount of AMPS inside clay galleries is relatively higher than the amount of Cops.

According to SAXS and TGA results for Cops-MMT, AMPS-MMT, and MET-MMT, the interaction between those compounds and clay was confirmed. This could further the possibility of interaction between AMPS and clay by adsorption via the sulphate group, instead of an ion exchange reaction as stated by Xu *et al*¹².

5.4.2 Interaction via the amide groups

The other interaction between AMPS onto and the clay could be via adsorption of AMPS into the clay via amide groups. In order to confirm the possibility of interaction between

Results and discussions

AMPS and clay via an amide group, NIPA was also used as clay modifier. NIPA is similar to AMPS in terms of chemical structure except NIPA does not have a sulphate group. NIPA was therefore used to determine whether adsorption can also occur through the amide group of AMPS onto clay.

The treatment of clay by NIPA was carried out according to the procedure described in Section 4.2.3. The samples of NIPA-MMT were characterized using FT-IR, TGA and SAXS.

5.4.2.1 Characterization of NIPA-MMT using FT-IR

The FT-IR spectra of modified clay were compared to the FT-IR spectrum of pristine clay. The FT-IR of NIPA-MMT exhibited several new adsorption bands in the spectrum as shown in Appendix B: Fig.1 (B). The strong band at 2920 cm^{-1} is related to the CH of NIPA. The FT-IR spectra of pure NIPA exhibited a strong NH band at 3300 cm^{-1} . This band shifted to a lower wavenumber, 3237 cm^{-1} , in the FT-IR spectrum of NIPA-MMT and also became very weak and broader. This is related to the formation of hydrogen bonds between the NH of the amide group of NIPA and the hydroxyl group of silicate. A similar result was observed with acetamide, the interaction of its NH with the hydroxyl groups of silicate via hydrogen bonding leads to a decrease in the NH stretching frequency, relative to that shown by unadsorbed molecules^{18,26}.

The appearance of new CH and NH bands in the FT-IR spectrum of NIPA-MMT indicates the presence of NIPA on the surface of silicate.

5.4.2.2 Amount of NIPA inside the clay galleries

Fig. 5.11(a) shows the TGA thermograms of unmodified clay, NIPA-MMT and AMPS-MMT. Clearly there is difference in weight loss between Na^+ -MMT and NIPA-MMT, this difference is due to the decomposition of NIPA. Therefore, NIPA interacts with clay. The decomposition behaviour of AMPS and NIPA are included in Fig. 5.11.

NIPA might interact with the clay in two ways: hydrogen bonds may form between the amide groups and hydroxyl groups on the clay surface, or the amide groups could form

Results and discussions

hydrogen bonds with water molecules or hydroxide groups coordinated to the interlayer cations as can be seen in Fig. 5.10(a and b) respectively ²⁶.

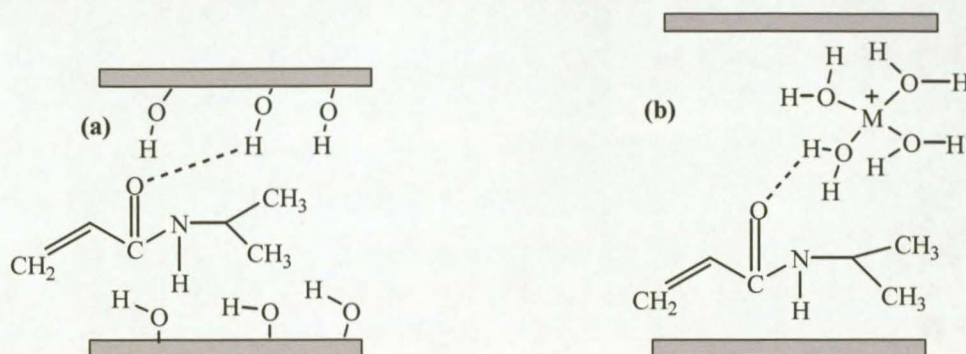


Fig. 5.10: Two possibilities for the interaction between NIPA and clay via hydrogen bonding between amide group of NIPA and (a) hydroxyl groups of silicate, and (b) with water molecules coordinated to the interlayer cations.

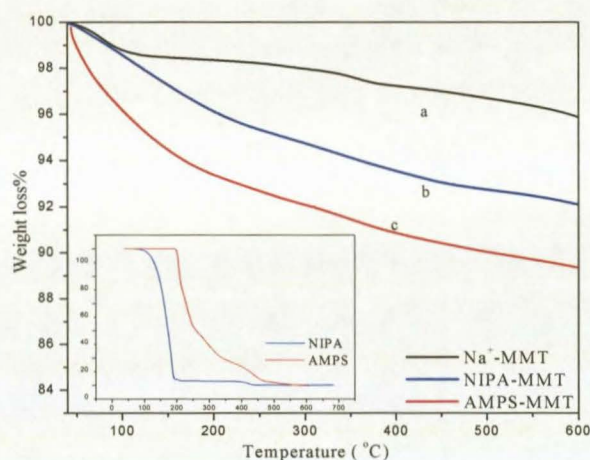


Fig. 5.11: TGA thermograms of (a) Na⁺-MMT, (b) NIPA-MMT, (c) AMPS-MMT. The insert shows thermal decomposition of dried NIPA and AMPS.

The reason for the difference in weight loss between NIPA-MMT and AMPS-MMT is most probably due to that, the quantity of AMPS inside the clay galleries is greater than the quantity of NIPA inside the clay galleries. This is because the AMPS can interact with clay more strongly than NIPA, since NIPA can only interact via amide groups, while AMPS can interact via both amide and sulphate groups. Furthermore, AMPS is more hydrophilic than NIPA, because AMPS has a sulphate group making it more hydrophilic than NIPA. Therefore the AMPS can more easily enter into the clay galleries.

Results and discussions

5.4.2.3 Study of the *d*-spacing of NIPA-MMT and AMPS-MMT

SAXS measurements were used in order to compare the *d*-spacing of AMPS-MMT with NIPA-MMT. The SAXS patterns for the modified clays in Fig. 5.12(b and c) below show an increase in interlayer distance relative to the unmodified clay in Fig. 5.12(a).

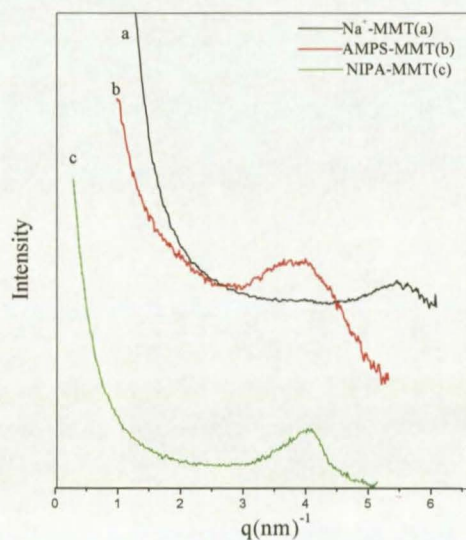


Fig. 5.12: SAXS patterns for (a) Na⁺-MMT, (b) AMPS-MMT, and (c) NIPA-MMT.

The increases in interlayer distances of Na⁺-MMT after modification by NIPA indicates that NIPA successfully interacts with clay. The interlayer distances of the two modified clays were different (i.e. 1.75 nm for AMPS-MMT and 1.57 nm for NIPA-MMT), this is due to higher packing of AMPS inside clay galleries compared to that of NIPA as shown by TGA results.

From Sections 5.4.1 and 5.4.2 it can be concluded that AMPS does not ion-exchange with clay, as stated by Xu *et al*¹². However, AMPS can strongly interact with the clay surface via adsorption of AMPS into clay by the amide and sulphate group sites.

Results and discussions

5.4 References

- (1) Utracki, L. A.; Kamal, M. R. *The Arabian Journal for Science and Engineering*, **2002**, *27*, 43 - 67.
- (2) Noh, M. W.; Lee, D. C. *Polymer Bulletin* **1999**, *42*, 619 - 626.
- (3) Alexandre, M.; Dubois, P. *Materials Science and Engineering*, **2000**, *28*, 1 - 63.
- (4) Zeng, C.; Lee, L. J. *Macromolecules* **2001**, *34*, 4098 - 4103.
- (5) Ray, S.; Okamoto, M. *Progress in Polymer Science* **2003**, *28*, 1539 - 1641.
- (6) Katti, K.; Katti, D. *Clays and Clay Minerals* **1992**, *40*, 722 - 730.
- (7) Bergaya, F.; Lagaly, G. *Applied Clay Science* **2001**, *19*, 1 - 3.
- (8) Noh, M. W.; Lee, D. C. *Polymer Bulletin* **1999**, *42*, 619 - 626.
- (9) Fu, X.; Qutubuddin, S. *Materials Letters* **2000**, *42*, 12 -15.
- (10) Beall, G. W.; Goss, M. *Applied Clay Science* **2004**, *27*, 179 - 186.
- (11) Luckham, P. F.; Rossi, S. *Advances in Colloid and Interface Science* **1999**, *82*, 43 - 92.
- (12) Xu, M.; Choi, Y. S.; Kim, Y. K.; Wang, K. H.; Chung, I. J. *Polymer* **2003**, *44*, 6387 - 6395.
- (13) Xu, M.; Choi, Y. S.; Wang, K. H.; Kim, J. H.; Chung, I. *Macromolecules Research* **2003**, *11*, 410 - 417.
- (14) Choi, Y. S.; Ham, H. T.; Chung, I. J. *Polymer* **2003**, *44*, 8147 - 8154.
- (15) Choi, Y. S.; Ham, H. T.; Chung, J. *Chemistry of Materials* **2004**, *16*, 2522 - 2529.
- (16) Choi, Y. S.; Wang, K. H.; Xu, M.; Chung, I. J. *Chemistry of Materials* **2001**, *14*, 2936 - 2939.
- (17) Choi, Y. S.; Choi, M. H.; Wang, K. H.; Kim, S. O.; Kim, Y. K.; Chung, I. J. *Macromolecules* **2001**, *34*, 8978 - 8985.
- (18) Shmuel, Y.; Harold, C. *Organo-Clay Complexes and Interactions*; Marcel Dekker, Inc: New York and Basel, 2002.
- (19) Xie, W.; Xie, R.; Pan, W.; Hunter, D.; Koene, B.; Tan, L.; Vaia, R. *Chemistry of Materials* **2002**, *14*, 4837 - 4845.
- (20) He, H.; Duchet, J.; Galy, J.; Gerard, J. *Journal of Colloid and Interface Science* **2006**, *295*, 202 - 208.

Results and discussions

- (21) Zheng, H.; Zhang, Y.; Peng, Z. *Journal of Applied Polymer Science* **2004**, *92*, 638 - 646.
- (22) Xi, Y.; Martnes, W.; He, H.; Forst, R. L. *Journal of Thermal Analysis and Calorimetry* **2005**, *81*, 91 - 97.
- (23) Davis, R. D.; Gilman, J. W.; Sutto, T. E.; Callahan, J. H.; Trulove, P. C.; De-long, H. C. *Clays and Clay Minerals* **2004**, *52*, 171 - 179.
- (24) Qutubuddin, S.; Tajuddin, Y. *Polymer Bulletin* **2002**, *48*, 143 - 149.
- (25) Rosorff, M. In *Nano Surface Chemistry*; Marcel Dekker Inc: New York and Basel, 2002; pp 653 - 673.
- (26) Theng, B. K. G. *The Chemistry of Clay-Organic Reactions*; Adam Hilger: London, 1974.
- (27) Biasci, L.; Aglietto, M.; Ruggeri, G.; Ciardelli, F. *Polymer* **1994**, *35*, 2296 - 3304.
- (28) Yermiyahu, Z.; Lapides, I.; Yariv, S. *Applied Clay Science* **2005**, *30*, 33 - 41.
- (29) Xi, Y.; Ding, Z.; He, H.; Frost, R. L. *Journal of Colloid and Interface Science* **2004**, *277*, 116 - 120.
- (30) Badran, A.; Youssef, A.; El-Hakim, A. A. *Polymer Bulletin* **2004**, *53*, 9 - 17.
- (31) Vaia, R. A.; Teukolsky, R. K.; Giannelis, E. P. *Chemistry of Materials* **1994**, *6*, 1017 - 1022.
- (32) Lee, S. Y.; Kim, S. J. *Journal of Colloid and Interface Science* **2002**, *248*, 231 - 238.
- (33) McMurry, J.; Begley, T. *The Organic Chemistry of Biological Pathways*; Roberts and Company Publishers, 2005.
- (34) Li, H.; Yu, Y.; Yang, Y. *European Polymer Journal* **2005**, *41*, 2016 - 2022.
- (35) Bunzli, J. G.; Chauvin, A.; Imbert, D. *Proton transfer reactions*; Swiss Federal Institute of Technology, 2003.
- (36) Choi, Y. S.; Chung, I. J. *Polymer* **2004**, *45*, 3827 - 3834.
- (37) Park, S.; Seo, D.; Lee, J. *Journal of Colloid and Interface Science* **2002**, *251*, 160 - 165.
- (38) Kalendova, A.; Pospisil, M.; Kovarova, L.; Merinska, D.; Valaskova, M.; Vlkova, H.; Simonik, J.; P. Capkova. *Plastics Rubbers Composites* **2004**, *33*, 279

Results and discussions

- 287.

- (39) Mermut, A. R.; Lagaly, G. *Clay and Clay Minerals* **2001**, *49*, 393 - 397.
- (40) Stadtmueller, I. M.; Ratinac, K. R.; Ringer, S. P. *Polymer* **2005**, *46*, 9574 - 9584.
- (41) Usuki, A.; Kawasumi, M.; Kojima, Y.; Okada, A.; Kurauchi, T.; Kamigaito, O. *Journal of Materials Research* **1993**, *8*, 1174 - 1178.

Characterization of poly(styrene-co-butylacrylate)-clay nanocomposites

6.1 Introduction

This chapter focuses on the characterization of the structures and determination of the properties of poly(S-co-BA) nanocomposites, which were synthesized via batch emulsion polymerization using the different clay modifiers (AMPS, Cops, NIPA, and MET). The chemical structure of the clay modifiers was shown in Table 5.1.

In order to study the effects of incorporation of clay into polymers, neat poly(styrene-co-butylacrylate) was synthesized under conditions similar to those used to synthesize the nanocomposites. The properties of the copolymer-clay nanocomposites were compared with those of pure copolymer.

Different organic compounds were used to modify clay (see Chapter 5), before it was used to prepare nanocomposites. In the literature, AMPS has been used to synthesize nanocomposites materials and exfoliated structures were obtained¹⁻³. On the other hand, attempts to prepare nanocomposites using Cops, NIPA, and MET as the clay modifiers have not been reported yet.

SAXS TEM and SEM were used to characterize the structures of nanocomposites (conventional, intercalated and exfoliated). The thermal properties of the products were characterized using TGA. DMA was used to determine the mechanical properties and T_g . FT-IR was used to determine the compositions of the nanocomposites. The molecular weight of the polymer in the nanocomposites was determined by GPC.

6.2 Synthesis of poly(styrene-co-butylacrylate)

The main purpose of the synthesis of poly(S-co-BA) was to use it as a reference, to study the effect of the presence of the clay filler on thermal and mechanical properties of poly(S-co-BA) relative to poly(S-co-BA) nanocomposites. Poly(S-co-BA) was prepared

Results and discussions

under conditions similar to those employed for the preparation of nanocomposites (see Section 4.8.1).

The ^1H NMR spectrum of poly(S-co-BA) is shown in Fig. 6.1. There are no ethylenic protons at $\sim 5.2, 5.75$ ppm. The small signal at $3.3\sim 3.8$ ppm is ascribed to the proton belonging to the butylacrylate. The relative amounts of styrene and butylacrylate monomer units incorporated into the copolymer were determined using ^1H NMR, by integration of specific peaks belonging to the styrene and butylacrylate monomer units. The following equation was used:

$$PS\% = \frac{A/5}{A/5 + B/2}$$

where PS% is the percentage of polystyrene in the copolymer, and A and B are the integrated peaks of styrene and butylacrylate respectively. Poly(S-co-BA) contained 64.0% styrene and 36.0% butylacrylate at 90% conversion. Poly(S-co-BA) was also characterized using FT-IR (see Section 6.4.1).

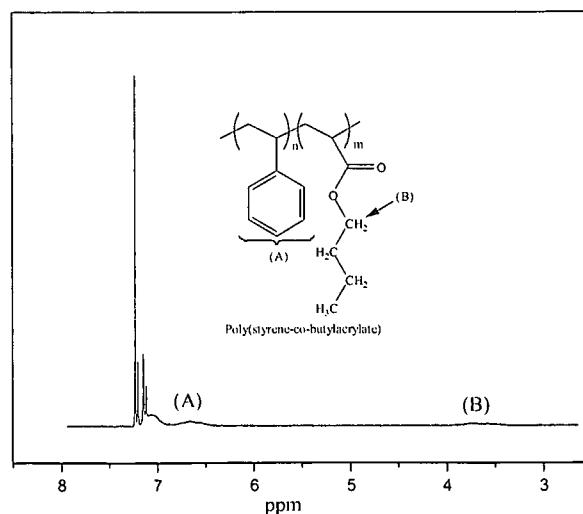


Fig. 6.1: ^1H NMR spectrum of poly(styrene-co-butylacrylate). Note that the distribution of monomer units in the copolymer is expected to be random.

6.3 Nanocomposites via batch emulsion polymerization

Batch emulsion polymerization was used to synthesise poly(S-co-BA) nanocomposites with different clay modifiers. The characterization of nanocomposite structures (conventional, intercalated and exfoliated), and the determination of their properties (thermal and mechanical) are described in the following sections.

6.3.1 Analysis of the composition of poly(styrene-co-butylacrylate) nanocomposites by FT-IR

Although FT-IR analysis of a polymer is rather complicated ⁴, FT-IR is the most widely used technique employed to characterize polymers. In the case of polymer-nanocomposites the FT-IR spectra are especially complicated due to the presence of clay particles plus the organic modifier molecules in the polymer ⁵. Table 6.1 shows the main vibration bands that can be seen in the FT-IR spectra of poly(S-co-BA) and poly(S-co-BA)-clay nanocomposites (at 100% CEC). The FT-IR spectra are shown in Appendix C: Fig. 1-5.

*Results and discussions***Table 6.1: FT-IR data of poly (S-co-BA)-clay nanocomposites (at 100% CEC)**

	Poly(S-co-BA)	Poly(S-co-BA)- AMPS-MMT	Poly(S-co-BA)- Cops-MMT	Poly(S-co-BA)- NIPA-MMT	Poly(S-co-BA)- MET-MMT
Groups	Wavelength (cm ⁻¹)	Wavelength (cm ⁻¹)	Wavelength (cm ⁻¹)	Wavelength (cm ⁻¹)	Wavelength (cm ⁻¹)
Si-O		464, 520, 1042	464, 520	531, 466	464, 520
Al-O		621	628	621	628
>C-C<	1023, 762, 692	1034, 761, 698	1034, 761, 698	1031, 762, 699	1036, 761, 698
-C-H	2936, 2873	2922, 2875	2922, 2875	2930, 2873	2930, 2875
C=O	1737	1737	1737	1737	1740
Ar-H	3022, 3056, 3078	3030, 3062, 3078	3031, 3061, 3085	3025, 3058, 3085	3024, 3070, 3085
-CH ₂ -	1454, 1490	1448, 1494	1448, 1494	1449, 19493	1448, 1494
>C=C<	1941, 1624	1947, 1604	1947, 1064	1949	1947

Evidence of the formation of poly(S-co-BA) nanocomposites was obtained by comparing the FT-IR spectrum of pure poly(S-co-BA) (Appendix C: Fig. 1) with that of a poly(S-co-BA) nanocomposite (Appendix C: Figs. 2- 4). The vibration bands at 465 and ~520 cm⁻¹ are associated with Si-O groups of clay ⁶, while the adsorption band at ~621cm⁻¹ is related to Al-O stretching of the clay ^{3,7}. The adsorption bands at 1737cm⁻¹ and the bands in the range 3022~3085cm⁻¹ are associated with C=O and with hydrogen atoms attached to aromatic carbon atoms (Ar-H) of poly(S-co-BA), respectively ⁸. Some expected bands could not be seen in the FT-IR spectrum due to the presence of different bands belonging to polymer, clay and surfactant, leading to complication of the FT-IR spectrum. However, FT-IR analysis shows at least that all the components that form nanocomposite materials were found to be present in the final material.

6.3.2 Characterization of nanocomposite structure

Three different nanocomposites structures can be distinguished, depending on the ordering and the dispersion of clay layers inside the polymer matrix, namely conventional, intercalated and exfoliated ¹.

The techniques most commonly used for characterization of the nanocomposite structures

Results and discussions

are SAXS and TEM⁹. SEM is another alternative method that can be utilized to characterize the structures of nanocomposites.

6.3.2.1 Characterization of nanocomposite structures by SAXS

The intercalation of the polymer chains into clay galleries leads to increases in the interlayer spacing relative to the original interlayer spacing of the modified clay. The change in interlayer distance can be observed by SAXS analysis¹⁰.

When the intercalated structure forms, some polymer chains penetrate between the clay galleries and the interlayer spacing is increased, leading to a shift of the diffraction peak towards lower angle values. In the case of an exfoliated structure no diffraction peaks appear in SAXS diffractograms due to loss of structural registry of the layers, i.e. the d-spacing becomes very large (>10 nm)^{11,12}, and consequently the individual clay sheets are no longer regularly oriented parallel to each other.

The SAXS patterns in Fig. 6.2 shows Na⁺-MMT peaks for all nanocomposites at 1% to 10% clay loading, proving that the SAXS equipment is able to detect such small quantities of clay dispersed through the polymer matrix.

Results and discussions

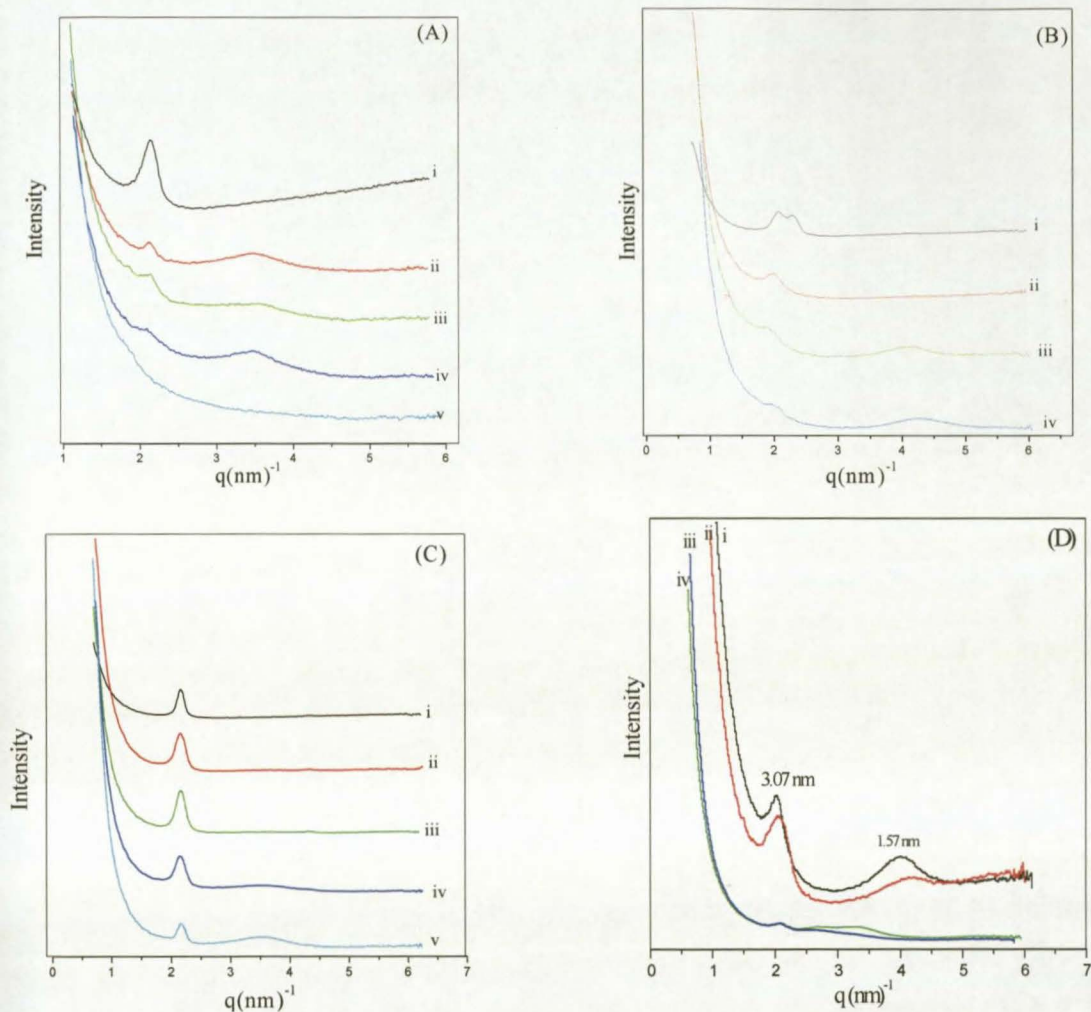


Fig. 6.2: SAXS patterns for poly(styrene-co-butylacrylate) nanocomposites: (A) poly(styrene-co-butylacrylate)-AMPS nanocomposites i-v represent nanocomposites containing 1%, 3%, 5%, 7% and 10% clay respectively, (B) poly(styrene-co-butylacrylate)-NIPA nanocomposites i-iv represent nanocomposites containing 1%, 3%, 7% and 10% clay respectively, (C) poly(styrene-co-butylacrylate)-Cops nanocomposites i-iv representing nanocomposites containing 1%, 5%, 7% and 10% clay, (D) poly(styrene-co-butylacrylate)-MET-nanocomposites i-iv representing nanocomposites containing 1%, 5%, 7% and 10% clay respectively.

The SAXS patterns in Fig. 6.2 (A) have different profiles, depending on the quantities of clay incorporated into the poly(S-co-BA). According to the SAXS patterns, the structure of the nanocomposites was found to be influenced by the clay content. The peak appearing for poly(S-co-BA)-AMPS nanocomposites at low clay loading (1% and 3%) (Fig. 6.2 A (i and ii)), indicated that an intercalated structure was obtained at low clay percentage. However, in the case of nanocomposites with 7% clay (Fig. 6.2 A (iv)), a broad peak was observed, indicating the formation of a partially exfoliated structure¹³.

Results and discussions

Even more surprisingly, no peak was found in the SAXS patterns of poly(S-co-BA)-AMPS nanocomposite with 10% clay, suggesting that the clay platelets are fully exfoliated within the polymer matrix.

The formation of an exfoliated structure at high clay level is unusual. It is known that the exfoliated structure is easily obtained when the clay percentage is less than 10%¹⁴. However, Choi *et al.*² successfully prepared nanocomposite structures at 20% clay loading. The author interpreted these results based on a thermodynamic factor. In the presence of high clay loading the clay platelets are close to each other, and consequent platelet movement can generate energy by friction. This energy might lead to more free movement of the clay platelets, thus randomizing their orientation. On the other hand, this energy cannot be generated at low clay loading due the huge distances between clay platelets.

In the present work, the use of high clay loading (i.e. more than 10%) yielded a very viscous latex after only 2 h of reaction, using the batch emulsion polymerization method. Semi-batch emulsion polymerization (see Section 6.4) was then used in an attempt to overcome these high viscosity problems.

The SAXS patterns in Fig. 6.2 prove that the final nanocomposite structure is influenced by the clay modifiers used to modify the clay surface. These results also demonstrated that the structure of the obtained nanocomposites depends on the clay/polymer ratio. SAXS patterns for nanocomposites prepared using AMPS (see Fig. 6.2 A (i-iii)) show peaks when the clay loading is 1-5%, indicate that an intercalated structure was formed. A broad peak at 7% clay loading indicated that partially exfoliated was obtained. No peak at a clay loading of 10% suggests the formation of a fully exfoliated structure. Fig. 6.2 (B) also shows SAXS patterns for a series of nanocomposites prepared using NIPA as clay modifier. The presence of Na⁺-MMT peaks for nanocomposites with 1-5% clay loading indicated that an intercalated structure was probably obtained. Broader peaks were observed as the clay loading increased, indicating that an exfoliated-intercalated (partially exfoliated) structure formed when the clay loading was between 7% and 10%. The nanocomposite structures obtained using AMPS and NIPA were found to be slightly different. An exfoliated structure was obtained with AMPS while a partially exfoliated

Results and discussions

structure was obtained when NIPA was used. This could be due to the high polarity of AMPS head groups compared to NIPA, and also because AMPS is adsorbed to the clay surface more strongly as was discussed in Section 5.4.2.

The SAXS patterns of nanocomposites prepared using Cops as clay modifier, Fig. 6.2 (C) show peaks for all clay loadings. This means that the intercalated structure was formed for the full range of clay content. Although Cops molecules have the ability to enlarge the basal spacing of clay, as was demonstrated in Section 5.2.3, only intercalated structures were obtained, showing that the formation of exfoliated nanocomposites might not always depend on the expansion of the interlayer by a clay modifier. Similarly, Wan *et al.*¹⁵ found that although the clay interlayer distance was extended to 2.1 nm, when the clay was surface-modified using dimethyldioctadecyl ammonium, only intercalated structures were obtained.

It was expected that nanocomposites obtained using Cops as clay modifier would result in an intercalated structure, due to the nature of the chemical structure of Cops itself. Cops molecules are hydrophilic molecules, due to the presence of the sulphate head group, and also due to a hydroxyl group on the main chain of the Cops molecule. The hydrophilicity of Cops may have limited the migration of hydrophobic monomers (styrene and butylacrylate) inside the clay galleries. Therefore, most of the monomers will polymerize outside the clay galleries (i.e. the rate of polymerization outside galleries will be greater than that inside), resulting only in intercalated structures. Furthermore, the formation of an intercalated nanocomposites structure by Cops could also be due to the very poor reactivity of its polymerizable group (i.e. the vinylic group) towards the monomers used (i.e. styrene and butylacrylate). Thus the few monomers which entered inside the clay galleries would not copolymerize with Cops molecules, and in turn acts as locus for more hydrophobic monomers. This subsequently limits changes to the interfacial adhesion between polymer matrix and clay, leading to the formation of an intercalated structure. Blumstein¹⁶ found that in order to improve the strength of the interface between clay and the polymer matrix the organic modifiers used to modify the clay should have functional groups that can interact with the polymer matrix or initiate the polymerization. Qutubuddin and Fu¹⁴ obtained intercalated structures when non-

Results and discussions

polymerizable surfactants were used, while exfoliated structures were obtained with polymerizable surfactants.

On the contrary, the MET molecule is hydrophobic due to the long hydrocarbon chain length, thus rendering it compatible with hydrophobic monomers¹⁷. This facilitated the monomer entry between the clay galleries¹⁸, allowing much of the polymerization to occur inside the clay galleries, leading to a partially exfoliated nanocomposite structure.

Furthermore, the nature of the polymerizable group of MET is an ester of methacrylic acid, and the methacrylic derivative is an example of a very reactive polymerizable surfmer¹⁹. The high reactivity of the polymerizable group of MET enables it to copolymerize easily with monomers. The copolymerization of monomers with MET resulted in the extensive movement of clay platelets, yielding the partially exfoliated nanocomposite as seen in Fig. 6.2 D (iv).

SAXS patterns of poly(styrene-co-butylacrylate)-MET nanocomposites in Fig. 6.2 (D), shows two peaks corresponding to a basal spacing at 3.07 nm and 1.57 nm. The second peak (i.e. 1.57 nm) is a second order peak due to the lamellar structure of clay.

The reason for the difference in nanocomposite structures might be the result of thermodynamic effects. Here it is necessary to look at the interactions between the clay and polymer, clay and organic modifiers, and polymer and organic modifiers. An optimum balance of all these interactions generally leads to an exfoliated nanocomposite²⁰. AMPS molecules seem to have favourable balance of all interactions, the presence of sulphate and amide groups in the AMPS structure allows it to interact easily with clay by formation of hydrogen bonding. Furthermore, because AMPS has an amphiphilic character³, it can also interact with monomer. All of these factors could be reasons for obtaining exfoliated structures when AMPS was used.

The complete intercalation of silicate layers cannot be judged only from SAXS diffractograms. TEM was used to confirm the morphology of nanocomposites

Results and discussions

6.3.2.2 Characterization of nanocomposite structures by TEM

TEM is an excellent qualitative analytical technique for the characterization of the extent of clay dispersion in polymer-clay nanocomposites¹³. Fig. 6.3 shows TEM images of poly(S-co-BA)-AMPS nanocomposites containing 1% and 5% clay, respectively.

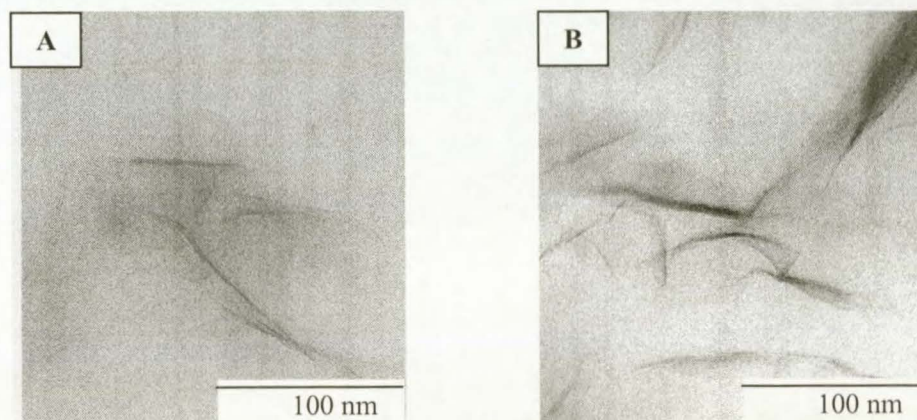


Fig. 6.3: TEM images of intercalated poly(S-co-BA)-AMPS nanocomposites containing: (A) 1% clay, and (B) 5% clay loading.

Fig. 6.3 shows high stacking of clay layers. This indicates that the silicate layers did not disperse very well in the polymer matrix, leading to the formation of intercalated structures. These results confirmed the results that were obtained by SAXS measurement (Section 6.4.2). Fig. 6.4 shows TEM images for poly(S-co-BA)-AMPS nanocomposites containing 7% and 10% clay loading respectively.

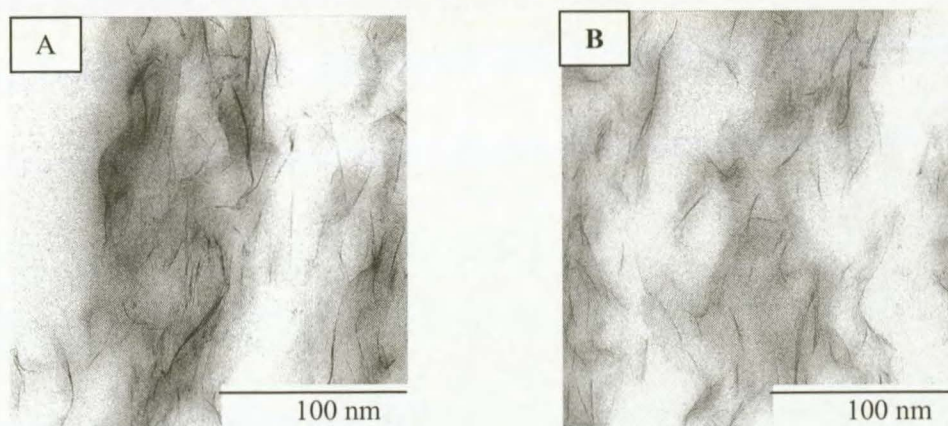


Fig. 6.4: TEM images for partially exfoliated poly(S-co-BA)-AMPS nanocomposites at: (A) 7% clay loading, and (B) exfoliated poly(S-co-BA)-AMPS nanocomposites at 10% clay loading.

The dark lines represent the silicate layers and the polymers matrix appears as relatively

Results and discussions

bright domains. The TEM image of poly(S-co-BA)-AMPS nanocomposites at 7% clay loading is shown in Fig. 6.4 (A). Results indicate that some of the clay platelets dispersed as single layers, while some other layers were still stacked in an orderly manner. This means that the silicate layers are partially exfoliated in the polymer matrix, and the nanocomposite structure was found to be dependent on the clay/polymer ratio. This confirmed the result of SAXS measurement. On the other hand, as the percentage of clay loading increased to 10%, the silicate layers are completely separated from each other, as can be seen in Fig. 6.4 (B). The silicate layer edges appear as thin dark lines, well distributed through the polymer matrix. Hence an exfoliated structure was obtained, which confirmed the SAXS results.

TEM images for poly(S-co-BA)-NIPA nanocomposites containing different clay loadings are shown in Figs. 6.5 and 6.6.

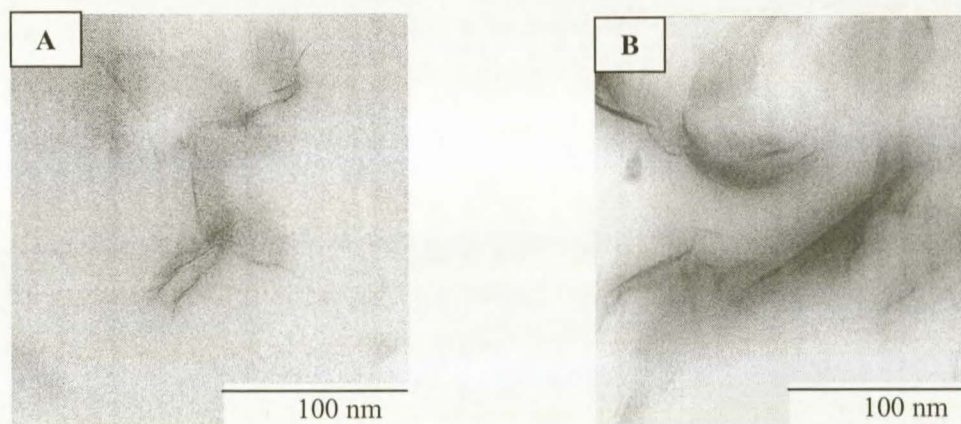


Fig. 6.5: TEM images for intercalated poly(S-co-BA)-NIPA nanocomposites at: (A) 1% clay loading and (B) 3% clay loading.

Fig. 6.5 shows high stacking of clay layers with the aggregation in micrometer size. This indicated an intercalated structure and that the silicate layers maintained their ordering. This confirmed SAXS results. The intercalated structure was formed when NIPA was used as clay modifier at a clay loading of 1% and 3%.

Results and discussions

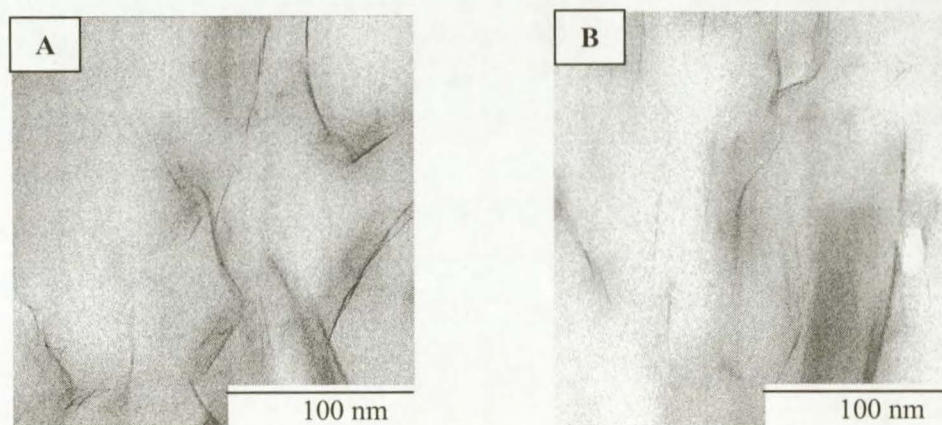


Fig. 6.6: TEM images for poly(S-co-BA)-NIPA nanocomposites at different clay loadings: (A) 7% and (B) 10% clay.

It is clear from the TEM images in Fig. 6.6 that some of the clay layers were still stacked with each other, as seen by the very dark areas, while some individual clay layers were well distributed into the polymer matrix. This means that the clay layers were partially exfoliated into the polymer matrix and an exfoliated/intercalated (partially exfoliated structure) was obtained. This is in agreement with SAXS results given in Section 6.4.2. On the other hand the completely intercalated structures were obtained when Cops was used as clay modifier. Fig. 6.7 TEM image shows an intercalated structure of poly(S-co-BA)-Cops nanocomposite at 10% clay loading.

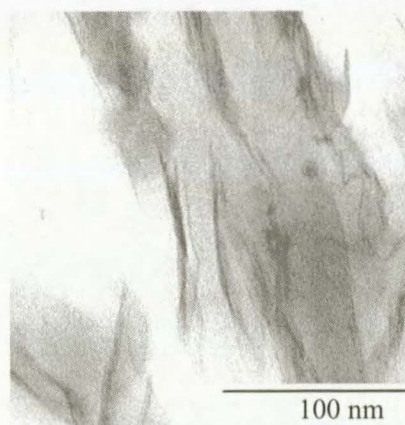


Fig. 6.7: TEM image of intercalated structure of poly(S-co-BA)-Cops nanocomposites at 10% clay loading.

The nanocomposites synthesized using Cops as clay modifier had an intercalated

Results and discussions

structure. This was confirmed by TEM analysis, as can be seen in Fig. 6.7, where the thick black lines are related to groups of clay layers still strongly bound to each other, yielding the intercalated structure. This was the case for all nanocomposites prepared using Cops as a clay modifier. The TEM results are in agreement with the SAXS results.

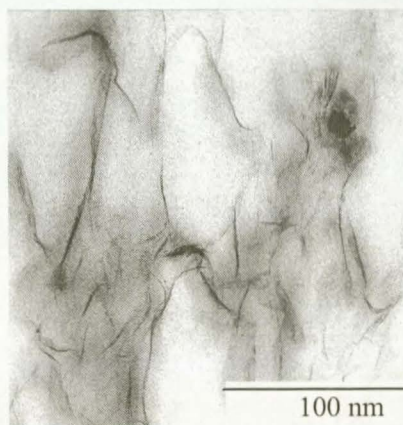


Fig. 6.8: TEM image of poly(S-co-BA)-MET nanocomposite at 10% clay loading.

The TEM image of the nanocomposite prepared using MET as clay modifier illustrates that some clay layers are bound to each other, while other clays layer are completely separated from each other. This result indicated that a partially exfoliated structure was obtained when MET was used.

6.3.2.3 Study of the morphology of nanocomposites using SEM

SEM analysis is not a commonly used method to characterize the morphology of nanocomposite materials, because of a limitation of this technique it is difficult to see the clay particles in the polymer matrix. However, SEM was used by Zaman²¹ to characterize the surface of nanocomposites; he used SEM to study the surface of unsaturated polyester nanocomposites. He found that the polymer region appears as a dark area, while the clay particles are appear as a light area, and finally concluded that the clay particles appeared to be not uniformly dispersed through the polymer matrix. SEM analysis was also used by Lei *at al.*²² who observed the clay particles using SEM. They found that clay particles are randomly dispersed into the polymer matrix. Fig. 6.9 shows the SEM images of the surface of a film of exfoliated and intercalated nanocomposites (i.e. nanocomposites synthesised using AMPS and Cops at 10% clay loading).

Results and discussions

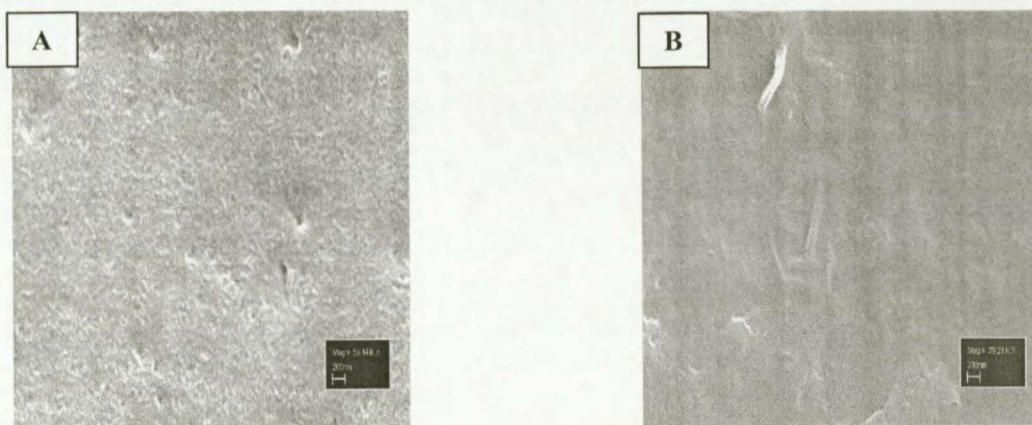


Fig. 6.9: SEM images of (A) poly(S-co-BA)-AMPS nanocomposite containing 10% clay, and (B) poly(S-co-BA)-Cops nanocomposite containing 10% clay.

From the SEM images in Fig. 6.9 it was not possible to see clay nanoparticles, this might be due to clay nanoparticles being completely covered by polymer matrix, and therefore the SEM images just show the smooth regions related to polymer, and the clay cannot be seen.

6.3.3 Determination of the molecular weights of nanocomposites

The molecular weights of the polymer in nanocomposites were determined after removal of all the clay. The results are shown in Table 6.2.

In general all of the synthesized polymers were found to have very high molecular weight. This is commonly observed for polymers prepared by polymerization in emulsion. Indeed in emulsion polymerization, termination by recombination is unlikely since theoretically only one radical is present in the micelle²³. This is verified in work done by Wang *at el.*²⁴ who synthesized polystyrene nanocomposites via different polymerization methods (bulk, suspension, solution, and emulsion polymerization), and showed that the highest molecular weight was observed for emulsion polymerization, followed by suspension, bulk, and solution polymerization²⁴.

Another reason for obtaining high molecular weight is the limitation of diffusion of propagating species during the polymerization system due to the high viscosity. The viscosity inside the polymer particles increases as the polymerization progresses, therefore the movement of propagating species will become extremely slow, making the

Results and discussions

termination unlikely. Table 6.2 shows the molecular weights of all the nanocomposites synthesised in this study, using emulsion polymerization.

Table 6.2: Variation of molecular mass and polydispersity index (PDI) with clay loading of the poly(S-co-BA)-clay nanocomposites

Sample	Clay content (%)	$\bar{M}_n \times 10^{-3}$ (g/mol)	$\bar{M}_w \times 10^{-3}$ (g/mol)	PDI \bar{M}_w/\bar{M}_n
Poly(S-co-BA)	0	277	848	3.05
Poly(S-co-BA)-AMPS nanocomposites	1	290	888	3.05
	3	338	839	2.56
	5	279	767	2.74
	7	293	721	2.45
	10	109	445	4.04
Poly(S-co-BA)-Cops nanocomposites	1	270	955	3.52
	3	299	942	3.14
	5	349	843	2.41
	7	305	763	2.49
	10	241	765	3.16
Poly(S-co-BA)-NIPAn Nanocomposites	1	417	971	2.33
	5	365	912	2.5
	7	367	880	2.4
	10	343	823	2.40
Poly(S-co-BA)-MET nanocomposites	1	380	1140	3.00
	5	391	961	2.46
	7	356	1245	3.5
	8	361	916	2.54

The concentration of clay has a significant effect on the molecular weight of polymer nanocomposites. The molecular weight of poly(S-co-BA) in the nanocomposites was found to slightly decrease as the clay concentration increased. Choi *et al.*⁶ observed a similar effect of clay on the molecular weight. They found that the molecular weight of nanocomposite materials is 60-90% lower in the presence of clay than in its absence, and interpreted their results as follows: clay acts as an additional micelle, thus polymerization occurs in more micelles and the molecular weight consequently decreases^{6,24}. Furthermore, the presence of clay particles in a polymerization system can hinder the growth of polymer chains, also leading to a decrease in molecular weight as the clay concentration increases.

Results and discussions

6.3.4 Study of the thermal properties of nanocomposites

Fig. 6.10 shows the thermal stability of pure poly(S-co-BA), and of some different poly(S-co-BA) nanocomposites, as determined by TGA analysis.

All synthesized nanocomposites are more thermally stable relative to neat poly(S-co-BA). This indicated that the incorporation of clay into the poly(S-co-BA) nanocomposite leads to improved thermal stability of the copolymer ²⁵.

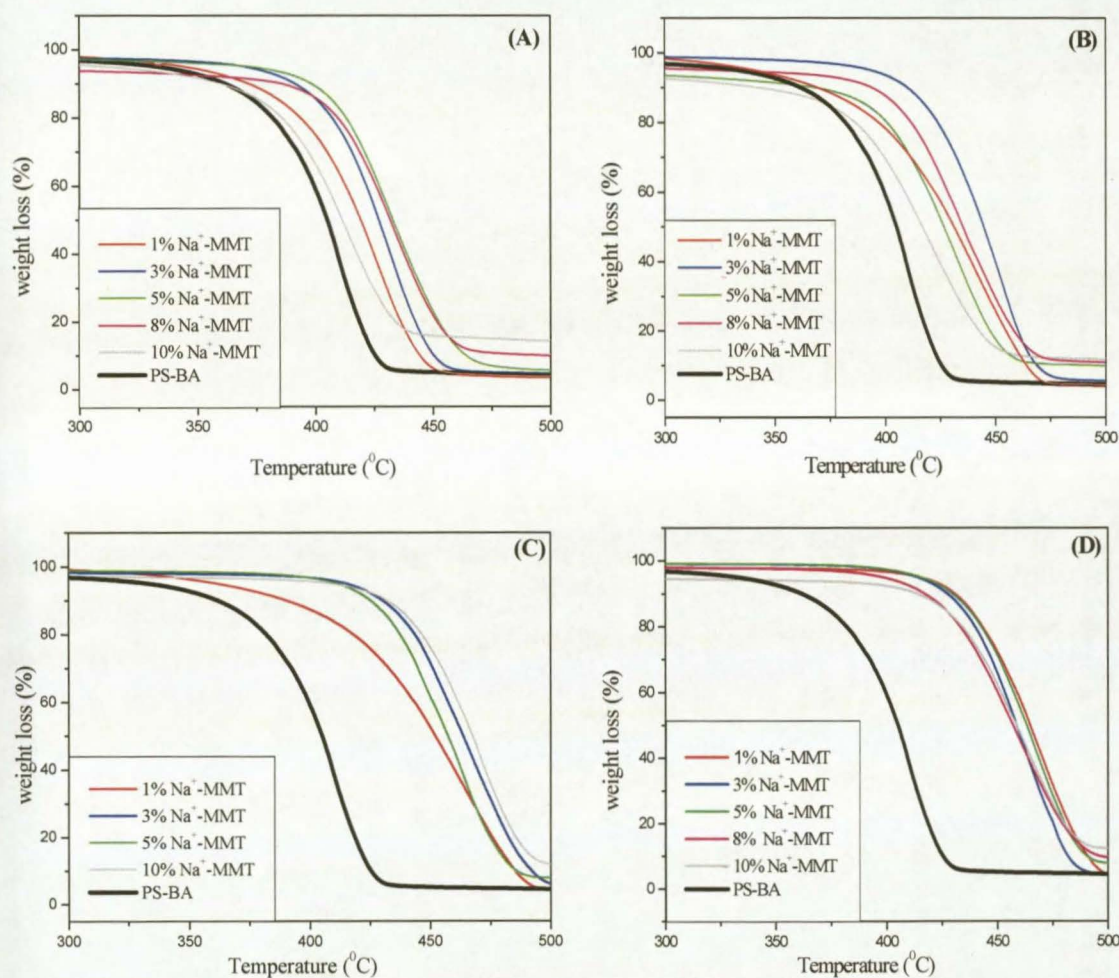


Fig. 6.10: (A-D) Thermal stability of poly(S-co-BA)-clay nanocomposites as a function of clay loading. The inserts show the amount of clay in the thermograms, as a percentage and the organic compounds used to make the organoclays: (A) Poly (S-co-BA)-AMPS nanocomposites (B) Poly(S-co-BA)-MET nanocomposites (C) Poly(S-co-BA)-Cops nanocomposites (D) Poly(S-co-BA)-NIPA nanocomposites.

The improvement in thermal stability of the polymer in the presence of clay is generally attributed to the formation of clay char that acts as a mass transport barrier and an

Results and discussions

insulator between the bulk polymer and surface area where the combustion of polymer occurs ^{26,27}. The presence of clay could also hinder the diffusion of volatile decomposition products within the nanocomposites ²⁶. The enhancement of the nanocomposites thermal stability has also been attributed to the restricted thermal motion of polymer chain inside the clay galleries ¹⁶.

TGA results shown in Fig. 6.10 indicate that the improvement in thermal stability is not simply a function of clay loading. For instance, the nanocomposites synthesized using AMPS as clay modifier (Fig. 6.10 (A)), showed the highest thermal stability for 3% clay loading. This is in accordance with findings of Doh and Choi ²⁸, who reported that the maximum thermal stability of polystyrene nanocomposites is reached when only 0.3% clay is used.

In order to see the effects of the dispersion states of clay on the thermal stability, four different nanocomposites containing similar clay loading are compared to each other, as shown in Fig. 6.11 and Table 6.3.

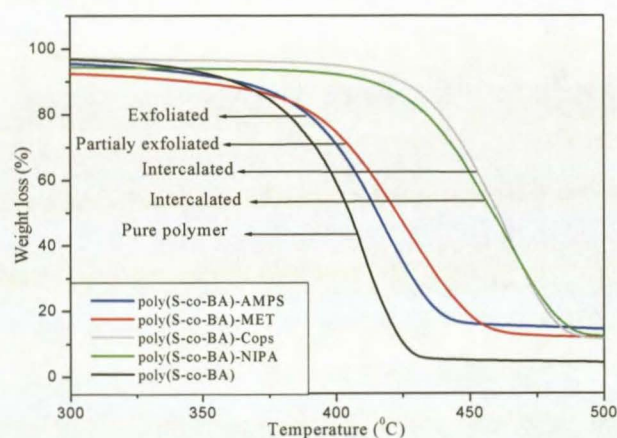


Fig. 6.11: Comparison of the thermal stability of four different nanocomposites at similar clay loadings. The thermogram of poly(S-co-BA) is included as a reference.

*Results and discussions***Table 6.3 : TGA data for poly(S-co-BA) nanocomposites at similar clay loading (10%)**

Sample	T10%	T50%	% Clay i.e. % Char * 600°C
Poly(S-co-BA)	363	405	-
Poly(S-co-BA)-AMPS-nanocomposites	365	415	10.00
Poly(S-co-BA)-MET-nanocomposites	365	434	11.02
Poly(S-co-BA)-Cops-nanocomposites	421	459	10.30
Poly(S-co-BA)-NIPA-nanocomposites	413	454	11.00

* $T_{10\%}$, $T_{50\%}$ and % clay in nanocomposites i.e. % Char $_{600^{\circ}\text{C}}$ represents the onset of decomposition taken at 10% decomposition, temperature at 50% decomposition and the % remains (char) at 600°C respectively.

Table 6.3 and Fig. 6.11 show that the onset temperature for exfoliated nanocomposites is limited when compared to neat polymer, while in the case of intercalated nanocomposites the temperature sharply increased by 50 - 58°C. In addition, the temperature at which 50% degradation occurs increased by 10 - 30°C in the case of exfoliated and partially exfoliated structures and by 55 - 60°C for the intercalated structure, relative to pure copolymer. These results indicate that the intercalated nanocomposites show higher thermal stability improvement than exfoliated and partially exfoliated nanocomposites, i.e. poly(S-co-BA)-cops-MMT is more thermally stable than the poly(S-co-BA)-MET-MMT and poly(S-co-BA)-AMPS-MMT nanocomposites. However, it was reported that exfoliated nanocomposite structures have higher thermal stability than intercalated structures ^{7,29}. Similar unexpected results have been reported by Giannelis *et al.* ³⁰ who synthesized exfoliated and intercalated poly(ethyleneimine), both at similar clay loading, and found intercalated nanocomposites to be more thermal stable than exfoliated ones. Samakande *et al.* ³¹ also observed similar results with polystyrene-clay nanocomposites prepared by bulk free radical polymerization. They interpreted their results as follows: in the case of the intercalated structure there are several closely packed layers of clay (stacked layers) which provide a more efficient barrier between the burning zone and the underlying flammable material that is being gasified.

Table 6.3 and Fig 6.11 show that the percentage of clay (i.e. %Char at 600°C), is slightly

Results and discussions

higher than the theoretical clay percentage. Initially it was expected that the %Char at 600°C would be close to the initial clay percentage. These unexpected results are probably because of incomplete conversion of polymerization. The conversion at the end of polymerization was found to be between 90 and 92%, giving an experimental clay content that is slightly higher than expected.

6.3.5 Study of the mechanical properties of nanocomposites

All nanocomposites that were synthesized showed higher storage modulus relative to that of the virgin copolymer, as shown in Table 6.4 below (where G^1 is storage modulus). The storage modulus found in the plateau below T_g increased slightly as the clay loading increased, in agreement with the literature^{1,14,32}. The incorporation of clay particles with a high aspect ratio, such as montmorillonite³³, leads to increases in the storage modulus. This could be due to an interaction between the polymer and silicate layers at the interface of layers and the polymer matrix, which can suppress the mobility in the polymer segments near the interface, leading to improved mechanical properties^{17,26,34}.

*Results and discussions***Table 6.4:** T_g values and storage modulus of nanocomposites

Sample	% clay	$G' \times 10^8$ (Pa)	T_g (°C)
Poly(S-co-BA)	0	2.07	24
Poly(S-co-BA)-MET nanocomposite	1	2.25	27
	5	2.81	32
	7	2.83	36
	10	3.00	36
Poly(S-co-BA)-NIPA nanocomposite	1	2.32	29
	5	2.60	29
	7	2.60	33
	10	2.77	33
Poly(S-co-BA)-Cops nanocomposite	1	2.54	27
	5	2.68	30
	7	2.77	33
	10	2.58	33
Poly(S-co-BA)-AMPS nanocomposite	1	2.40	30
	5	2.40	34
	7	2.73	38
	10	2.95	41

Exfoliated poly(S-co-BA)-AMPS-MMT nanocomposites show a relatively higher storage modulus in comparison to the intercalated poly(S-co-BA)-Cops-MMT nanocomposites, and to the partially exfoliated poly(S-co-BA)-NIPA-MMT nanocomposites. Similar results were reported by Choi *et al.*¹, who found that the exfoliated structure of poly(styrene-co-acrylonitrile) has a storage modulus higher than the intercalated structure of a similar copolymer.

Fig. 6.12 shows the variation in storage modulus and $\tan \delta$ vs. temperature for pure poly(S-co-BA) and of four different nanocomposites.

Results and discussions

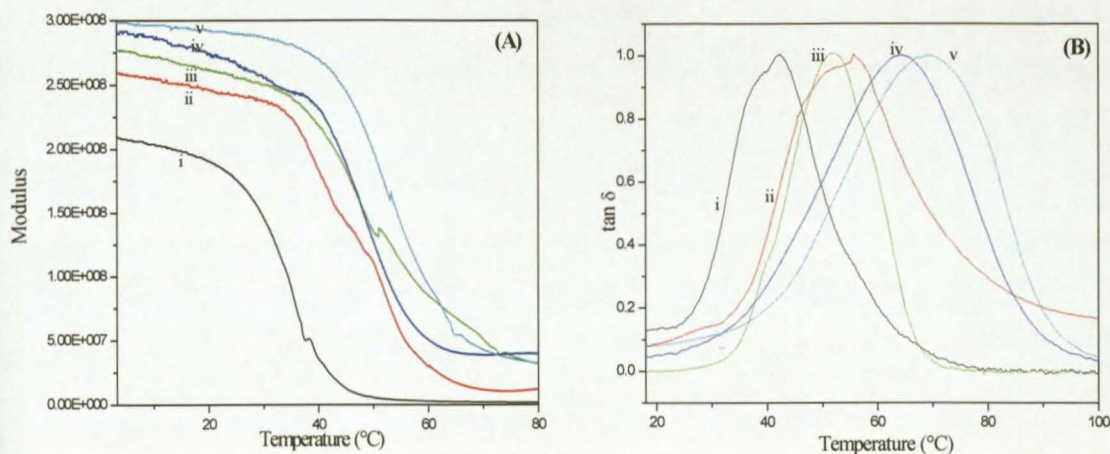


Fig. 6.12: Variation of (A) storage modulus and (B) $\tan \delta$ vs. temperature for (i) pure poly(S-co-BA) and for different nanocomposites at 10% clay loading: (ii) poly(S-co-BA)-cops nanocomposite, (iii) poly(S-co-BA)-NIPA nanocomposite, (iv) poly(S-co-BA)-MET nanocomposite, and (v) poly(S-co-BA)-AMPS nanocomposite.

All of the T_g values in Table 6.4 were obtained from the onset of $\tan \delta$ plot (see Appendix D). Fig. 6.12 (B) shows that the $\tan \delta$ peaks for the nanocomposites (ii-v) shifted to higher temperature relative to that for the virgin copolymer (i), indicating that the T_g value of the nanocomposites were higher than that of the virgin copolymer. The T_g values increased slightly with an increase in clay content, as shown in Fig. 6.13. This is generally attributed to the restriction of the molecular chain motion of the copolymer, therefore the motion or relaxation of chain segments becomes difficult at the original T_g , but becomes easier at a higher temperature, i.e. the clay layers act as cross-linkers in the nanocomposite systems, leading to the restriction of motion^{1,2,34}. Although Qutubuddin and Fu¹⁴ obtained a fully exfoliated structure in polystyrene at the whole clay loading range, they observed decreases in T_g as the amount of clay increased. In their case, they interpreted these results as being due to the decrease in molecular weight of the nanocomposite with clay content. In our case the slight decrease in the molecular weight could not cause a decrease in the T_g due to the overall high molecular weight obtained.

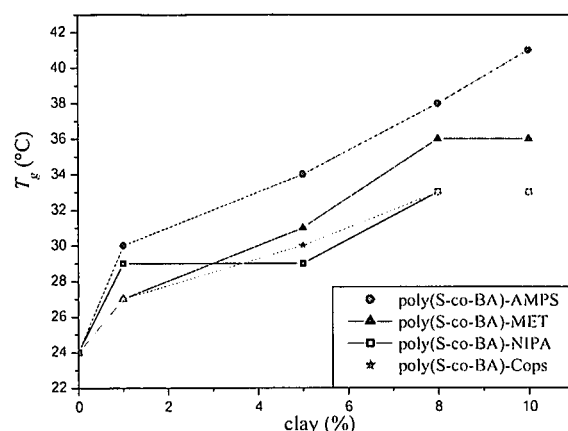
Results and discussions

Fig. 6.13: T_g values vs. clay content of four types of nanocomposites

The exfoliated nanocomposite prepared using AMPS at 10% clay loading showed a higher T_g than that for the intercalated structures of the other types of nanocomposites at similar clay loading.

In Fig. 6.12 (B) the $\tan \delta$ peaks for the nanocomposites are broader than the peak for the virgin copolymer. This also could be ascribed to the restricted polymer chain mobility due to the presence of clay fillers³⁴. The broadening of the $\tan \delta$ peak is more pronounced with exfoliated nanocomposites than with intercalated structures because the highly dispersed exfoliated clay inhibits the mobility to a greater extent than when clay is only intercalated; this could also interpret the higher T_g for exfoliated nanocomposites compared to the T_g of intercalated nanocomposites³¹.

6.4 Nanocomposites via semi-batch emulsion polymerization

In order to study whether the method of monomer addition during polymerization influences the structure and properties of the final nanocomposites, the polymerization was carried out in two stages, following a semi-batch process (see Section 4.2.3). The idea was to add only 10% of the monomers in the initial stage so as to ensure that the clay galleries become wider. In the second stage of the polymerization a slow feeding of monomers was done in order to allow time for the monomers to diffuse into the clay galleries. The objective here was to promote propagation inside the galleries at the expense of polymerization outside the clay galleries, so as to favour exfoliation.

Results and discussions

Poly(S-co-BA) nanocomposites were prepared using AMPS as clay modifier, at range clay loading from 3% - 15%.

The structures of nanocomposites were studied by TEM and SAXS. The thermal stability and mechanical properties of nanocomposites were studied by TGA and DMA respectively.

6.4.1 Characterization of the structure nanocomposites prepared via semi-batch emulsion polymerization.

TEM was used to monitor the distribution of the clay through the polymer matrix. Fig. 6.14 shows the TEM image of the poly(S-co-BA)-AMPS nanocomposite at 3% clay loading.

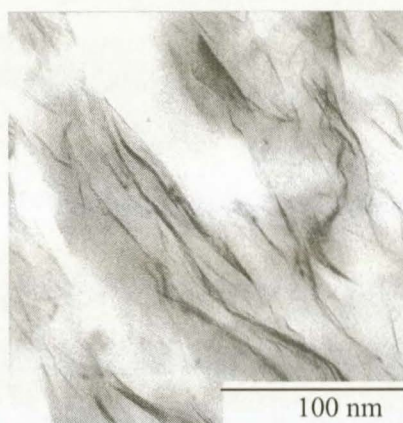


Fig. 6.14: TEM image of poly(S-co-BA)-AMPS nanocomposite at 3% clay loading

The silicate layers of clay appear as dark lines stuck to each other, indicating an intercalated structure. The same intercalated structure was obtained by batch free radical emulsion polymerization (also using also 3% clay). This shows that the semi-batch polymerization method does not bring any improvement in terms of exfoliation in these conditions. Fig. 6.15 below shows a TEM image of poly(S-co-BA)-AMPS nanocomposite at 10% clay loading.

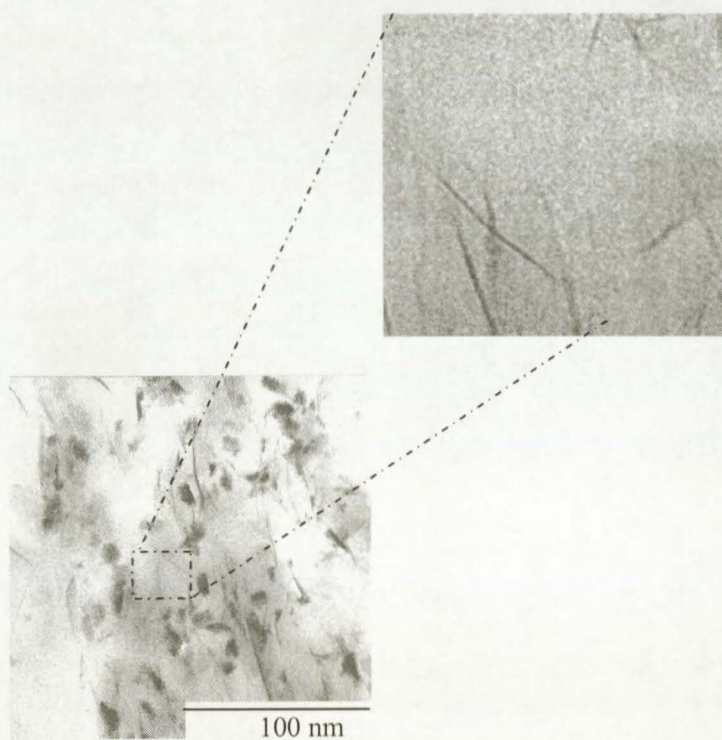
Results and discussions

Fig. 6.15: TEM image of a poly(S-co-BA)-AMPS nanocomposite at 10% clay loading.

For a 10% clay loading it is clear that the individual clay layers are dispersed uniformly in the polymer matrix. Silicate layers look like dark strips, and poly(S-co-BA) copolymer appears as relatively bright domains. Delaminated layers of silicate are well distributed through the entire copolymer matrix, so an exfoliated morphology of poly(S-co-BA) nanocomposites at 10% was obtained. Fig. 6.16 show TEM image of a poly(S-co-BA) nanocomposite at 15% clay loading.



Fig. 6. 16: TEM image for poly(S-co-BA)-AMPS at 15 % clay loading.

Results and discussions

The TEM image in Fig. 6.16 indicates that the silicate layers are still bound to each other; they appear as dark lines, meaning that the intercalated structure is obtained at 15% clay loading.

Fig. 6.17 shows the SAXS patterns of poly(S-co-BA)-AMPS nanocomposites at different clay loadings (3%, 10% and 15%).

Fig. 6.17 shows a difference in the nanocomposite structure. SAXS patterns for nanocomposites with 3% and 15% clay loading show a diffraction peak. This indicated that an intercalated structure was obtained at 3% and 15% clay loading. On the contrary, no peak was observed in the SAXS patterns of the nanocomposite with 10% clay loading, confirming the fully exfoliated structure observed by TEM.

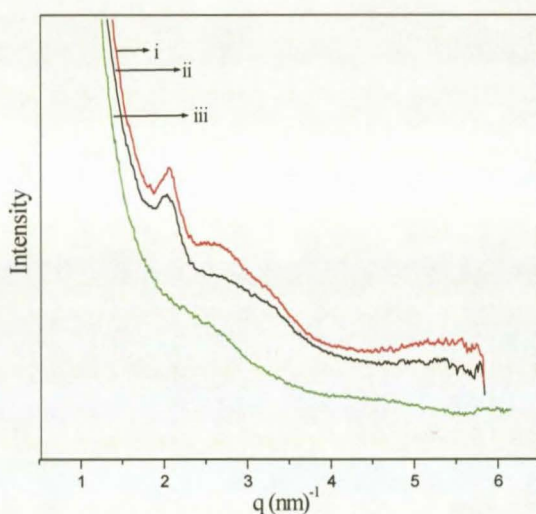


Fig. 6.17: SAXS patterns for poly(S-co-BA)-AMPS nanocomposites at different clay loading: (i) 3%, (ii) 15% and (iii) 10%

The structure of the nanocomposites prepared using semi-batch free radical emulsion polymerization was found to be identical to that observed for nanocomposites prepared using a batch emulsion polymerization process. This confirms that a slow rate of monomers does not play a significant role in the structure of the final nanocomposites obtained.

More surprisingly, the nanocomposite with 15% clay loading was found to have an intercalated structure. This is probably linked to thermodynamic and kinetic

Results and discussions

considerations, and more research in this area is recommended. The author believes that at this clay loading, the proximity of the clay platelets seems to hinder a full exfoliation as the polymerization takes place.

6.4.3 Study of the thermal stability of nanocomposites synthesized via semi-batch emulsion polymerization, by TGA

The nanocomposites (see Fig 6.18 below) were found to be more stable than neat poly(S-co-BA), as shown by a slight increase in thermal stability as clay loading increased.

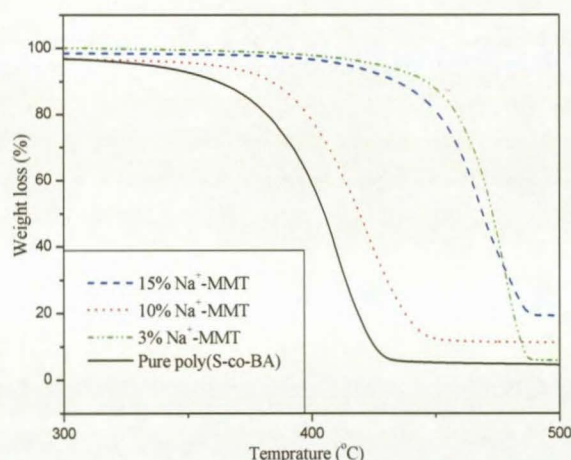


Fig. 6.18: Thermal stability of poly(S-co-BA)-AMPS nanocomposites at different clay loading. Pure poly(S-co-BA) is included in the figure as reference.

The thermal stabilities of the nanocomposites synthesized from semi-batch emulsion polymerization were found to be similar to those synthesized using batch emulsion polymerization. The intercalated nanocomposites with 15% and 3% clay loadings displayed greater thermal stability relative to the exfoliated structure with 10% clay. This could be related to the presence of some close packed layers in the case of intercalated structure, which can provide a suitable barrier between the burning zone and the underlying flammable material being gasified³¹.

Results and discussions

6.4 References

- (1) Xu, M.; Choi, Y. S.; Kim, Y. K.; Wang, K. H.; Chung, I. J. *Polymer* **2003**, *44*, 6387 - 6395.
- (2) Choi, Y. S.; Ham, H. T.; Chung, J. *Chemistry of Materials* **2004**, *16*, 2522 - 2529.
- (3) Choi, Y. S.; Ham, H. T.; Chung, I. J. *Polymer* **2003**, *44*, 8147 - 8154.
- (4) Young, R. J. *Introduction to Polymers*; Chapman and Hall Ltd: London, 1981.
- (5) Morgan, A. B.; Gilman, J. W.; Harris, R. H.; Jackson, C. L. *Materials Science and Engineering* **2000**, *83*, 52 - 54.
- (6) Choi, Y. S.; Choi, M. H.; Wang, K. H.; Kim, S. O.; Kim, Y. K.; Chung, I. J. *Macromolecules* **2001**, *34*, 8978 - 8985.
- (7) Alexandre, M.; Dubois, P. *Materials Science and Engineering*, **2000**, *28*, 1 - 63.
- (8) Zou, M.; Wang, S.; Zang, Z.; Ge, X. *European Polymer Journal* **2005**, *41*, 2602 - 2613.
- (9) Causin, V.; Mareigo, C.; Ferrara, G. *Polymer* **2005**, *46*, 9533 - 9537.
- (10) Poreter, D.; Metcalfe, E.; Tomas, M. J. K. *Fire and Materials* **2000**, *24*, 45 - 52.
- (11) Eckel, D. F.; Balogh, M. P.; Fasulo, P. D.; Rodgers, W. R. *Journal of Applied Polymer Science* **2004**, *93*, 1110 - 1117.
- (12) Haraguchi, K.; Jun, H.; Matsuda, K.; Takehisa, T.; Elliott, E. *Macromolecules* **2005**, *38*, 3482 - 3490.
- (13) Morgan, A. B.; Gilman, J. W. *Journal of Applied Polymer Science* **2003**, *87*, 1329 - 1338.
- (14) Qutubuddin, S.; Fu, X. *Polymer* **2001**, *42*, 807 - 813.
- (15) Wan, C.; Qiao, X.; Zhang, Y.; Zhang, Y. *Polymer Testing* **2003**, *22*, 453 - 461.
- (16) Blumstein, A. *Journal of Polymer Science : Part A : Polymer Chemistry* **1965**, *3*, 2653 - 2661.
- (17) Nalwa, H. S. In *Encyclopedia of Nanoscience and Nanotechnology*; American Scientific Publishers: California, 2004; Vol. 8, pp 791 - 843.
- (18) Choi, Y. S.; Chung, I. J. *Macromolecules Research* **2003**, *11*, 425 - 430.
- (19) Unzue, M. J.; Schoonbrood, H. A. S.; Asua, J. M.; Goni, A. M.; Sherrington, D. C.; Stahler, K.; Goebel, K.; Taure, K.; Sjoberg, M.; Holmberg, K. *Journal of*

Results and discussions

- Applied Polymer Science* **1997**, *66*, 1803 - 1820.
- (20) Fornes, T. D.; Hunter, D. L.; Paul, D. R. *Macromolecules* **2004**, *37*, 1793 - 1798.
- (21) Zaman, A. A. *Journal of Undergraduate Research* **2003**, *5*, 215 - 221.
- (22) Lei, S. G.; Hoa, S. V.; T-That, M. T. *Composites Science and Technology* **2005**, *In press*.
- (23) Stevens, M. P. *Polymer Chemistry : An Introduction*; Oxford University Press: New York, 1990.
- (24) Wang, D.; Zhu, J.; Yao, Q.; Wilkie, C. A. *Chemistry of Materials* **2002**, *14*, 3837 - 3843.
- (25) Lebaron, P. C.; Wang, Z.; Pinnavaia, T. J. *Applied Clay Science* **1999**, *15*, 11 - 29.
- (26) Ray, S.; Okamoto, M. *Progress in Polymer Science* **2003**, *28*, 1539 - 1641.
- (27) Wang, J.; Du, J.; Zhu, J.; Wilkie, C. A. *Polymer Degradation and Stability* **2002**, *77*, 249 - 252.
- (28) Doh, J. H.; Cho, I. *Polymer Bulletin* **1998**, *41*, 511 - 519.
- (29) Fischer, H. *Materials Science and Engineering* **2003**, *23*, 763 - 772.
- (30) Giannelis, P. E. *Advanced Materials* **1996**, *8*, 29 - 40.
- (31) Samakande, A.; Hartmann, P. C.; Cloete, V.; Sanderson, R. D. *Polymer* **2006**, *Accepted*.
- (32) Kawasumi, M.; Hasegawa, N.; Kato, K.; Usuki, A.; Okada, A. *Macromolecules* **1997**, *30*, 6333 - 6338.
- (33) Song, K.; Sand, G. *Clays and Clay Minerals*. **2001**, *49*, 119 - 125.
- (34) Zhang, Y.; Lee, J.; Jang, H.; Nah, C. *Composites: Part B* **2004**, *35*, 133 - 138.

Conclusions and recommendations

7.1 Conclusions

- AMPS was used as an organic modifier for the modification of clay. (SAXS analysis showed that increasing the concentration of AMPS caused an increase in the *d*-spacing from 1.14 nm (for virgin clay) up to 1.82 nm for modified clay). Depending on the quantity of AMPS inside the clay galleries, four different types of arrangements can occur namely: mono-layer, bi-layer, paraffin-type mono-layer and paraffin-type bi-layer.
- The interaction mechanism between AMPS and the clay was studied in depth. Firstly, it was proved that AMPS cannot interact with Na⁺-MMT via an ion-exchange reaction as suggested in the literature. The interaction of AMPS with clay is however likely to occur by adsorption, via formation of hydrogen bonds between both the amide and sulphate groups of AMPS, and the hydroxyl groups of the clay surface. This was confirmed by modifying the clay using other organic compounds (modifiers) having similar chemical groups to those of AMPS. Among the alternate compounds used as modifiers for clay, Cops and MET contain sulphate groups, whereas N-isopropylacrylamide (NIPA) has amide groups. These three compounds all readily adsorbed into the clay galleries, but to a lesser extent than AMPS, showing that AMPS interacts with the clay surface via both the amide and the sulphate groups.
- Styrene and butylacrylate were copolymerized by emulsion polymerization in the presence of various amounts of clays. The clay was first modified with AMPS, Cops, MET, and NIPA respectively. The morphology of the nanocomposites obtained was found to be dependent on both the organic

Conclusions and recommendations

modifier and the ratio of clay to polymer. Cops, NIPA, and MET-modified clays yielded intercalated to partially exfoliated structures, while AMPS-modified clay gave a fully exfoliated structure (only for 10% clay loading). This was attributed to two features of AMPS, namely the high reactivity of its polymerizable group with styrene and butylacrylate, and its capacity to strongly adsorb into clay by hydrogen bonding. Surprisingly, the degree of exfoliation was found to be enhanced as the AMPS-MMT loading increased, with an optimum at 10% clay/polymer

- All polymer-clay nanocomposites were found to be more thermally stable than neat poly(S-co-BA). The extent of thermal stability was directly correlated to the structure of the nanocomposite and not to the amount of clay dispersed in the polymer matrix. Thermal stability was found to be higher for intercalated than for exfoliated nanocomposites.
- An increase in the storage modulus of the nanocomposites was found to be directly correlated to the morphology of the nanocomposites. Exfoliated structures exhibited higher G' than partially exfoliated structures, and intercalated structures showed the lowest G' values.
- Batch and semi-batch emulsion polymerizations of styrene and butylacrylate in the presence of clay, were carried out so as to evaluate what effect the monomer feeding rate would have on the structures and properties of nanocomposites. Both methods (batch and semi-batch) yielded nanocomposites with similar properties and morphologies, showing that the exfoliation driving force is not monomer diffusion controlled, but the ability of the clay modifiers to adsorb inside clay galleries and their ability to copolymerize with the monomers.

7.2 Recommendations for future work

The following areas require further research:

- To study the isotherm adsorption of AMPS and other organic molecules into

Conclusions and recommendations

clay. This could provide more understanding of the interaction between organic molecules and the clay surface, and support the results obtained using TGA and SAXS.

- Study the kinetics of free radical polymerization inside and outside the clay galleries.
- Using surfactant-free, starved-free emulsion polymerization to prepare nanocomposites seeds, which on further reaction could enable us to encapsulate these clay layers inside latex particles which probably provide more improvement of nanocomposite properties.

Appendixes

Appendixes

Appendix A: The amount of Amps onto clay vs. time of clay modification

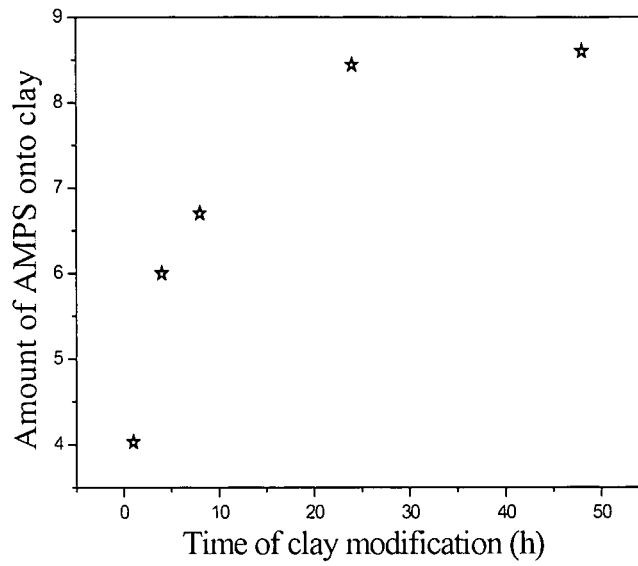


Fig. A 1: The amount of AMPS onto clay vs. the time of clay modification

Appendixes

Appendix B: FT-IR spectra of modified clay

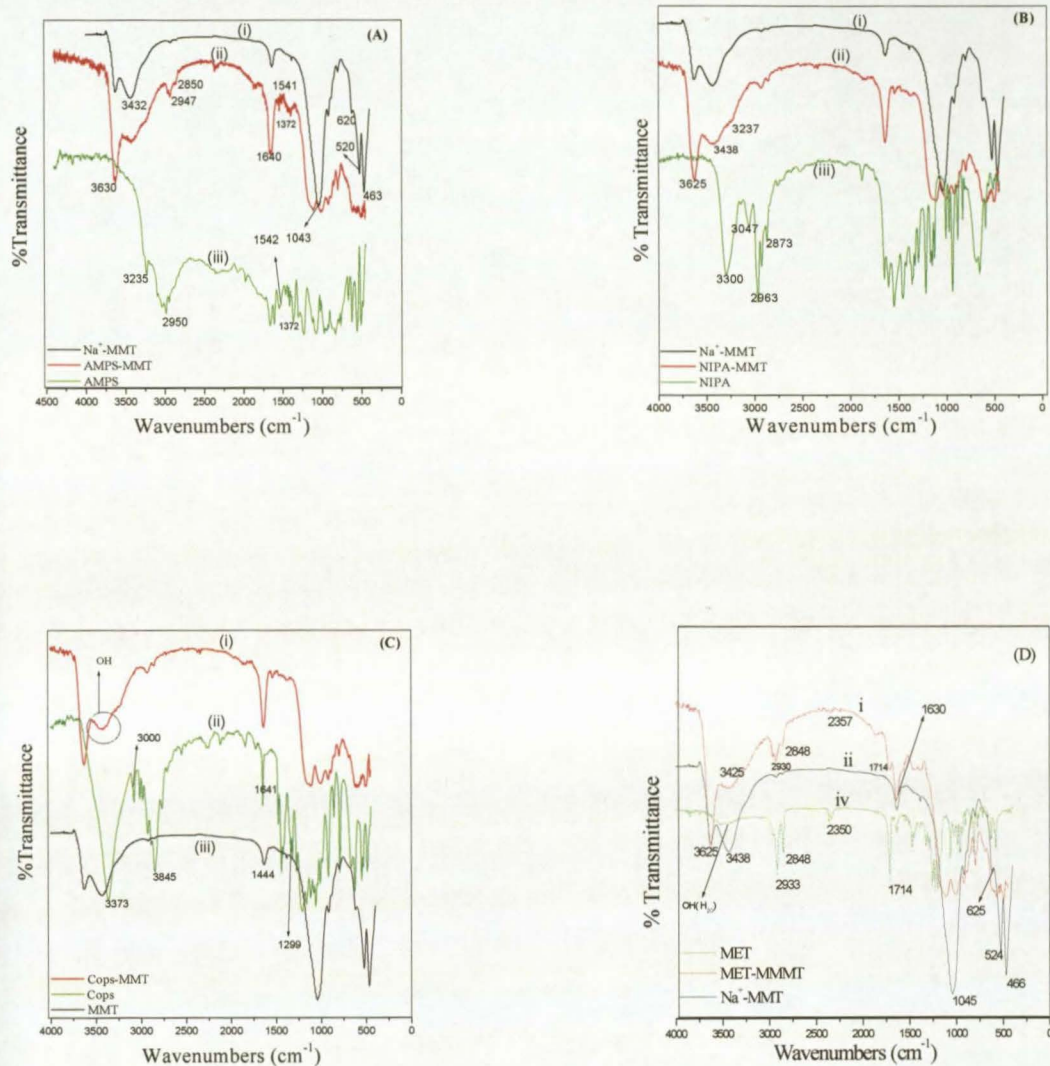


Fig. B 1: FT-IR spectra of the clay modified with different clay modifiers. (A) i-iii, represents: Na⁺-MMT, AMPS-MMT, AMPS (B) i-iii, represents: Na⁺-MMT, NIPA-MMT and NIPA (C) i-iii, represent Cops-MMT, Cops and Na⁺-MMT, (D) i-iii, represents Na⁺-MMT, MET-MMT and MET.

Appendixes

Appendix C: FT-IR spectra of poly(S-co-BA) nanocomposites

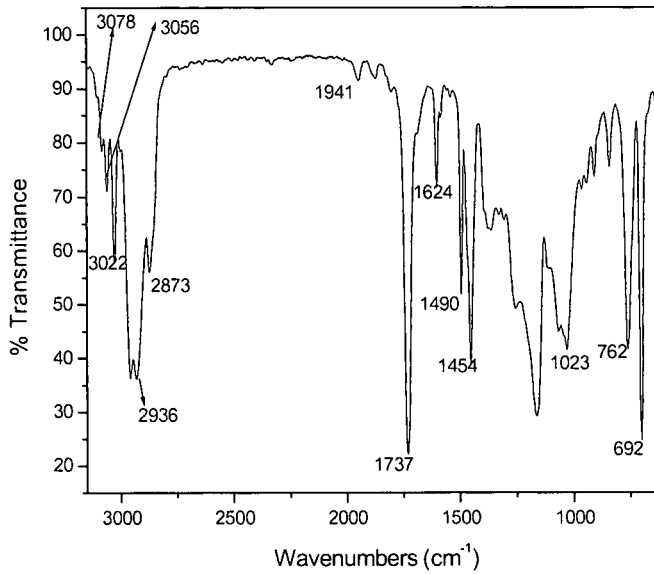


Fig. B 1: FT-IR spectrum of poly(S-co-BA).

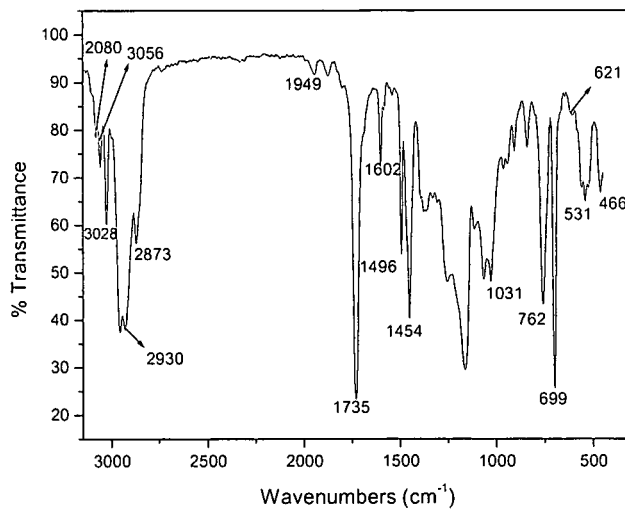


Fig. C 2: FT-IR spectrum of poly(S-co-BA)-NIPA nanocomposites.

Appendixes

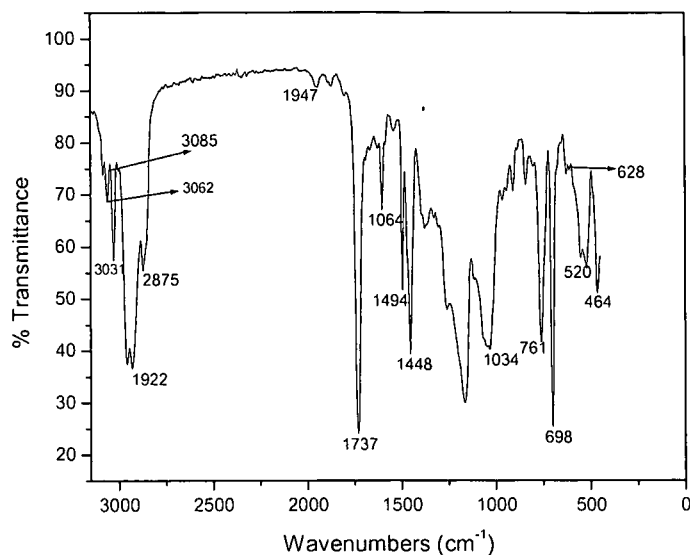


Fig. C 3: FT-IR spectrum for poly(S-co-BA)-Cops nanocomposite.

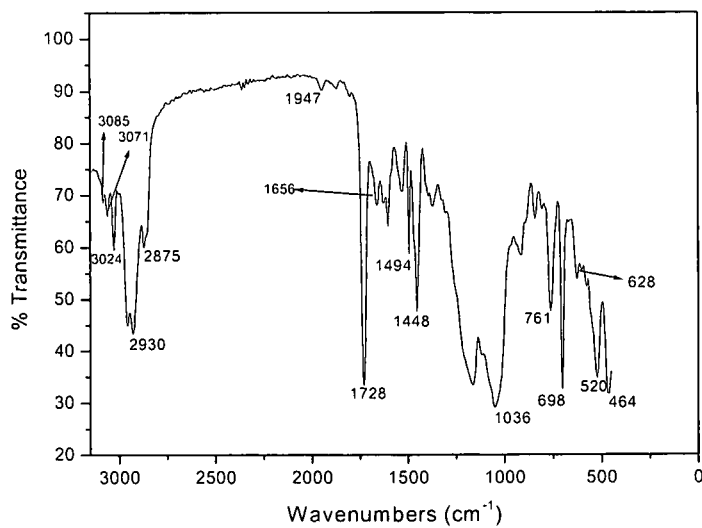


Fig. C 4: FT-IR spectrum of poly(S-co-BA)-MET nanocomposite.

Appendixes

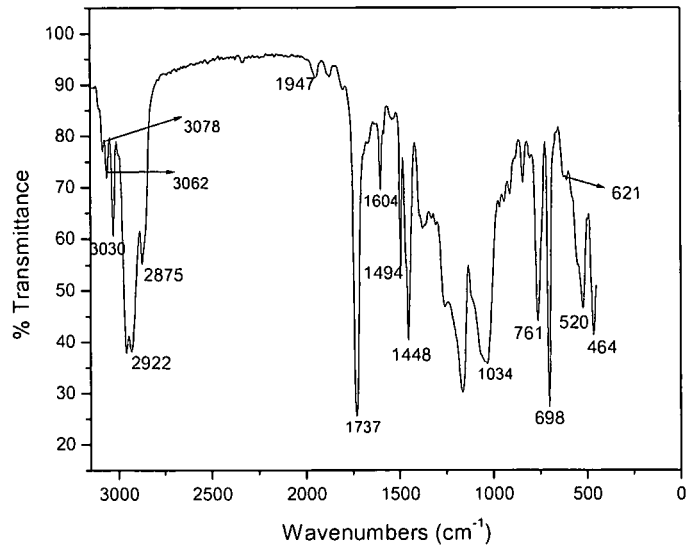


Fig. C 5: FT-IR spectrum of poly(S-co-BA)-AMPS nanocomposite.

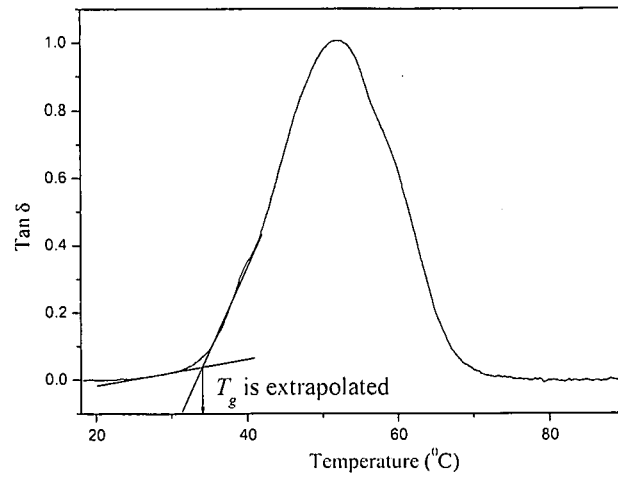
*Appendixes***Appendix D: T_g measurement by using DMA**

Fig.C1: The determination of T_g of nanocomposites from the onset temperature of $\tan \delta$ peak.